View metadata, citation and similar papers at core.ac.uk

brought to you by CORE

provided by King Fahd University of Petroleum and Minerals

COOPERATIVE UPLINK TRANSMISSION SCHEMES FOR WIRELESS MIMO SYSTEMS

BY

SUHAIB MOHAMMED AL-BASIT

A Thesis Presented to the

DEANSHIP OF GRADUATE STUDIES

KING FAHD UNIVERSITY OF PETROLEUM & MINERALS

DHAHRAN, SAUDI ARABIA

In Partial Fulfillment of the

Requirements for the Degree of

MASTER OF SCIENCE

In

TELECOMMUNICATION ENGINEERING

JUNE 2012

KING FAHD UNIVERSITY OF PETROLEUM & MINERALS
DHAHRAN 31261, SAUDI ARABIA

DEANSHIP OF GRADUATE STUDIES

This thesis, written by **Suhaib Mohammad Ismail Albasit** under the direction of his thesis advisors and approved by his thesis committee, has been presented to and accepted by the Dean of Graduate Studies, in partial fulfillment of the requirements for the degree of **MASTER OF SCIENCE IN TELECOMMUNICATION ENGINEERING**

Thesis Committee

Prof. Salam A. Zummo
(Chairman)

Dr. Samir Alghadhban
(Co-Chairman)

Dr. Azzedine Zerguine
(Member)

Dr. Maan Kousa
(Member)

Dr. Ali Muqaibel
(Member)

Dr. Ali Al-Shaikhi
Department Chairman

Prof. Salam A. Zummo
Dean of Graduate Studies

30/12/12
Date

My Father, Mother, Wife, Brothers, Sisters

ACKNOWLEDGMENTS

In the name of Allah, the Most Beneficent, the Most Merciful

All praise is due to Allah (Subhanahu wa-ta'ala) who gave me the knowledge, courage and patience to accomplish this research, and I ask Him to accept it as an act of worship. I ask for His blessings, mercy, and forgiveness. May the peace and blessings of Allah be upon Prophet Muhammad (Peace Be upon Him).

My deep appreciation goes to my advisor Dr. Salam Zummo. He was always there when I needed him, and even with his tight schedule, he has always found time for me. I am extremely grateful to him for his prompt replies and his numerous proofreads. Also, I acknowledge, with deep gratitude the guidance of Dr. Samir Al-Ghadhban, my co-advisor. His support and guidance were very important, especially in Matlab. Dr. Samir has provided me with many subroutines that were essential to my work. I am also very grateful to my thesis committee members, Dr. Azzedine Zerguine, Dr. Maan A. Kousa, and Dr. Dr. Ali Muqaibel, for their care, cooperation and constructive advice.

I would like to express my deepest indebtedness to my father, and to my mother, to my wife, sisters and brothers for their constant prayers, guidance, encouragement and support throughout my career. They are the source of power, inspiration, and confidence in me. I also like to thank my colleagues and friends for their concern and help.

Acknowledgement is due to the King Fahd University of Petroleum and Minerals and the Department of Electrical Engineering, for the support and the excellent facilities given for this research, and for granting me the opportunity to pursue my graduate studies with financial support.

TABLE OF CONTENTS

LIST OF TABLES **vii**

LIST OF FIGURES **viii**

ABSTRACT (ENGLISH) **xiv**

ABSTRACT (ARABIC) **xvi**

CHAPTER 1. INTRODUCTION **1**

1.1 Background 2

1.1.1 Multi-Antenna Systems 2

1.1.2 Multi-hop Relaying 6

1.2 Literature Survey 7

1.3 Thesis Contributions 11

1.4 Thesis Outline 12

CHAPTER 2. VIRTUAL MIMO RELAYING BASED ON AMPLIFY-AND-FORWARD (AF) **13**

2.1 System Model 14

2.1.1 AF using the V-BLAST scheme 14

2.1.2 AF using non-orthogonal STBC 16

2.2 Performance Analysis 19
2.2.1 AF using the V-BLAST scheme 19
2.3 Capacity Analysis 22
2.3.1 AF using the V-BLAST scheme 22
2.4 Numerical Results 23
2.4.1 AF using the V-BLAST scheme 23
2.4.2 AF Using non-orthogonal STBC 25
2.5 Chapter Conclusions 40

CHAPTER 3. VIRTUAL MIMO RELAYING BASED ON DETECT-SPLIT-FORWARD (DSF) 41

3.1 System Model 42
3.1.1 DSF Using the V-BLAST Scheme 42
3.1.2 DSF Using the STBC Scheme 43
3.1.3 A Hybridization system 45
3.2 Performance Analysis 46
3.2.1 DSF Using the V-BLAST Scheme 46
3.2.2 DSF Using the STBC Scheme 49
3.3 Capacity Analysis 49
3.4 Numerical Results 51
3.4.1 DSF Using the V-BLAST Scheme 51
3.4.2 DSF Using the STBC Scheme 58
3.4.3 Comparison Between the AF and the DSF V-BLAST Schemes . . . 75
3.5 Chapter Conclusions 77

CHAPTER 4. MIMO RELAYING BASED ON SPATIAL MODULATION 78

4.1 System Model 79

4.2 Performance Analysis 80

4.2.1 MIMO V-BLAST Relaying 80

4.2.2 MIMO STBC Relaying 80

4.2.3 MIMO SMod Relaying 81

4.3 Capacity Analysis 84

4.3.1 MIMO V-BLAST Relaying 84

4.3.2 MIMO STBC Relaying 84

4.3.3 MIMO SMod Relaying 84

4.4 Numerical Results 86

4.5 Chapter Conclusions 111

CHAPTER 5. CONCLUSIONS AND FUTURE RESEARCH 112

References 114

VITAE 120

LIST OF TABLES

2.1 AF vMIMO for $1 \times 2 \times 2$ relays using V-BLAST 23

2.2 AF vMIMO for $1 \times 2 \times 2$ relays using non-orthogonal STBC 25

3.1 DSF vMIMO for $1 \times 2 \times 2$ relays 51

3.2 DSF vMIMO with STBCfor $1 \times 2 \times 2$ relays 58

4.1 MIMO V-BLAST Relaying 86

4.2 MIMO STBC Relaying 86

4.3 MIMO SMod Relaying 86

LIST OF FIGURES

1.1 V-BLAST Detection Algorithm [1]. 5

1.2 Spectral efficiency for SIMO and cMIMO with power density reduction [2] 10

2.1 Cooperative relay in multi-hop cMIMO wireless networks. 14

2.2 AF system model $1 \times 2 \times 2$. 16

2.3 Time slotting in AF scheme. 16

2.4 AF non-orthogonal STBC $1 \times 2 \times 2$ example. 17

2.5 Time slotting in AF using non-orthogonal scheme. 17

2.6 Simulation and analysis results of AF vMIMO for $1 \times 2 \times 2$ relays 26

2.7 BER performance for multi hop at same throughput. 27

2.8 BER performance various source-relay distances for AF. 28

2.9 Average capacity with various source-relay distances for AF vMIMO using V-BLAST. 29

2.10 Average capacity with various source-relay distances for AF vMIMO using V-BLAST at certain SNR value. 30

2.11 Simulation results of AF with non-orthogonal STBC for QPSK and 64-QAM relays 0.3 from the source. 31

2.12 Simulation results of AF with non-orthogonal STBC for QPSK and 64-QAM relays 0.5 from the source. 32
2.13 Simulation results of AF with non-orthogonal STBC for QPSK and 64-QAM relays 0.7 from the source. 33
2.14 Simulation results of AF spatial multiplexing with sphere decoder for QPSK, 16-QAM and 64-QAM relays 0.3 from the source. 34
2.15 Simulation results of AF spatial multiplexing with sphere decoder for QPSK, 16-QAM and 64-QAM relays 0.5 from the source. 35
2.16 Simulation results of AF spatial multiplexing with sphere decoder for QPSK, 16-QAM and 64-QAM relays 0.7 from the source. 36
2.17 Comparing between AF non-orthogonal STBC and spatial multiplexing relays 0.3 from the source. 37
2.18 Comparing between AF non-orthogonal STBC and spatial multiplexing relays 0.5 from the source. 38
2.19 Comparing between AF non-orthogonal STBC and spatial multiplexing relays 0.7 from the source. 39

3.1 DSF-V-BLAST system model $1 \times 2 \times 2$. 43
3.2 Time slotting in DSF-V-BLAST scheme. 44
3.3 DSF STBC system model $1 \times 2 \times 2$. 45
3.4 Time slotting in DSF STBC scheme. 46
3.5 Detection process at each relay. 47
3.6 Splitting 16-QAM to two 4-ASK. 48

3.7 Detection process at each relay. 53
3.8 Splitting 64-QAM to two 8-ASK. 53
3.9 Simulation and analysis results of DSF-V-BLAST vMIMO for $1 \times 2 \times 2$ relays 54
3.10 256-QAM with different relaying setting of DSF-V-BLAST vMIMO. . . . 55
3.11 BER performance various source-relay distances for DSF V-BLAST. 56
3.12 Simulation and analysis results of DSF V-BLAST for 16-QAM. 57
3.13 Simulation and analysis results of DSF with STBC for 64-QAM and 256-QAM relays 0.3 from the source. 61
3.14 Simulation and analysis results of DSF with STBC for 64-QAM and 256-QAM relays 0.5 from the source. 62
3.15 Simulation and analysis results of DSF with STBC for 64-QAM and 256-QAM relays 0.7 from the source. 63
3.16 64-QAM with different relay location of DSF-STBC vMIMO for $1 \times 2 \times 2$ relays. 64
3.17 BLER performance various source-relay distances for DSF using STBC. . . 65
3.18 Average capacity with various source-relay distances for DSF using STBC. 66
3.19 Average capacity with various source-relay distances for DSF using STBC at certain SNR value. 67
3.20 Comparing BLER performance for DSF using STBC and V-BLAST at d=0.3 from source-relay 68

3.21 Comparing BLER performance for DSF using STBC and V-BLAST at d=0.5 from source-relay 69
3.22 BLER performance for various source-relay distances of the DSF using STBC and V-BLAST. 70
3.23 BLER performance for various source-relay distances of the hybrid vMIMO system for $1 \times 2 \times 2$ relays at 2 bit/s/Hz 71
3.24 Average capacity with d=0.3 from source-relay for DSF using STBC and V-BLAST. 72
3.25 Average capacity with d=0.7 from source-relay for DSF using STBC and V-BLAST. 73
3.26 Average capacity with various source-relay distances for DSF-STBC and DSF-V-BLAST at certain SNR value. 74
3.27 Comparing between AF and DSF 76
3.28 Comparing between AF and DSF source-relay distances. 76

4.1 MIMO relayed system model. 79
4.2 SMod relayed system model. 79
4.3 MIMO relaying versus DSF relays at 0.3 from the source with rate 2bit/s/Hz. 91
4.4 MIMO relaying versus DSF relays at 0.5 from the source with rate 2bit/s/Hz. 92
4.5 MIMO relaying versus DSF relays at 0.7 from the source with rate 2bit/s/Hz. 93
4.6 BLER performance various source-relay distances for MIMO relaying versus DSF with rate 2bit/s/Hz SNR=10 dB. 94

4.7 BLER performance various source-relay distances for MIMO relaying versus DSF with rate 2bit/s/Hz SNR=20 dB. 95
4.8 Average capacity at distance d=0.3 from source-relay for MIMO relaying versus DSF relaying. 96
4.9 Average capacity at distance d=0.9 from source-relay for MIMO relaying versus DSF relaying. 97
4.10 Average capacity various source-relay distances for MIMO relaying versus DSF with SNR=20 dB. 98
4.11 MIMO relaying versus DSF relays at 0.3 from the source with rate 4bit/s/Hz. 98
4.12 MIMO relaying versus DSF relays at 0.5 from the source with rate 4bit/s/Hz. 99
4.13 MIMO relaying versus DSF relays at 0.7 from the source with rate 4bit/s/Hz. 99
4.14 BLER performance various source-relay distances for MIMO relaying versus DSF with rate 4bit/s/Hz SNR=10 dB. 100
4.15 BLER performance various source-relay distances for MIMO relaying versus DSF with rate 4bit/s/Hz SNR=20 dB. 101
4.16 MIMO relaying versus Relayed Spatial Modulation at 0.3 from the source with rate 2bit/s/Hz. 102
4.17 MIMO relaying versus Relayed Spatial Modulation at 0.5 from the source with rate 2bit/s/Hz. 103
4.18 MIMO relaying versus Relayed Spatial Modulation at 0.7 from the source with rate 2bit/s/Hz. 104

4.19 BLER performance various source-relay distances for MIMO relaying versus SMod with rate 2bit/s/Hz SNR=10 dB 105
4.20 BLER performance various source-relay distances for MIMO relaying versus SMod with rate 2bit/s/Hz SNR=10 dB with 4×4 configuration. 106
4.21 Average capacity various source-relay distances for MIMO relaying versus SMod with SNR=20 dB. 107
4.22 MIMO relaying versus Relayed Spatial Modulation at 0.3 from the source with rate 2bit/s/Hz. 108
4.23 MIMO relaying versus Relayed Spatial Modulation at 0.5 from the source with rate 2bit/s/Hz. 109
4.24 MIMO relaying versus Relayed Spatial Modulation at 0.7 from the source with rate 2bit/s/Hz. 110

THESIS ABSTRACT

NAME: Suhaib Mohammed Al-Basit

TITLE OF STUDY: Cooperative Uplink Transmission Schemes for Wireless MIMO Systems

MAJOR FIELD: Telecommunication Engineering

DATE OF DEGREE: June 2012

Cooperative multi-input multi-output (MIMO) schemes in wireless communication systems improve coverage, throughput, capacity, and quality of service. We propose to evaluate the performance of uplink cooperative MIMO using hopping over MIMO relays. Both simulations and analysis are performed to evaluate the proposed system in terms of several physical parameters such as distance, modulation type, number of relays, and number of hops.

We derive the analytical error performance for virtual MIMO relaying schemes using the V-BLAST amplify-and forward scheme (AF) and detect-split-and-forward scheme (DSF). The performance of the non-orthogonal virtual MIMO systems for both non-orthogonal spacetime block code (STBC) and spatial multiplexing (SM) are studied.

We introduce and analyze the performance of relayed spatial modulation, by deriving expression for the average capacity and the probability of symbol error rate. The main

contribution of this thesis is to provide analytical tools to evaluate the performance of distributed and virtual MIMO relaying schemes, including V-BLAST, STBC and spatial modulation.

Keywords: *Cooperative multi-input multi-output, Detect-Split-and-Forward Scheme, Non-orthogonal Virtual MIMO, Relayed spatial modulation.*

ملخص الرسالة

الاسم الكامل: صهيب محمد إسماعيل البسيط

عنوان الرسالة: أنضمة الارسال التعاونية الاسلكية للنظم متعددة المدخلات والمخرجات الاسلكية

التخصص : هندسة الاتصالات.

تاريخ الدرجة العلمية: يونيو 2012

أنضمة الارسال التعاونية الاسلكية للنظم متعددة المدخلات والمخرجات الاسلكية (MIMO) في أنظمة الاتصالات اللاسلكية تحسن التغطية، والإنتاجية فى وقت واحد، والقدرة، ونوعية الخدمة. في هذا البحث اقترحنا لتقييم أداء أنضمة الارسال التعاونية الاسلكية للنظم متعددة المدخلات والمخرجات الاسلكية (MIMO) باستخدام القفزات على أنظمة (MIMO) الترحيلية تنفيذ كل من المحاكاة والتحليل لتقييم النظام المقترح من حيث عدة معاملات مادية مثل المسافة، ونوع التحوير، وعدد من التبديلات، وعدد من القفزات.

في هذا البحث اوجدنا نسبة الخطأ في الارسال لأنظمة ترحيل MIMO الظاهرية باستخدامV-BLAST بعدة طرق ترحيلية, تضخيم وارسال(AF) وكشف تقسيم وارسال(DSF). وتم دراسة الأداء الغير متعامدة الارسال لأنظمة ترحيل MIMO الظاهرية سواء الأنظمة الغير متعامدة للشيفرات المكانية الزمانية (STBC) و المكانية المتعددة (SM).

وفي هذا البحث أدخالنا الترحيل عن طريق التشكيل المكاني وحللنا الأداء عن طريق اشتقاق متوسط القدرة ونسبة الخطأ في ارسال الرمز. المساهمة الرئيسية لهذه الأطروحة هو توفير أدوات تحليلية لتقييم أداء أنظمة الارسال الموزعة والافتراضية الترحيليه MIMO بما في ذلك V-BLAST، STBC والتشكيل المكاني.

CHAPTER 1

INTRODUCTION

Since the introduction of the multiple-input-multiple-output (MIMO) technology concept in the 90's, there have been great advancements in data rate speeds and wireless network efficiency. The main purposes of MIMO implementation is to resolve the problem of fast random fading and to improve the quality of data transmission. Using MIMO technology, the capacity of a propagation environment will decrease with increasing the correlation of the channel coefficients. Practically, for none-line-of-sight (NLOS) and omni-directional wireless mobile communications, there are restrictions on handset manufacture implied by wavelengths. Hence, the designers should select applicable wavelengths to realize the full potential of MIMO fetchers. Obviously, large antenna arrays of different sizes are not always practical for handsets or laptops.

Furthermore, the developers of the next generation of wireless systems are investing in virtual or cooperative spatial multiplexing and space-time block code (STBC) techniques. The goal is to provide better quality-of-service (QoS) at higher data rates, especially for users who are at the cell edge. These techniques resemble multi-user multi-input multi-

output (MU-MIMO) techniques in the uplink side. They are also called Network MIMO [3]. They are based on the concept of relaying and virtual antenna arrays which enhance the end-to-end link performance, offer good QoS and coverage range capability in NLOS environment.

Cooperative communication is a recent model adapted from the broadcasting model of wireless channels where all communicated nodes support each other. Cooperative communications execute the communication process in a distributed way for gaining the advantages of the MIMO systems. Besides, reducing consumption of battery, improving capacity and expanding the network lifetime can be achieved [4]. Carrying a higher data rate over wireless environments motivates us to investigate virtual MIMO relay based schemes.

1.1 Background

1.1.1 Multi-Antenna Systems

Space-Time Block Codes (STBC)

The error probability decays inversely with SNR. This is one of the main challenges of communication over Rayleigh fading channels, comparing to the exponential decay observed on additive white Gaussian noise (AWGN) channels. STBC is a simple method that improves the reliability by increasing the decay of error probability [5].

STBC encoder can be described as follows: At the encoder, n symbols $(x_1, x_2, \ldots, x_n)$ are mapped to an $m \times l$ orthogonal transmission matrix, where the i^{th} row stands for the transmitted symbols from the i^{th} antenna and the j^{th} column stands for the transmitted

symbols in the j^{th} time slot. As n symbols are transmitted during l time slots, the rate of STBC is $R_s = \frac{n}{l}$ $\quad$ symbols/time slot, the maximum transmission rate of STBC is equal to one symbol/time slot. For orthogonal STBC, the maximum rate is reached just for the two transmit antennas in Alamouti's scheme [6]. Traditionally, the transmit diversity technique proposed by Alamouti is considered to be the first STBC. The encoding and decoding operations are carried out in sets of two modulated symbols. The two symbols are transmitted at two subsequent time instances t_1 and t_2. The times t_1 and t_2 are parted by a constant time duration T_s. The STBC block $\mathbf{s} = [x_1, x_2]^T$ consists of two symbols. The transmission rate is equal to the transmission rate of a single-input single-output (SISO) system. The space-time encoding mapping of Alamouti's two-branch transmit diversity technique can be represented by the coding matrix

$$\mathbf{C}_A = \begin{pmatrix} x_1 & -x_2^* \\ x_2 & x_1^* \end{pmatrix}. \tag{1.1}$$

The above coding matrix is orthogonal because the dot product $\mathbf{C}_A \cdot \mathbf{C}_A^H$ is a diagonal matrix according to $\mathbf{C}_A \cdot \mathbf{C}_A^H = \left[\sum_{i=1}^{n} |x_i|^2\right] \cdot I_m$, where C_A^H is the hermitian of C_A, I_m is the identity matrix of size $m \times m$, where m represents the number of transmit antennas, and n is the number of symbols transmitted per transmission block in C_A. The decoding process supposes that the fading channel coefficients during the two consecutive transmission times, t_1 and t_2, are the same.

Vertical Bell Labs Layered Space-Time Architecture (V-BLAST)

A high-level block diagram of a single user V-BLAST system is exposed in Figure1.1 where the number of receive antennas is M_R and the number of transmit antennas is N_T. A single bit stream is demultiplexed into several layers, and then every layer is modulated separately and sent through separated transmitting antenna. The state of procedure for the V-BLAST system is that M_R is equal or greater than N_T , so if that is content, and there is rich scattering in the channel such that the layer channel vectors are independent, one can use the V-BLAST detection algorithm to demodulate the layers, which is based only on the spatial characteristics antenna array form.

The block diagram of a V-BLAST transmitter with N_T antennas is shown in Figure 1.1. The data stream is demultiplexed into N_T sub-streams, and each sub-stream is then encoded into symbols and fed to its relevant transmitter. Transmitters 1 to N_T function using the same channel at a symbol rate of $1/T_s$ symbols/sec, where T_s is the symbol duration and the symbol timing is synchronized. Figure 1.1 also shows the vertical encoding in V-BLAST where each frame is partitioned over the transmit antennas and sent in a vertical manner [1].

Sphere Decoder (SD)

The method of SD places a hyper sphere of initial radius (R) centered at the received vector then starts searching for a valid point on its surface. The detection is done consecutively on all coordinates of the transmitted vector with an itemizing process that reduces the search array. When SD finds a valid point, it decreases the hyper sphere radius so that the new point lies on the surface of the searched sphere. After that, the search is recurred until

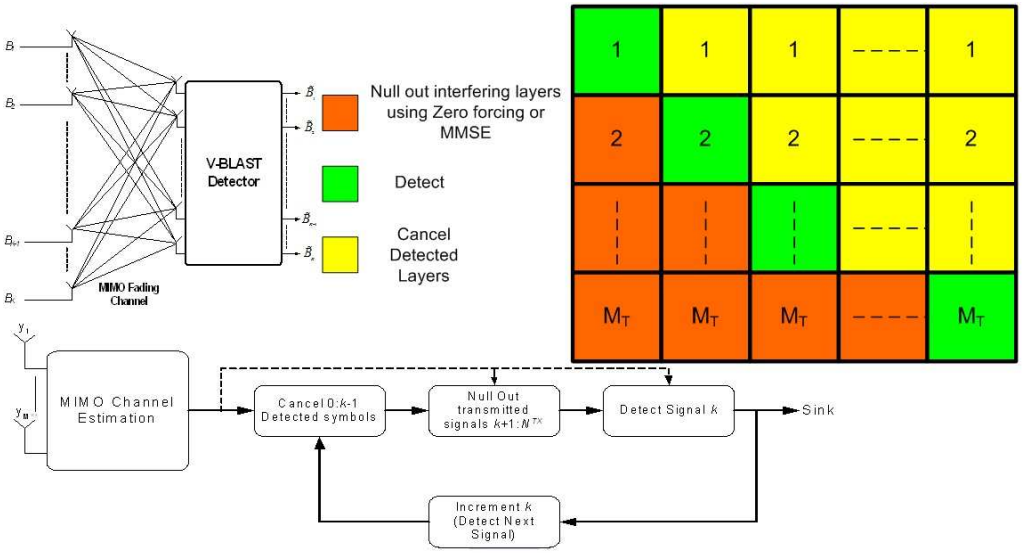

Figure 1.1: V-BLAST Detection Algorithm [1].

the closest point close to the received vector is found which is when the algorithm results in an empty sphere. If the SD doesn't find a valid point within the initial sphere, it increments the radius and explores again [1].

Spatial Modulation (SMod)

Spatial modulation is a newly developed transmission technique [7]. The essential design is to map information bits to two information carrying units: 1) the symbol from a constellation diagram and 2) the transmit antenna. SMod shows a decrease of nearly 90% in the receiver complexity for V-BLAST with the same spectral efficiency and nearly the same receiver complexity as Alamouti [8]. In [9] the new detector shows an improvement as compared to the original detector of around 4 dB. Recently, [10] has been applied for indoor optical MIMO wireless systems.

1.1.2 Multi-hop Relaying

In this era where mobile communications has been very much in demand, telecommunication operators face the need to compete with their counterparts to provide end users with better coverage and higher data rates. The topology of a wireless communication system comprises of a fixed base station (BS) and a user equipment (UE). To cope up with the market demands, a radio device node called relay node (RN), which comprises of passive repeaters that forward analog signals, is used in scenarios where a wired system is not possible or would be more costly [11]. Relay nodes play a very important role in this as they help operators lessen their deployment costs. There are three layers of relay nodes:

- Layer 1 - Amplify and Forward which is a repeater that makes use of control signaling.
- Layer 2 - Decode and Froward which uses protocols such as Medium Access Control and Radio Link Control.
- Layer 3 - resembles a set of Base Stations with wireless backhaul.

The deployment of relay nodes can be categorized in three different scenarios as they are flexible in terms of construction, position and transmission of power:

- **Network densification**, where the aim is to increase the network capacity with the introduction of new BS sites.
- **Coverage extension** relates to dead zones not covered by the network in urban and suburban environments. Using relays extends the coverage to these zones without the

need for a wired backhaul. On the other hand, the lack of a dense network can cause bad coverage in indoor environments. So, the use of indoor relay is one solution to cover them.

- **Fast roll-out**, where the fast penetration with new wireless services requires a very dynamic and fast change of an operator's infrastructure. Relay nodes can be deployed much faster and support operators to be the first to offer new services.

Relay Nodes can be further differentiated into those operating in half-duplex and those operating in full-duplex. Half-duplex relays are subject to an orthogonality constraint, which implies that they either transmit or receive on a time-frequency resource and therefore must operate in a half-duplex mode. In the case of full duplex relays, they receive the signal on one carrier frequency, process it and transmit it on the same frequency with a small delay compared to the received frame duration. This assumes that there is good isolation between the receiver antennas and the transmit antennas of relays [11].

1.2 Literature Survey

The relaying technique, as introduced by Van der Meulen [12], has transpired through the years as the most well known approach to improve the reliability and performance of wireless networks. It makes use of node cooperation and it allows a network to extend its coverage without exhausting its power resources. There are several relaying protocols, namely: Amplify-and Forward (AF), Decode-and Forward (DF), and Coded Cooperation (CC) [13]. AF is the simplest; as it only amplifies a signal then forwards it. This sys-

tem however, has a drawback. As it amplifies the signal, it also amplifies the noise. This technique, as described in the IEEE802.16j standard, does not require the mobile station (MS) to be aware of intermediate relays [14]. DF is a protocol that uses error correction as it decodes data once received and confirms its correctness then forwards the data. This technique is generally used with Hybrid Automatic Repeat-reQuest (HARQ) to ensure that correct data was decoded and intact. CC is a Wyner-Ziv (WZ) coding technique [15]. The first message is transmitted during the first slot then WZ-compressed by the relay while a second message is sent through a second slot directly from the source to its destination [16].

Relay structures have evolved by the introduction of Virtual Antenna Arrays and MIMO relays [17, 18, 19]. MIMO provides higher data rate, more spectral efficiency and better link reliability than single antenna systems. The authors of [20] apply relaying concepts to MIMO. They study an infrastructure relay system for several relay transmission and topology schemes (e.g. parallel, serial and hybrid relay) taking into consideration cooperative MIMO. In particular, the end-to-end transmission rate has been optimized and derived over several factors. Others [21] investigate the performance of spacetime block codes (STBCs) with MIMO relaying using AF as an effective way to introduce spatial diversity. In [22], DF cooperative relaying scheme for MIMO systems is analyzed. All the previous studies focus on diversity concepts. Cooperative spatial multiplexing with AF relaying was investigated in [23] and new closed-form expressions were derived for high-SNR performance of relay schemes under different design criteria. IEEE802.16e describes the uplink collaborative MIMO (UL-cMIMO) as the following: each user is equipped with single antenna and shares the same channel resources with other users (same burst size) [24]. By utiliz-

ing simultaneous transmissions over common burst, cMIMO will allow increasing the peak transmission rate and improve the system performance. Unlike the conventional single user MIMO, cMIMO lets the powers of RN sum, so greater spectral efficiency can be reached [2]. One of the difficulties is to expand the interference level since combined sub-channels have increased interference similar to SIMO. Moreover, it is required that users match the same burst size. In order to overcome these challenges, the authors in [2] propose a novel algorithm for cMIMO. The major factor of this algorithm is to decrease the power-densities of the cMIMO transmissions related to those of SIMO transmissions. For example, two users seeking cMIMO transmissions at the same sector using the same burst (same OFDMA slots) will generate twice the interference level generated by SIMO. If the power density of the two users was reduced by a factor of two, they will result in the same interference level as a SIMO [2]. The factoring of cMIMO power should be met especially for users that are on the boundary of the cell to keep the same interference level compared to SIMO. Actually, the bisecting of the power density will reduce the user's signal to interference noise ratio (SINR) relative to the SIMO case. Another point is to take into account the outcome of spatial orthogonality. Consider a 2×2 MIMO system, the spectral efficiencies for SIMO is $\log_2(1 + \mathrm{SNR})$ and the spectral efficiencies for cMIMO is $2\log_2(1 + \frac{\mathrm{SNR}}{2})$. The cMIMO signal-to-noise ratio (SNR) stabilizes the power density reduction and the cMIMO spectral efficiency accounts for two transmissions at the same SNR.

There are several relaying techniques, such as amplification, compressing, coding and splitting. In [25] an amplify-and forward cooperative spatial multiplexing scheme is proposed in which each transmitter is equipped with a single antenna. The transmitters form

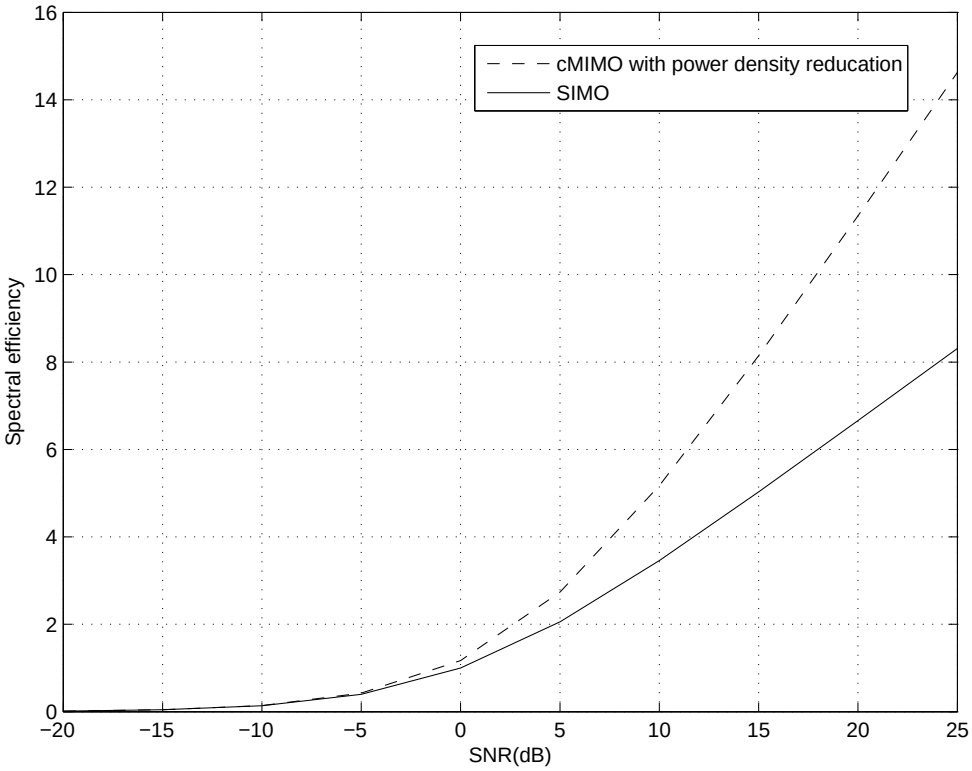

Figure 1.2: Spectral efficiency for SIMO and cMIMO with power density reduction [2]

a virtual antenna array and broadcast identical signal to relays that amplify and forward different portions of the signal at a reduced data rate to the destination. The receiver is equipped with multiple antennas in order to nullify and cancel the interference from the different relays and detect the original signal transmitted from the source. Another approach proposed by [26] is to let the relays detect a sub-stream from the original stream. Then all relays forward their low rate sub-streams simultaneously over the same physical channel.

1.3 Thesis Contributions

The contributions of this thesis can be summarized as follows:

- We derive the analytical error performance for virtual MIMO (vMIMO) relaying schemes using the V-BLAST amplify-and-forward scheme (AF) and the detect-split-and-forward scheme (DSF). The analytical results are supported by simulation in terms of several physical parameters (such as distance, modulation type, number of relays, and number of hops) and by the derivation of an expression for the average capacity of both systems. We study the performance of the non-orthogonal vMIMO systems for both non-orthogonal STBC and spatial multiplexing. Comparisons are supported by simulation with different physical parameters such as distance and modulation type.

- We compare STBC and V-BLAST vMIMO based systems using DSF. This scheme suggests the configuration and the modulation scheme in order to improve the performance. The main results of this study show that there is a tradeoff between those two schemes. The analytical results are supported by simulation results and an expression for the average capacity of both systems.

- We introduce and analyze the performance of relayed spatial modulation, by deriving expressions for the average capacity and the probability of symbol error rate. Also, we compare relayed spatial modulation with other relayed systems such as STBC and V-BLAST.

1.4 Thesis Outline

In Chapter 2, cooperative MIMO with amplify-and-forward relaying schemes using V-BLAST, non-orthogonal STBC and non-orthogonal spatial multiplexing are described. The system models of the systems are introduced with necessary details. For these systems, the average capacity and the probability of block error rate are derived. Moreover, the tradeoff between diversity and multiplexing is discussed. Chapter 3 compares STBC and V-BLAST cMIMO based systems using DSF, where we find formulas for the average capacity and the probability of block error rate. Also, like in Chapter 2, we discuss the tradeoff between diversity and multiplexing. In Chapter 4, we introduce a Relayed Spatial Modulation based system. The system is evaluated and compared with different MIMO relaying-based systems (i.e. STBC and V-BLAST). Also we find formulas for the average capacity and the probability of symbol error rate. Finally, the main conclusions from the thesis and the possible future research directions are discussed in Chapter 5.

CHAPTER 2

VIRTUAL MIMO RELAYING BASED ON AMPLIFY-AND-FORWARD (AF)

Virtual MIMO allows for increasing the peak transmission rate and improving the system performance. Unlike the usual single user MIMO, vMIMO allows the powers of its users to sum, so higher spectral efficiency can be accomplished [2]. In this chapter the performance of uplink cooperative Spatial Multiplexing using amplify-and forward (AF) and non-orthogonal STBC schemes over MIMO relays is evaluated. Both simulations and analysis have been carried out to evaluate the system's performance in terms of several physical parameters such as distance, modulation type, and number of hops.

The chapter is structured as follows: Section 2.1 gives a detailed description of the systems models. Sections 2.2 and 2.3 present the performance analysis of vMIMO (AF), in which we derive a formula for the block error rate. Section 2.4 presents the simulation results conducted to evaluate the vMIMO AF systems. Finally, Section 2.5 presents the chapter's conclusions.

2.1 System Model

Figure 2.1 shows a general multi-hop vMIMO system. The mobile unit (MS) or the source is equipped with a single antenna and it transmits to two relays. Based on the hopping scheme, the relays forward the signal to the second stage of relays. At the end, the signal is received by the base station (BS) which is equipped with multiple antennas.

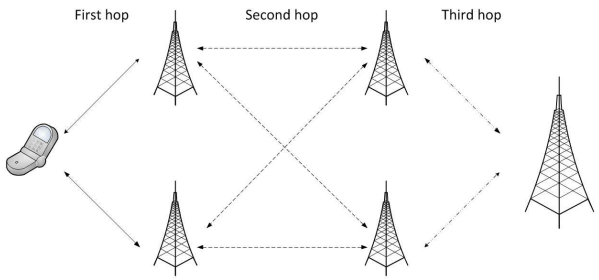

Figure 2.1: Cooperative relay in multi-hop cMIMO wireless networks.

2.1.1 AF using the V-BLAST scheme

The AF V-BLAST scheme is illustrated in Figure 2.2. This system was proposed in [27]. The transmitter and relays are equipped with single antennas. The source sends symbols $x_1, x_2...x_N$ to N relays $R_1, R_2....R_N$ with transmission power P_S at rate R_S bits/sec (bps) as depicted in Figure 2.3. The source transmits data to relays R_i which are equipped with single antenna. The received signal at the first hop is given by

$$Y_{R_i}^{(1)} = h_{R_i,S}^{(1)} x_i + n_{R_i}^{(1)}, \tag{2.1}$$

where $h^{(1)}_{R_i,S}$ is the channel gain between T_x of the source (S) and the targeted relay (R_i). We assume that the channel is rich-scattering complex Gaussian distributed with mean zero and variance $E[|h^{(1)}_{R_i,S}|^2] = d^{-m}_{R_i,S}$ where $d_{R_i,S}$ is the distance between the source (S) and relay (R_i). In addition m is the path loss exponent. Typical values for m are $2 \leq m \leq 4$ and x_i is the transmitted symbol from the source and $n^{(1)}_{R_i}$ is the complex gaussian noise with mean zero and variance $N_0/2$

The received signal at each hop is written as follows

$$Y^{t+1}_{R_i} = \prod_{l=1}^{t} H^{t+1}_{R_i,S} G^{l}_{i-1} Y^1 + n^{t+1}_{R_i}, \tag{2.2}$$

where H^t is the channel matrix at certain time slot, and $n^{t+1} = H^{t+1}G^t n^t + n^{n+1}$is the equivalent noise vector accumulated over all relay stages. Furthermore, we assume that all the relays are perfectly synchronized such that the forwarding should be within the same time at rate R_S/R_N bits/sec. R_N is the number of relays that need to be active in order to exploit the capacity of MIMO transmission. The amplification factor G_{R_i} scales the relay transmit power (P_{R_i}) before forwarding it to the destination and it is given in [28] as:

$$G_{R_i} = \sqrt{\frac{P_{R_i}}{([\overline{H_{R_i}}]P_s + N_0)}}, \tag{2.3}$$

On the last stage, all relays amplify their data and forward them to the destination using V-BLAST with successive interference cancellation (SIC) algorithm that perform nulling, cancelation and ordering. SIC can be based on zero forcing (ZF) as well as minimum mean square error (MMSE) equalizers.

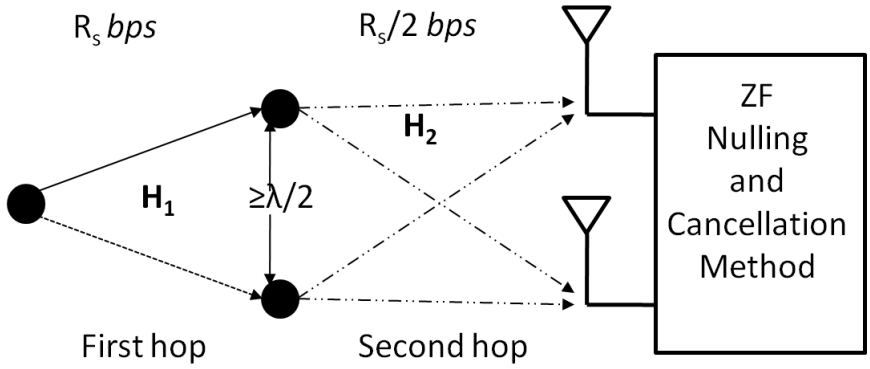

Figure 2.2: AF system model $1 \times 2 \times 2$.

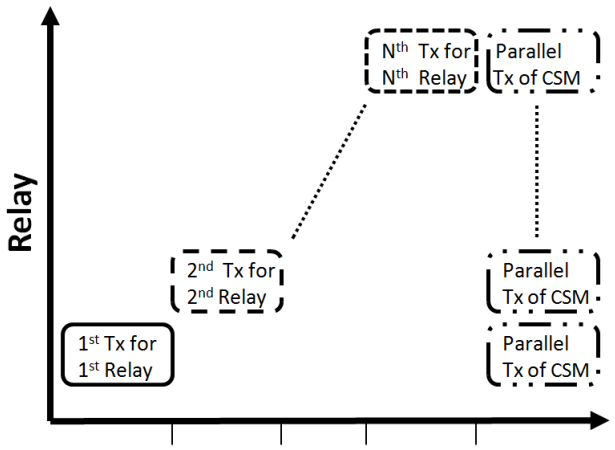

Figure 2.3: Time slotting in AF scheme.

2.1.2 AF using non-orthogonal STBC

To apply STBC for vMIMO by the AF scheme, the signals reach at each relay to be amplified will be affected by variant channels so that signals are not orthogonal. Let consider the case $1 \times 2 \times 2$ as shown in Figure 2.4 . signals at each relay will be

$$Y_{R_1}^1 = h_{SR_1}^1 x_1 + n_{R_1}^1, \tag{2.4}$$

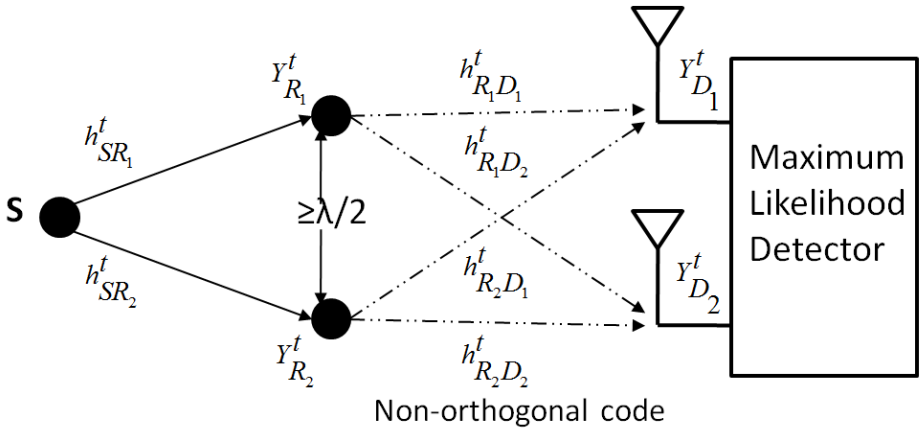

Figure 2.4: AF non-orthogonal STBC $1 \times 2 \times 2$ example.

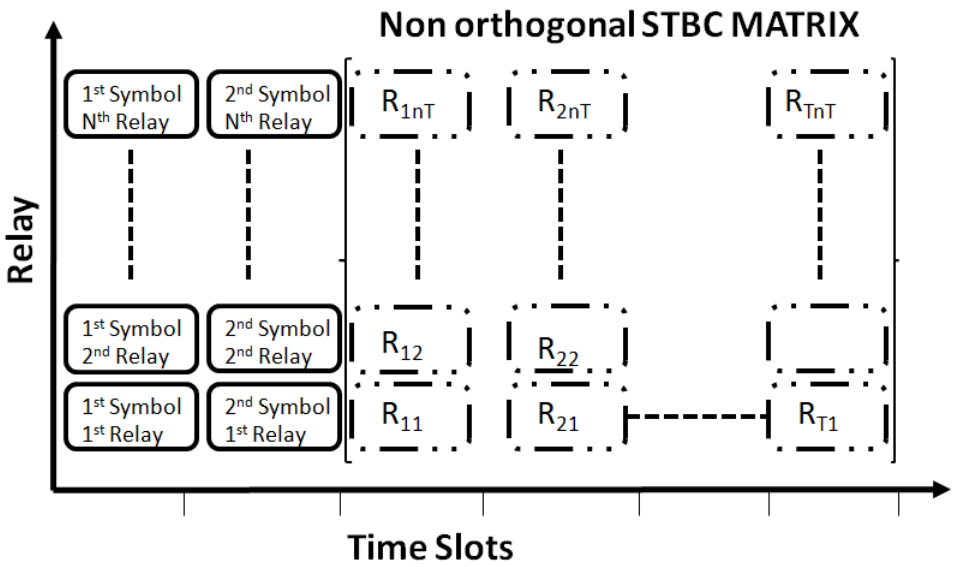

Figure 2.5: Time slotting in AF using non-orthogonal scheme.

$$Y_{R_2}^1 = h_{SR_2}^1 x_1 + n_{R_2}^1, \tag{2.5}$$

$$Y_{R_1}^2 = h_{SR_1}^2 x_2 + n_{R_1}^2, \tag{2.6}$$

and

$$Y_{R_2}^2 = h_{SR_2}^2 x_2 + n_{R_2}^2, \tag{2.7}$$

where $Y_{R_i}^t$ is the received signal at time slot t and relay R_i. Then all relays amplify the received signals with amplification factor G_{R_i} that can be found from equation 2.3.

Since the channel gains are statically independent, the rank of the combined channel matrix is M_R. For example the combined channel matrix of two relays cooperated with a single node is

$$\begin{pmatrix} Y_{D_1}^3 \\ Y_{D_1}^4 \\ Y_{D_2}^3 \\ Y_{D_2}^4 \end{pmatrix} = \begin{pmatrix} G_{R_1}^3 h_{R_1D_1}^3 h_{SR_1}^1 & G_{R_2}^4 h_{R_2D_1}^3 h_{SR_2}^2 \\ G_{R_2}^3 h_{R_2D_1}^4 h_{SR_2}^1 & G_{R_1}^4 h_{R_1D_1}^4 h_{SR_1}^2 \\ G_{R_1}^3 h_{R_1D_2}^3 h_{SR_1}^1 & G_{R_2}^4 h_{R_2D_2}^3 h_{SR_2}^2 \\ G_{R_2}^3 h_{R_2D_2}^4 h_{SR_2}^1 & G_{R_1}^4 h_{R_2D_2}^4 h_{SR_1}^2 \end{pmatrix} \begin{pmatrix} x_1 \\ x_2 \end{pmatrix} + \begin{pmatrix} G_{R_1}^3 h_{R_1D_1}^3 n_{R_1}^1 + G_{R_2}^4 h_{R_2D_1}^3 n_{R_2}^2 + n_{D_1}^3 \\ G_{R_1}^4 h_{R_1D_1}^4 n_{R_1}^1 + G_{R_2}^3 h_{R_2D_1}^3 n_{R_2}^2 + n_{D_1}^4 \\ G_{R_1}^3 h_{R_1D_2}^3 n_{R_1}^1 + G_{R_2}^4 h_{R_2D_2}^3 n_{R_2}^2 + n_{D_2}^3 \\ G_{R_1}^4 h_{R_1D_2}^4 n_{R_1}^1 + G_{R_2}^3 h_{R_2D_2}^3 n_{R_2}^2 + n_{D_2}^4 \end{pmatrix}, \tag{2.8}$$

where

$$\overrightarrow{Y} = H\overrightarrow{x} + \overrightarrow{n} \tag{2.9}$$

the received vector will be passed to the sphere decoder and process according [29].

2.2 Performance Analysis

In this section we derive the exact block error probability analysis for AF using a V-BLAST receiver employing M-QAM and M-PSK modulation schemes. In the analysis, we consider the effect of errors propagating from the previous erroneous layers. We analyze the system assuming that the power is equally splitted among antenna relays at the transmitters.

2.2.1 AF using the V-BLAST scheme

In order to calculate the Block Error Rate (BLER) of the multi-hop AF spatial multiplexing scheme, the combined channel matrix of AF V-BLAST for one hop and two relays can be described as follows:

$$H = \begin{pmatrix} h^2_{R_1D_1} G^2_{R_1} h^1_{R_1} & h^2_{R_1D_2} G^2_{R_2} h^1_{R_2} \\ h^2_{R_2D_1} G^2_{R_1} h^1_{R_1} & h^2_{R_2D_2} G^2_{R_2} h^1_{R_2} \end{pmatrix}, \tag{2.10}$$

Detection is done iteratively by detecting first the strongest layer. Then the effect of this strongest layer is removed from each received signals. The detection continues with the strongest remaining layer, and so on. To maximize the SNR, the optimal detection order is formed by choosing the row of W_{ZF} with minimum Euclidean norm. Where W_{ZF} is a matrix that represents the linear processing in the receiver:

$$W_{ZF} = (H^H H)^{-1} H^H. \tag{2.11}$$

The equivalent SNR at the destination is

$$\gamma_{eq} = \left[\prod_{n=1}^{N_H}(1+\frac{1}{\gamma_n})-1\right]^{-1}, \tag{2.12}$$

then the post-processing calculated SNR at each layer i is

$$\gamma_i = \frac{\gamma_{eq}}{R||W_{ZF,i}||_F^2}, \tag{2.13}$$

where $W_{ZF,i}$ is the zero forcing ZF projection vector of the i^{th} layer, and R_N is the total number of relays.

γ_i will be substituted at equations 2.14 and 2.20 to get the symbol error probability for the l^{th} layer M-QAM over Rayleigh fading channels ($P_{e,i}$) is given by [30]

$$\begin{aligned} P_{e,i} &= 4(1-\frac{1}{\sqrt{M}})(\frac{1-\zeta_i}{2})^{D_i}\sum_{j=0}^{D_i-1}\binom{D_i-1+j}{j}(\frac{1+\zeta_i}{2})^j \\ &\quad -4(1-\frac{1}{\sqrt{M}})^2\{\frac{1}{4}-\frac{\zeta_i}{\Pi}\{(\frac{\Pi}{2}-\tan^{-1}\zeta_i)\sum_{j=0}^{D_i-1}\binom{2j}{j}(\frac{1-\zeta_j}{4})^j \\ &\quad +\sin(\tan^{-1}\zeta_i)\sum_{j=1}^{D_i-1}\sum_{r=1}^{j}\frac{Jrj}{(1+\beta_i)^j}[\cos(\tan^{-1})\zeta_i]^{2(j-r)+1}\}\}, \end{aligned} \tag{2.14}$$

where

$$D_i = M_R - R_n + i, \tag{2.15}$$

where M_R is the total number of receiver antenna.Let d be the distance between each relay

and the source, and v be the path loss, then the parameters in (2.14) are defined as

$$\zeta_i = \frac{\beta_i}{1+\beta_i} \tag{2.16}$$

$$\beta_i = \frac{3d^{-v}\gamma_D}{2R_N(M-1)} \tag{2.17}$$

$$J_{rj} = \frac{\binom{2j}{j}}{\binom{2(j-r)}{(j-r)}4^i(2(j-r)+1)}. \tag{2.18}$$

The BLER of the V-BLAST at the second hop can be calculated as in [1]

$$P_{B,H} = 1 - \prod_{l=1}^{L}(1-P_{e,i}), \tag{2.19}$$

where $L = R_N$ for the V-BLAST. For M-PSK case, the probability error is substituted with [30]

$$P_{e,i} = \frac{M-1}{M} - \frac{\mu_t}{\sqrt{\mu_t^2+1}}(\frac{1}{2}+\frac{\omega_t}{\Pi})\sum_{\tau=0}^{D_t-1}\binom{2\tau}{\tau}[4(\mu_t^2+1)]^{-\tau}$$

$$-\frac{\mu_t}{\sqrt{\mu_t^2+1}}\frac{1}{\Pi}\sin(\omega_t)\sum_{\tau=1}^{D_t-1}\sum_{i=1}^{\tau}\frac{Ji\tau}{(\mu_t^2+1)^\tau}[\cos(\omega_t)]^{2(\tau-i)+1}, \tag{2.20}$$

where

$$\mu_t = \sqrt{\rho_t}\sin(\frac{\Pi}{M}) \tag{2.21}$$

$$\rho_t = d^{-v}\cdot\gamma_D \tag{2.22}$$

$$\omega_t = \tan^{-1}(\frac{\sqrt{\rho_t}\cos(\frac{\Pi}{M})}{\sqrt{\mu_t^2+1}}). \tag{2.23}$$

2.3 Capacity Analysis

2.3.1 AF using the V-BLAST scheme

Channel capacity is the maximum information rate that can be transmitted and received with a randomly low probability of error. A regular representation of the channel capacity is within a unit bandwidth of the channel and can be expressed in bps/Hz. This representation is also known as the spectral (bandwidth) efficiency. The instantaneous capacity of V-BLAST with R_N relays and with zero forcing interference nulling (ZF) and serial cancellation is given by [31]:

$$C_{V-BLAST}^{ZF} = R_N.\min_{i=1,2,\ldots,R_N}\{\log_2(1+\frac{\gamma_i}{R_N\|W_{ZF,i}\|_F^2})\}, \tag{2.24}$$

where $W_{ZF,i}$ is the ZF projection vector of the i^{th} layer, γ_i is the post-processing SNR per receive antenna includes distance effect as defined in equation 2.11, and $\|(\cdot)\|_F^2$ is the squared Frobenius norm.

with AF V-BLAST, the instantaneous capacity of the system is:

$$C_{AF-V-BLAST} = \frac{C_{V-BLAST}^{ZF}}{N_H}, \tag{2.25}$$

where N_H is the total number of hops.

2.4 Numerical Results

2.4.1 AF using the V-BLAST scheme

In this section we illustrate the numerical results of vMIMO using the AF scheme. Figure 2.6 shows the BLER performance of $1 \times 2 \times 2$ relays. The source is equipped with a single antenna, each relay has a single antenna and the destination has two antennas. vMIMO with different modulation is shown in Table 2.1

Table 2.1: AF vMIMO for $1 \times 2 \times 2$ relays using V-BLAST

Number of time slots	Modulation type	Spectral efficiency
3	QPSK	1.3
3	8PSK	2
3	64QAM	4

Where, in this thesis, the spectral effeciency is computed as the total number of bits received at the destination divided by the total number of time slots.

Figure 2.6 compares the block error rate of an AF vMIMO system with the 64-QAM, 8-PSK and QPSK. modulation techniques. The figure compares the analytical results obtained for the AF vMIMO to those obtained from the simulation. Clearly, our analysis seems to match the Monte Carlo simulation, which demonstrates the validity of the proposed analysis.

In Figure 2.7 the multi-hops are examined by implementing a second hop with adding two relays. In this case, we observe 3-4 dB gain at low SNR. The gain diminishes at high SNR to 2-1 dB. According to [32] the noise and interference are also amplified along with the amplified signals, so the performance will not enhance in proportion with the number of MIMO hops.

We also examine the effect of relay location on the performance of the vMIMO. At fixed SNR, we evaluate the performance of the system with different relay locations and the best place for the relay is in the center between source and destination as shown in Figure 2.8.

Figure 2.9 compares the channel average capacity of an AF vMIMO system with different relay locations at d=0.3, 0.5 and 0.9 from the source. As we can notice, when the relays are located farther from the source, the average channel capacity increases. Figure 2.10 shows the average performance capacity at certain SNR of AF vMIMO system with different relay locations.

2.4.2 AF Using non-orthogonal STBC

In this section, we illustrate the numerical results of AF the vMIMO non-orthogonal STBC scheme. Figures 2.11, 2.12 and 2.13 show the BLER performance of $1 \times 2 \times 2$ relays. The source is equipped with a single antenna, each relay has a single antenna and the destination has two antennas. The different modulations shown in Table 2.2 were applied to show the performance with different spectral efficiency. For fair comparison with the system model proposed in 2.1.1, we replace the V-BLAST decoder with SD considering the same spectral efficiency for both systems. The results of the simulation of the BLER performance for the spatial multiplexing model presented in Figures 2.14, 2.15 and 2.16. By comparing the two different systems, we notice that when the spectral efficiency is low the non-orthogonal STBC dominates the performance. However, when the source needs to transmit on higher spectral efficiency, the spatial multiplexing scheme dominates on non-orthogonal STBC.

Table 2.2: AF vMIMO for $1 \times 2 \times 2$ relays using non-orthogonal STBC

Number of time slots	Modulation type	Spectral efficiency
4	QPSK	1
4	16-QAM	2
4	64-QAM	3
4	256-QAM	4

Figures 2.16, 2.17 and 2.18 compare non-orthogonal STBC and spacial multiplexing for different relay locations. Notice that STBC performs better than SM for low rates. For high rates, SM performs slightly better than STBC, where the gain increases with distance.

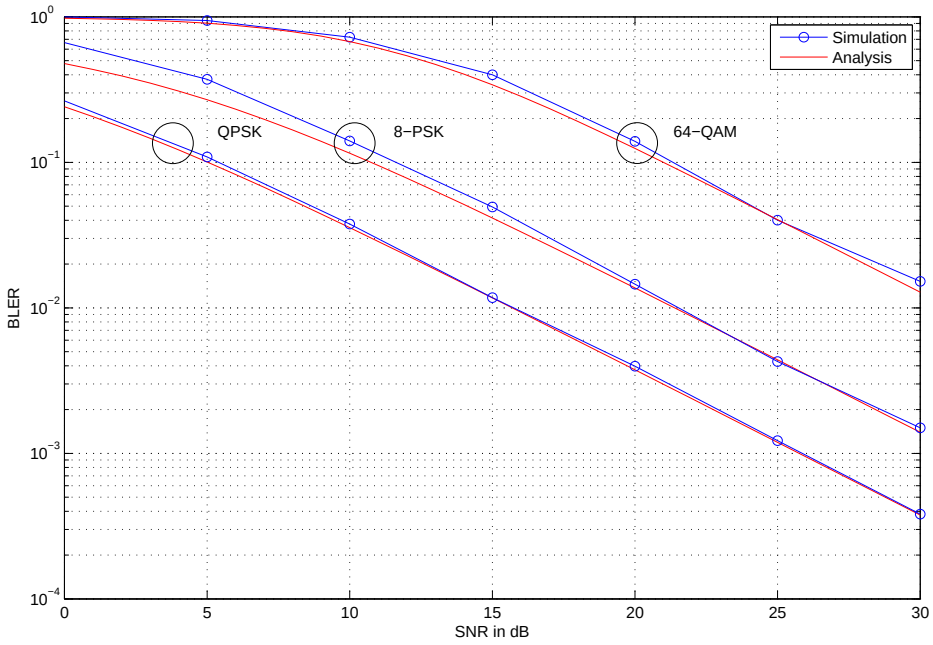

Figure 2.6: Simulation and analysis results of AF vMIMO for $1 \times 2 \times 2$ relays .

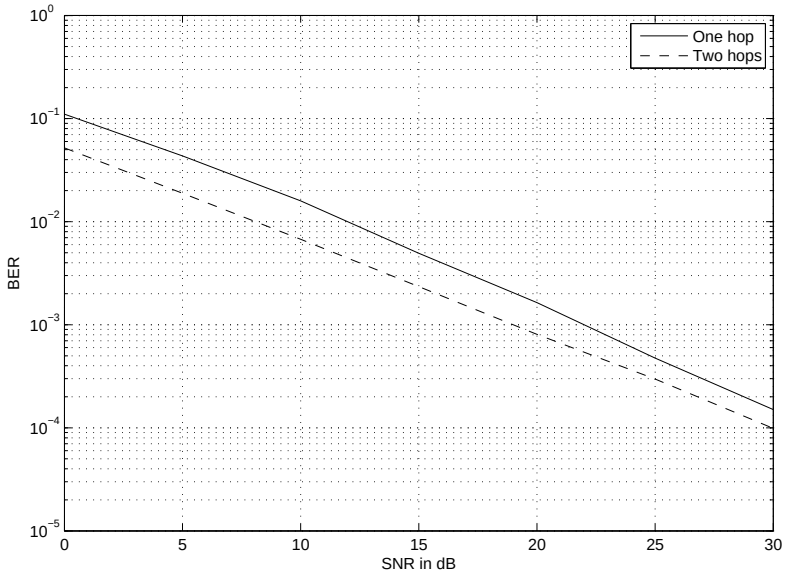

Figure 2.7: BER performance for multi hop at same throughput.

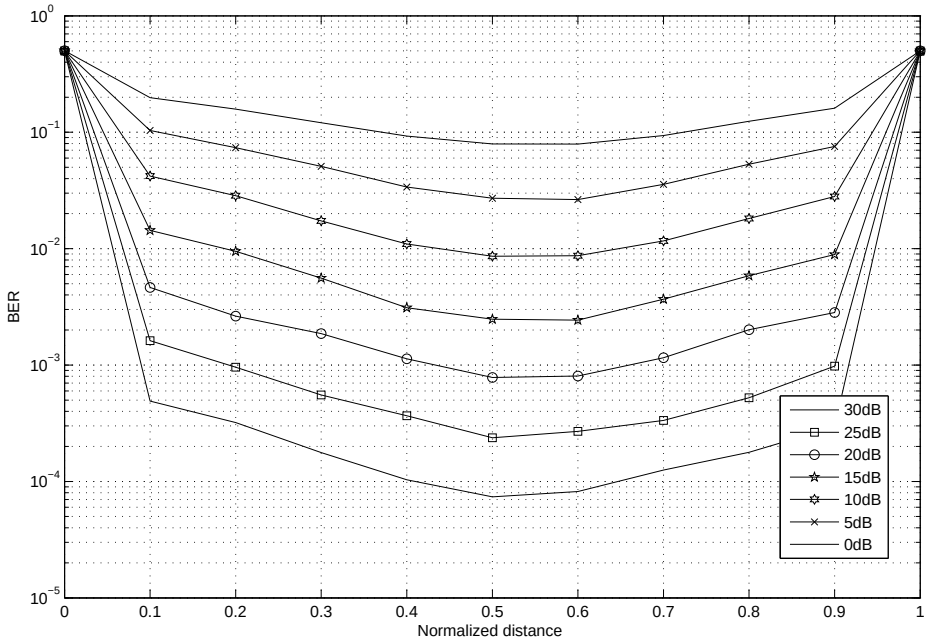

Figure 2.8: BER performance various source-relay distances for AF.

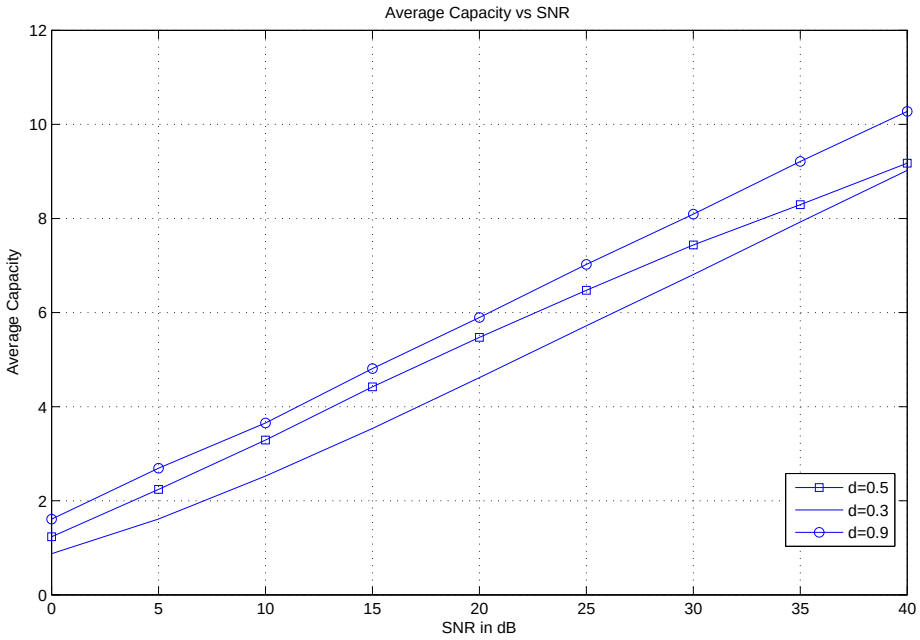

Figure 2.9: Average capacity with various source-relay distances for AF vMIMO using V-BLAST.

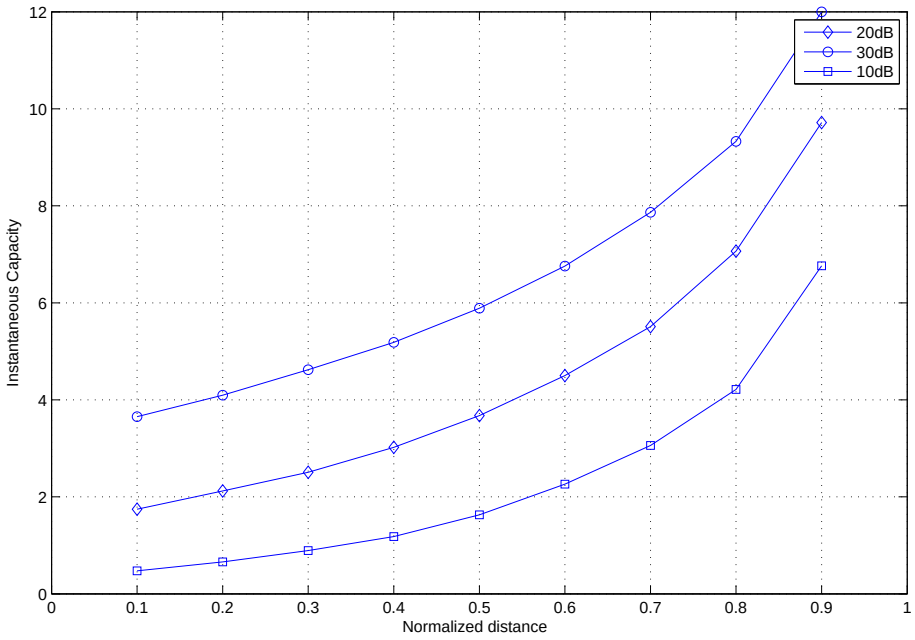

Figure 2.10: Average capacity with various source-relay distances for AF vMIMO using V-BLAST at certain SNR value.

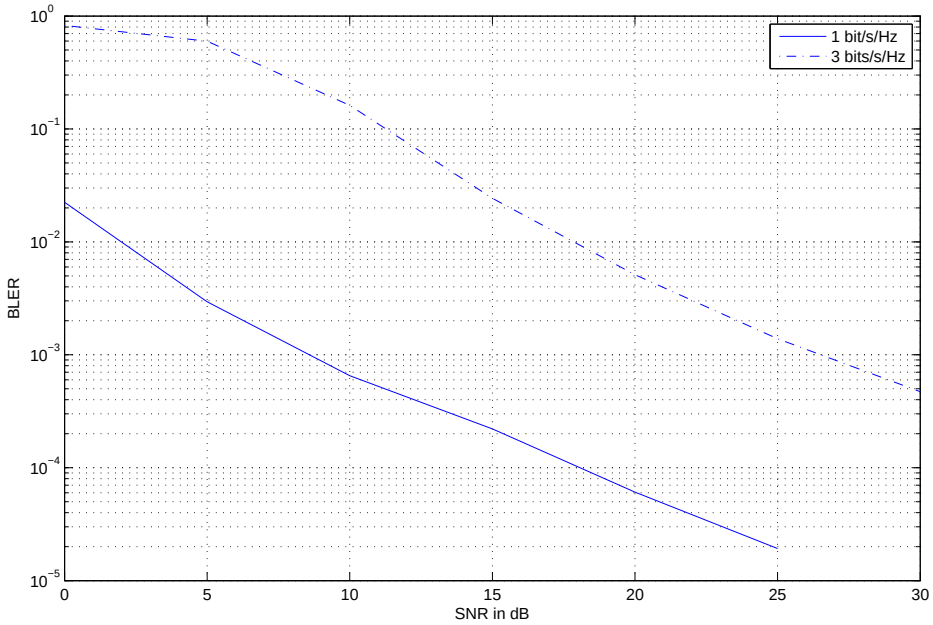

Figure 2.11: Simulation results of AF with non-orthogonal STBC for QPSK and 64-QAM relays 0.3 from the source.

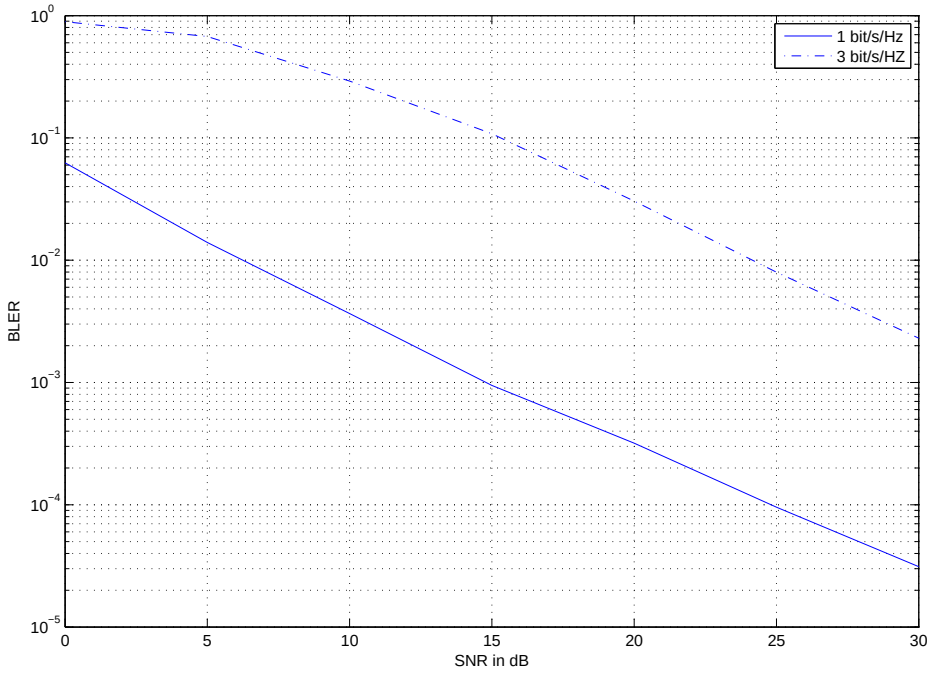

Figure 2.12: Simulation results of AF with non-orthogonal STBC for QPSK and 64-QAM relays 0.5 from the source.

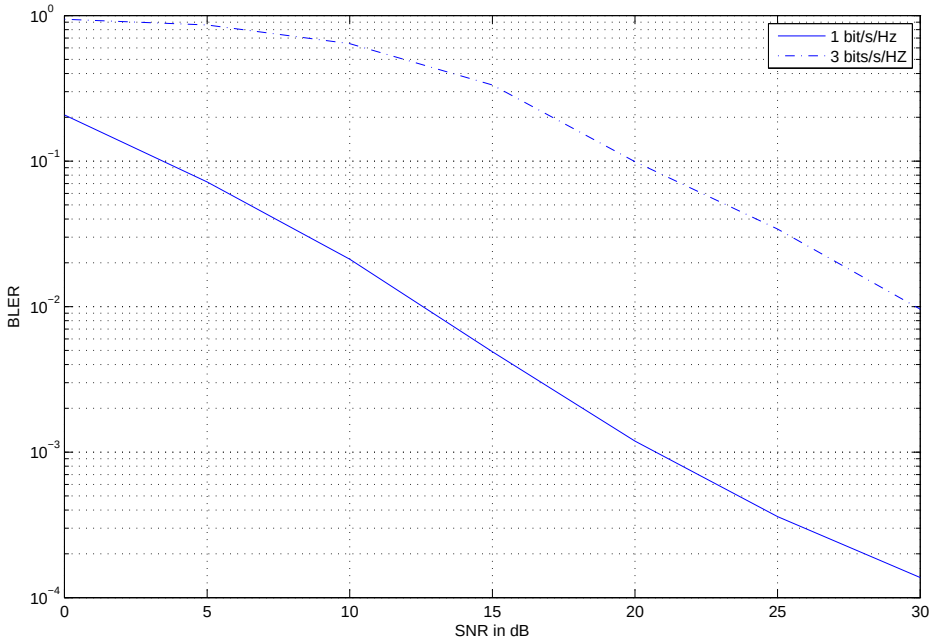

Figure 2.13: Simulation results of AF with non-orthogonal STBC for QPSK and 64-QAM relays 0.7 from the source.

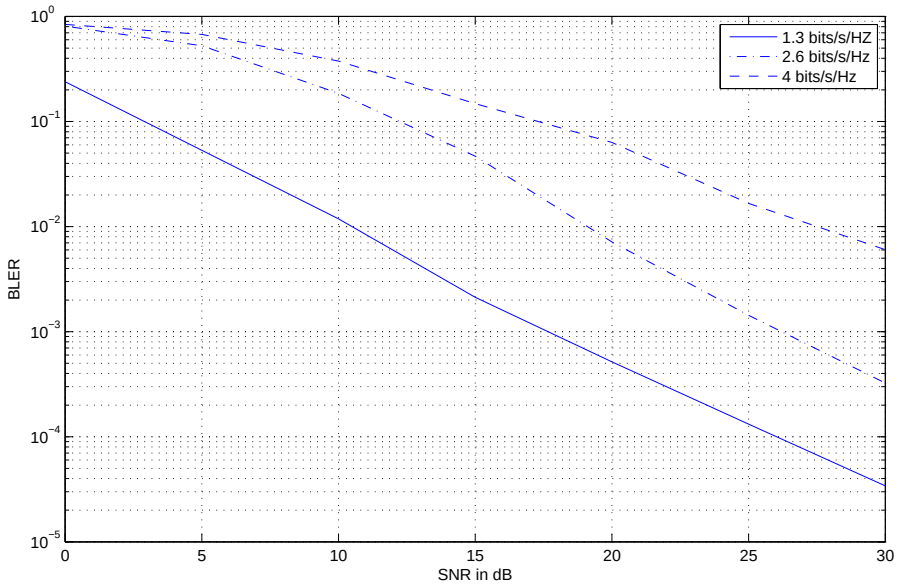

Figure 2.14: Simulation results of AF spatial multiplexing with sphere decoder for QPSK, 16-QAM and 64-QAM relays 0.3 from the source.

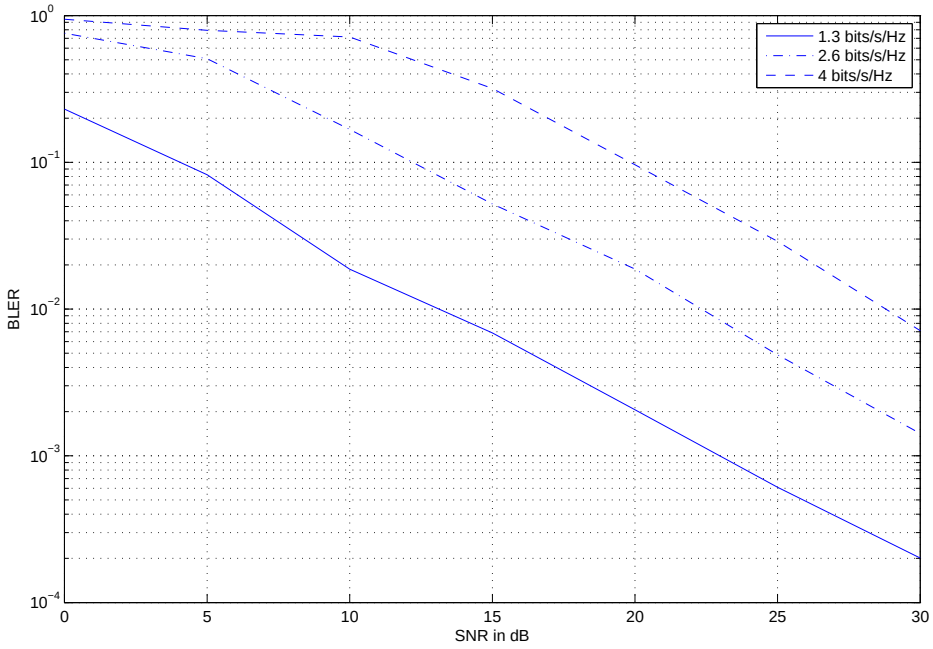

Figure 2.15: Simulation results of AF spatial multiplexing with sphere decoder for QPSK, 16-QAM and 64-QAM relays 0.5 from the source.

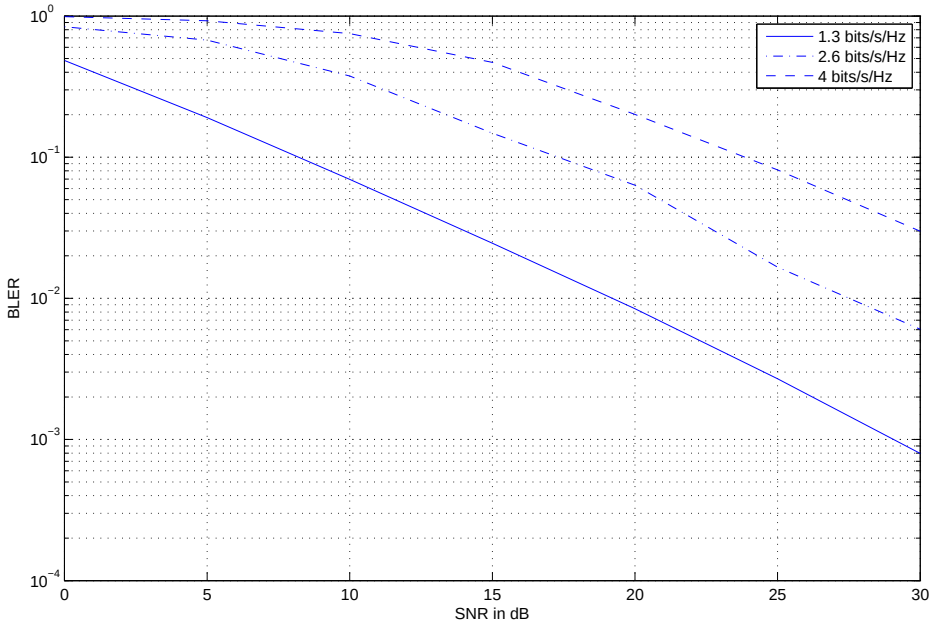

Figure 2.16: Simulation results of AF spatial multiplexing with sphere decoder for QPSK, 16-QAM and 64-QAM relays 0.7 from the source.

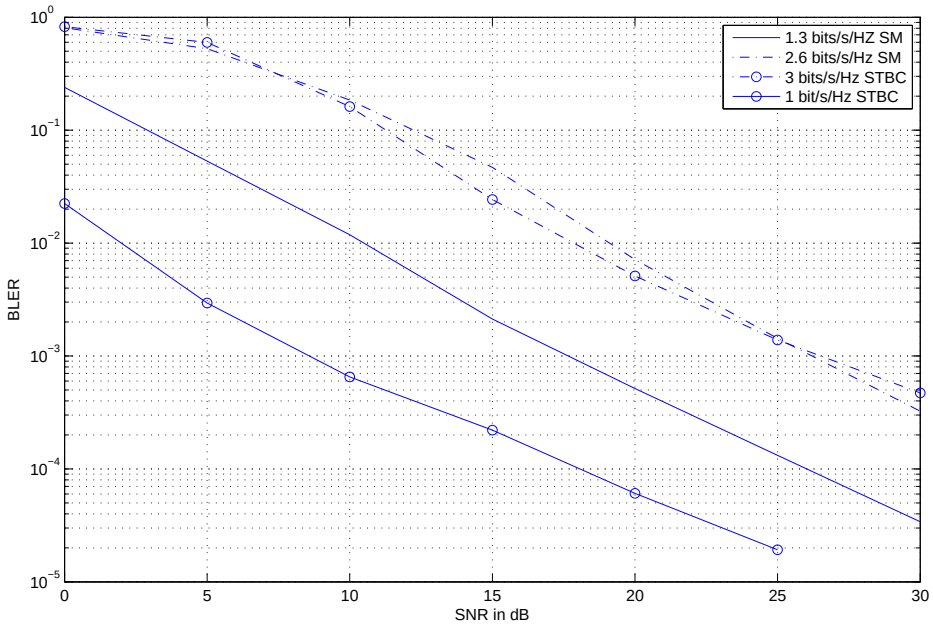

Figure 2.17: Comparing between AF non-orthogonal STBC and spatial multiplexing relays 0.3 from the source.

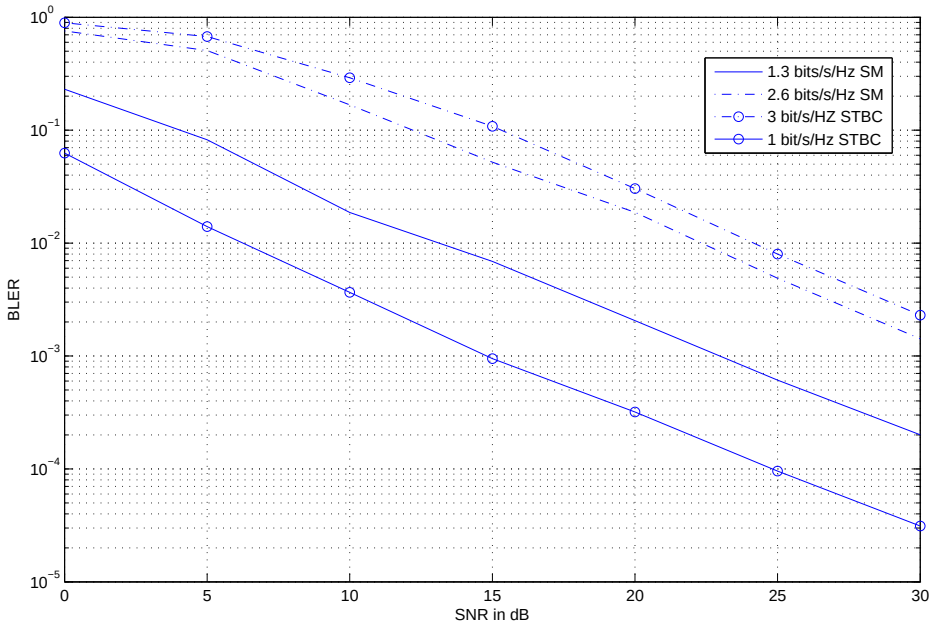

Figure 2.18: Comparing between AF non-orthogonal STBC and spatial multiplexing relays 0.5 from the source.

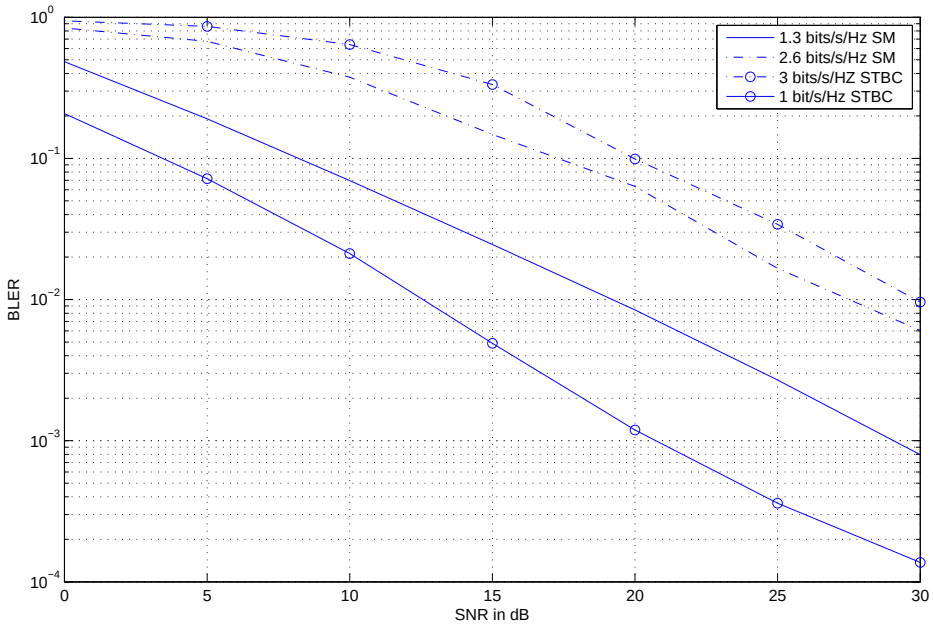

Figure 2.19: Comparing between AF non-orthogonal STBC and spatial multiplexing relays 0.7 from the source.

2.5 Chapter Conclusions

In this chapter, we investigate the performance of uplink cooperative Spatial Multiplexing and non-orthogonal STBC MIMO using Amplify-and Forward (AF) relays. The analytical results match the simulation results. We evaluate the system performance in terms of several physical parameters such as distance, modulation type, and number of hops. The gain, as we increase hops or relays, becomes limited because the noise and interference are also amplified along with the signal. Hence, performance does not enhance in proportion with the hop increase.

CHAPTER 3

VIRTUAL MIMO RELAYING BASED ON DETECT-SPLIT-FORWARD (DSF)

In the previous chapter, different schemes of uplink virtual spatial multiplexing and non-orthogonal STBC using AF were evaluated. Both simulations and analysis were conducted to evaluate the performance of the systems in terms of several physical parameters such as distance, modulation type, number of relays and number of hops. In this chapter, another vMIMO scheme, the detect-split-forward (DSF), is evaluated with different MIMO schemes such as V-BLAST and STBC to show the trade-off between using spatial multiplexing and increasing the diversity order in vMIMO systems. The performance of DSF is examined by simulation, analysis and comparison of the results with DSF using V-BLAST. Also, a formula for the average capacity of both DSF-STBC and DSF-V-BLAST is derived.

The rest of the chapter is organized as follows: The system model is described in the next section. In Sections 3.2 and 3.3, the BLER and the average capacity of the DSF-STBC and DSF-V-BLAST systems are analyzed. Simulation results are presented in Section 3.4

and Section 3.5 present's the chapter's conclusions.

3.1 System Model

The system configuration setup can be described as follows: $1 \times R_N \times M_R$ where 1 indicates a single user, R_N is number of relays at each hop and M_R is, total receiving antennas at the destination. The source data symbol (x) is sent in several time slots based on the number of relays and hops. At the first time slot, the source sends the data symbol then all relays detect the data and split them as a 2^m-ary symbol representing m bits $b_1, b_2, ...b_m$ to N relays $R_1, R_2, ..., R_N$ with symbol average energy $E_s = E[|x|^2]$, and a rates of $1/T$ symbols per second. For the example shown in Figure 3.1 the relay will receive the following signals

$$Y_{R_1} = h_{SR_1}x + n_{R_1} \tag{3.1}$$

$$Y_{R_2} = h_{SR_2}x + n_{R_2}. \tag{3.2}$$

At the last time slot (last hop), all the relays send their data simultaneously in a vMIMO scheme. Different vMIMO schemes for the last forwarding hop are described in the following sections:

3.1.1 DSF Using the V-BLAST Scheme

The DSF scheme [26] detects the signal, splits it then forwards it to the next relay as shown in Figure 3.1. Figure 3.2 shows that each of the relays, illustrated in Figure 3.1, sends part of the received signal which allows a higher rate of transmission.

For example, the source sends 16-QAM symbol x then the relays split the detected signals as illustrated in Figure 3.6. In the last time slot, all relays forward the new symbols to the destination simultaneously as in (3.4)

$$\begin{pmatrix} Y_{D_1} \\ Y_{D_2} \end{pmatrix} = \begin{pmatrix} h_{R_1D_1} & h_{R_2D_1} \\ h_{R_2D_2} & h_{R_1D_2} \end{pmatrix} \begin{pmatrix} \hat{x}_1 \\ \hat{x}_2 \end{pmatrix} + \begin{pmatrix} n_{D_1} \\ n_{D_2} \end{pmatrix}. \tag{3.3}$$

The destination using V-BLAST with the successive interference cancellation (SIC) algorithm performs nulling, based on zero forcing (ZF), cancelation and ordering.

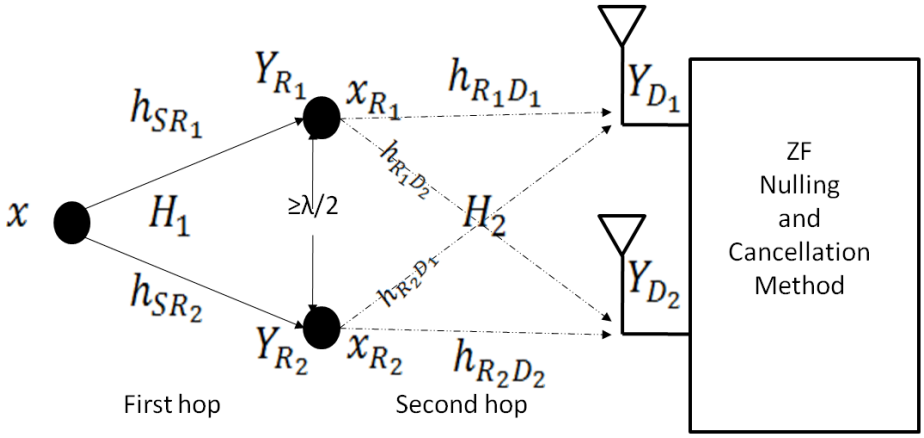

Figure 3.1: DSF-V-BLAST system model $1 \times 2 \times 2$.

3.1.2 DSF Using the STBC Scheme

In this section, we propose a new vMIMO scheme based on the STBC. This system model is built on the DSF scheme proposed but with the forwarding scheme being STBC as shown in Figure 3.3. Figure 3.4 shows that each relay transmits the same number of bits it receives (encoded into new symbols) in order to increase redundancy for error control.

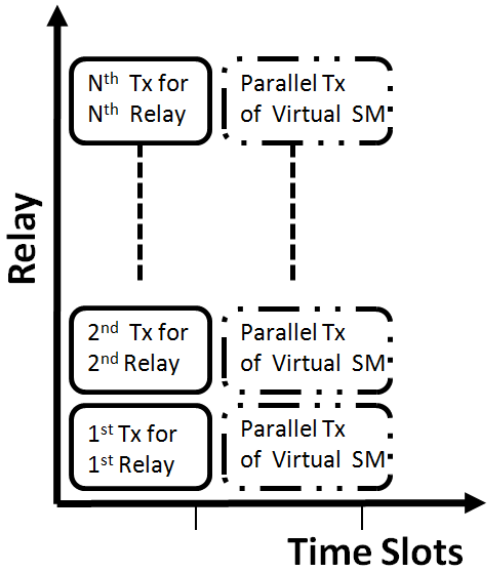

Figure 3.2: Time slotting in DSF-V-BLAST scheme.

In the first time slot, the symbol is broadcasted to the relays that detect,split and forward it with lower modulation. If the source sends 64-QAM symbol (x) to a hop that contain two relays: then the second and third time slots become the STBC transmission. The received signals on the last hop could be expressed as:

$$\begin{pmatrix} Y^2_{D_1} \\ Y^2_{D_2} \\ Y^{3*}_{D_1} \\ Y^{3*}_{D_2} \end{pmatrix} = \begin{pmatrix} h^2_{R_1D_1} & h^2_{R_1D_2} \\ h^2_{R_2D_1} & h^2_{R_2D_2} \\ h^{3*}_{R_1D_1} & -h^{3*}_{R_1D_2} \\ h^{3*}_{R_2D_1} & -h^{3*}_{R_2D_2} \end{pmatrix} \begin{pmatrix} \hat{x}_1 \\ \hat{x}_2 \end{pmatrix} + \begin{pmatrix} n^2_{D_1} \\ n^2_{D_1} \\ n^{3*}_{D_1} \\ n^{3*}_{D_1} \end{pmatrix}. \tag{3.4}$$

where $Y^t_{D_i}$ is the received signal at time slot t and antenna destination D_i, $h^t_{R_nD_i}$ is the channel from the relay R_n and destination at tim slot t.

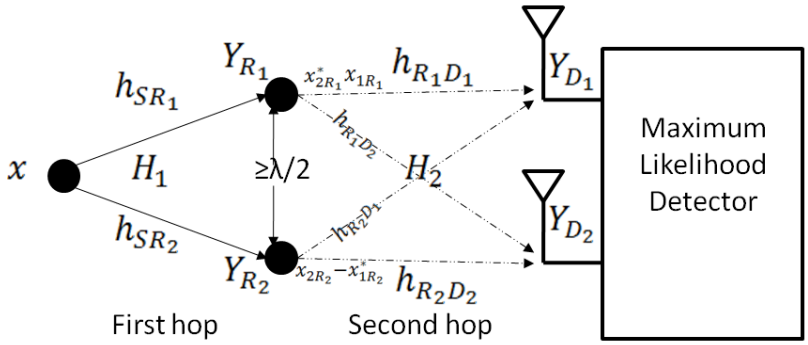

Figure 3.3: DSF STBC system model $1 \times 2 \times 2$.

3.1.3 A Hybridization system

V-BLAST and STBC manifest the well-known tradeoff between diversity and spatial multiplexing. Such tradeoff can be exploited by making a hybrid system that adaptively switches between the two systems. We propose a technique by which the relays determine the best scheme to use based on their distances from the source.

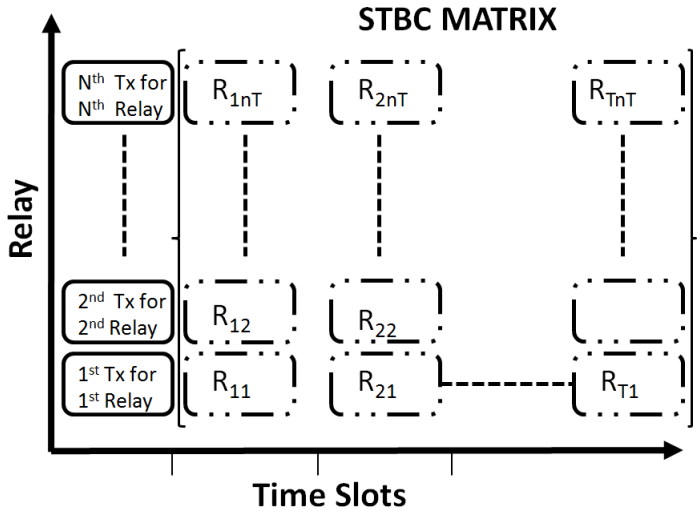

Figure 3.4: Time slotting in DSF STBC scheme.

3.2 Performance Analysis

3.2.1 DSF Using the V-BLAST Scheme

To calculate the block error rate (BLER) for the DSF V-BLAST scheme, we have to analyze the detection process (shown in Figure 3.5) on each hop. The symbol error rate (SER) at each relay after the detection and splitting process will be [33]

$$P_{e,R_n} = \left(\frac{M-1}{M}\right)\left(1-\sqrt{\frac{1.5\gamma_R}{M^2-1-3\gamma_R}}\right), \tag{3.5}$$

for $n = 1, 2, ..., N$ where $M = 2^{(\frac{m}{N})}$ M is the new cardinality of the signal set after spliting it and γ_R denotes the average SNR at each relay per symbol. The BLER at the first hop will be

$$P_{B,H_1} = 1-(1-P_{e,R_n})^2. \tag{3.6}$$

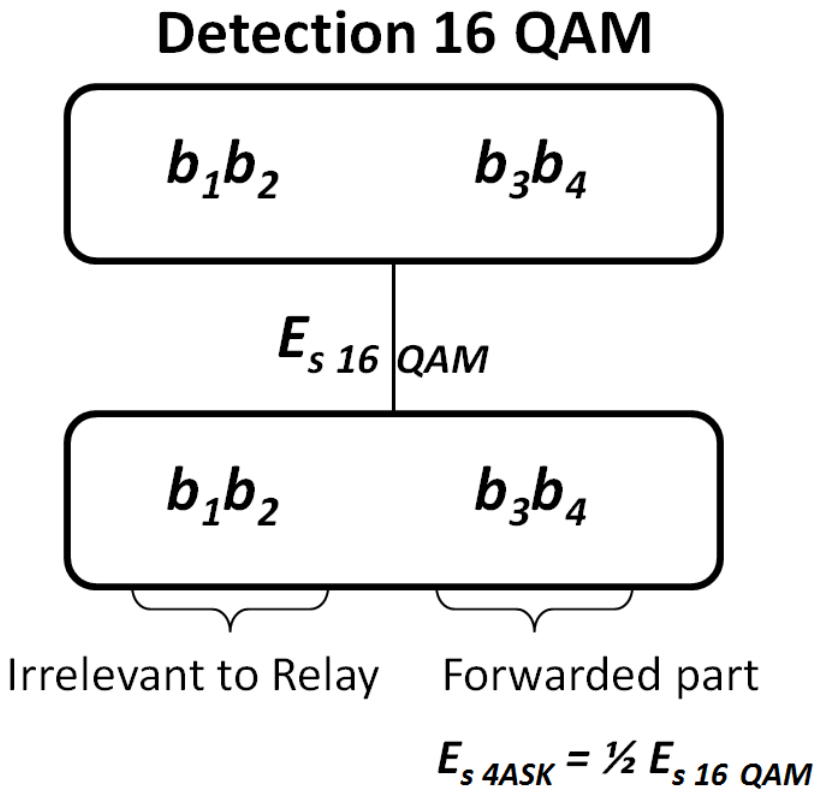

Figure 3.5: Detection process at each relay.

At the second hop, the symbol error probability for the l^{th} layer M-QAM over Rayleigh fading channels ($P_{e,i}$) can be calculated from Equation 2.19. Then, the total BLER at the destination will be

$$P_B = 1 - (1 - P_{B,H_1})(1 - P_{B,H_2}), \tag{3.7}$$

where P_{B,H_1} is the BLER probability of the first hop and P_{B,H_2} is the BLER probability of the second hop.

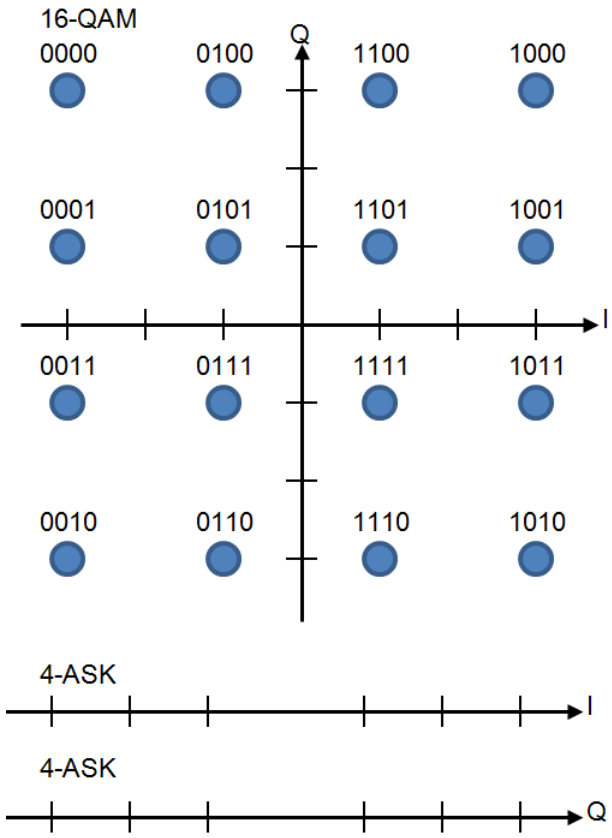

Figure 3.6: Splitting 16-QAM to two 4-ASK.

3.2.2 DSF Using the STBC Scheme

To calculate the BLER for the DSF scheme using STBC, we have to analyze the detection process (illustrated in Figure 3.7) at each hop. For example if we have a two relay system that sends 2 $bit/s/Hz$, then the Ms will send 64-QAM symbol at the first hop (as shown in Figure 3.8), and the two relays will detect the same symbol, split it and resend it with a lower modulation scheme to the base station or to the destination. For the M-QAM STBC, we use (2.14) to calculate SER at the second hop with a diversity order $M_R \cdot R_n$ and with one layer $(L = 1)$. Then, $P_{B,H_2} = P_{e,1}$ at $D = M_R \cdot R_N$. Finally we use (3.7) to find the total BLER.

3.3 Capacity Analysis

Early capacity analysis [1] of single-input single output (SISO) flat Rayleigh fading channels showed that the channel capacity in bps/Hz can be expressed as:

$$C_{SISO} = E_h\{\log_2(1 + \gamma_R|h|^2)\}, \tag{3.8}$$

where $E_h\{\cdot\}$ is the expectation operator with respect to the channel coefficient h, which is a complex Gaussian random variable with zero mean and a variance of 0.5 per dimension, and SNR is the average signal-to-noise-ratio for each receiving antenna. This is often called the ergodic capacity [1]. For a given h, there is only one way to increase the capacity of the SISO channel and that is by increasing SNR. Also, the capacity increases logarithmically with increasing SNR.

The instantaneous capacity of V-BLAST with R_N relays and with ZF interference nulling and serial cancelation is given by [31]

$$C_{V-BLAST}^{ZF} = R_N.min_{n=1,2,...,R_N}\{\log_2(1 + \frac{\gamma_D}{R_N\|W_{ZF,i}\|_F^2})\}, \tag{3.9}$$

where $W_{ZF,i}$ is the ZF projection vector of the R_N^{th} relay, γ_D is the SNR per receive antenna, and $\|(\cdot)\|_F^2$ is the squared Frobenius norm.

Furthermore, the instantaneous capacity of an orthogonal STBC of rate r_c and R_N relays is [34]

$$C_{STBC} = r_c\{\log_2(1 + \frac{\gamma_D}{R_N}\|\mathbf{H}\|_F^2)\}. \tag{3.10}$$

To derive a formula for the capacity of DSF for V-BLAST and STBC, the instantaneous capacity of the system is determined by the weakest link. DSF consists of two SISO channels and one MIMO channel. The second MIMO hop can be either V-BLAST or STBC. The instantaneous capacity of DSF using V-BLAST can be calculated from

$$C_{DSF-V-BLAST} = \frac{\min\{C_{SISO1}, C_{SISO2}, C_{V-BLAST}^{ZF}\}}{N_H}, \tag{3.11}$$

and the capacity of DSF using STBC

$$C_{DSF-STBC} = \frac{\min\{C_{SISO1}, C_{SISO2}, C_{STBC}\}}{N_H}, \tag{3.12}$$

where N_H is the total number of hops.

3.4 Numerical Results

3.4.1 DSF Using the V-BLAST Scheme

Table 3.1: DSF vMIMO for $1 \times 2 \times 2$ relays

Number of time slots	Modulation type	Spectral efficiency
2	QPSK	1
2	16-QAM	2
2	64-QAM	3
2	256-QAM	4

In this section, we illustrate the numerical results of vMIMO using the DSF-V-BLAST scheme. Figure 3.9 shows the BLER performance of $1 \times 2 \times 2$ relays cMIMO with different modulation as shown in Table 2. The analytical results match the simulation results. In Figure 3.10, a gain of 2 dB is obtained as the number of relays doubled from 2 to 4. At a fixed SNR, we evaluate the performance of the system with different relay locations and the best place for the relay is at the center between the source and the destination as shown in Figure 3.11. Figure 3.12 compares the block error rate of a DSF-V-BLAST vMIMO system employing 16-QAM modulation. The Figure compares the analytical results obtained for the DSF-V-BLAST vMIMO for 16-QAM. The BLER for the first hop is found and sent as QPSK in the second hop. The total BLER performance is shown in Figure 3.12. The simulation matches the proposed analysis methods at each hop. Figure 3.10 compares the symbol error rate of a DSF-V-BLAST vMIMO system with different numbers of relays and receive antennas. The transmitter sends the 256-QAM symbols on two, four and eight relays. It is clear that increasing the number of relays will improve the performance since it will lower the modulation techniques from 16-QAM to QPSK to BPSK, a

fact that leads to a better error probability curve versus SNR. At a fixed SNR, we evaluate the performance of the system with different relay locations and the ultimate place for the relay is the center between the source and the destination as shown in Figure 3.11.

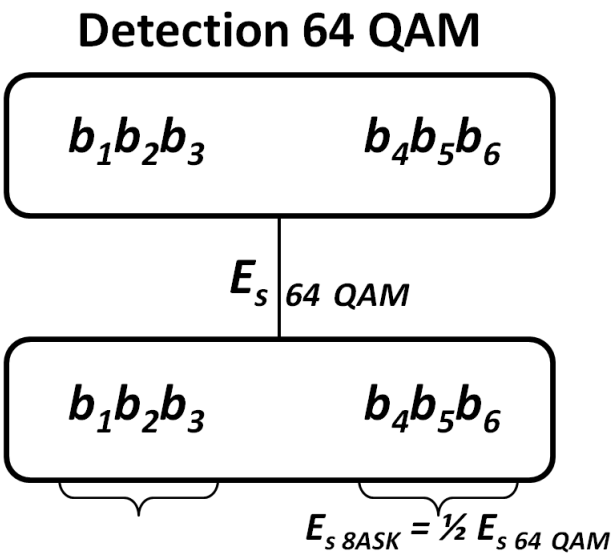

Figure 3.7: Detection process at each relay.

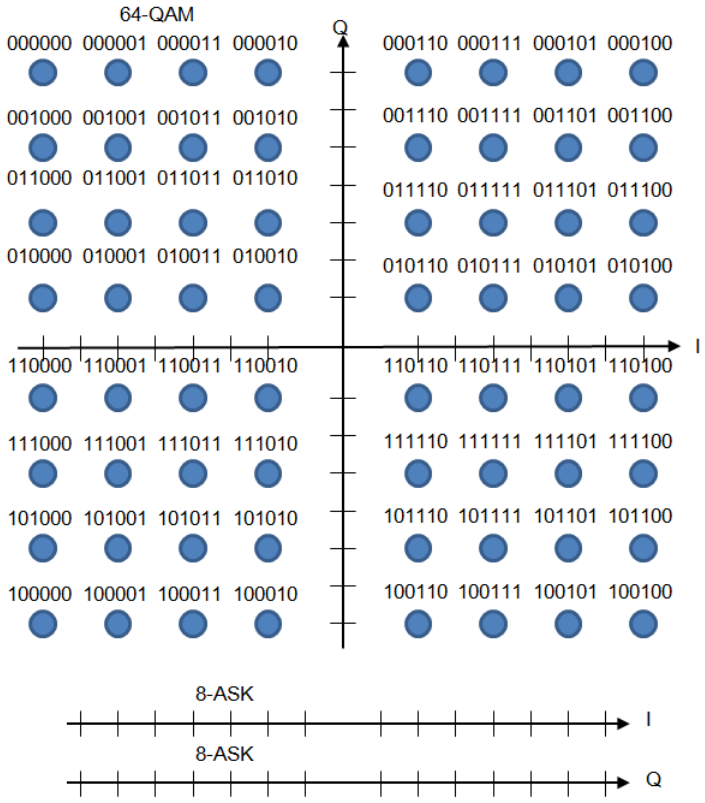

Figure 3.8: Splitting 64-QAM to two 8-ASK.

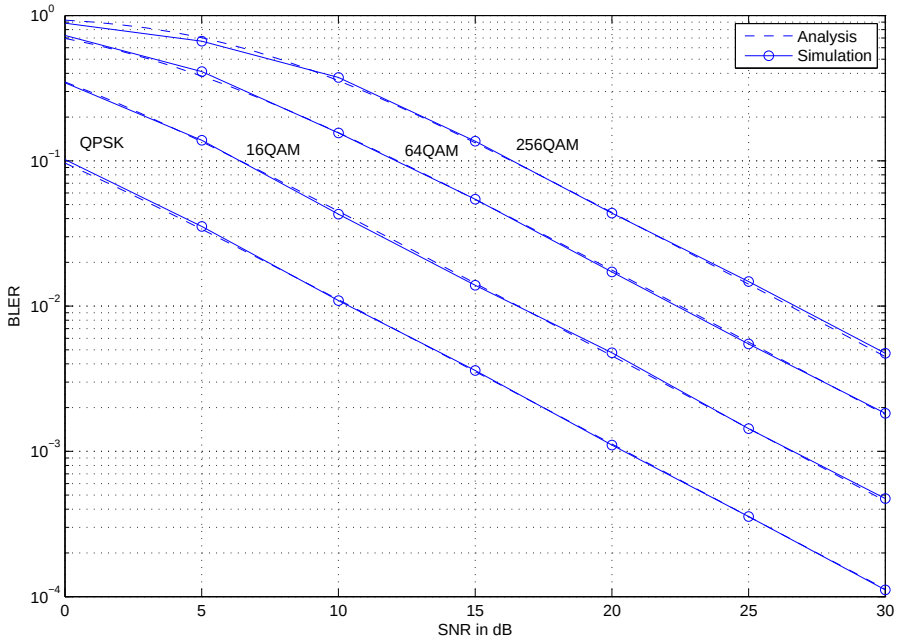

Figure 3.9: Simulation and analysis results of DSF-V-BLAST vMIMO for $1 \times 2 \times 2$ relays
.

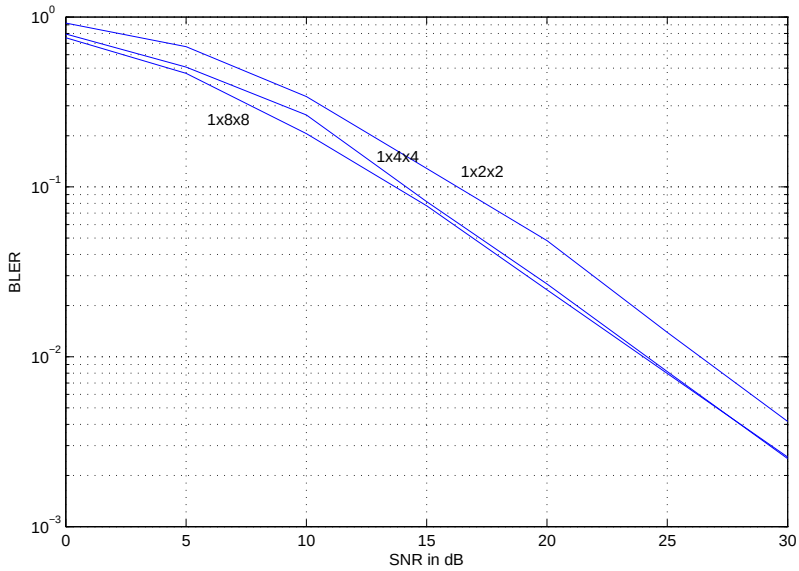

Figure 3.10: 256-QAM with different relaying setting of DSF-V-BLAST vMIMO.

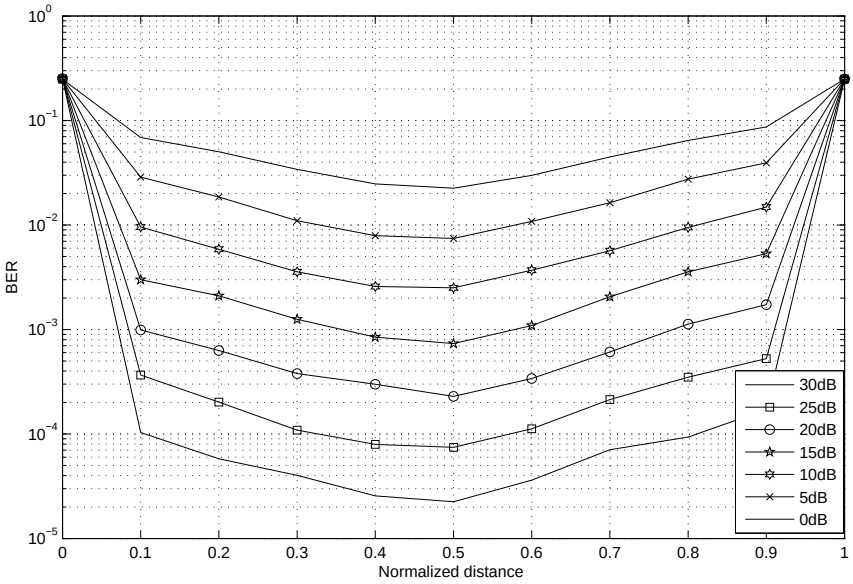

Figure 3.11: BER performance various source-relay distances for DSF V-BLAST.

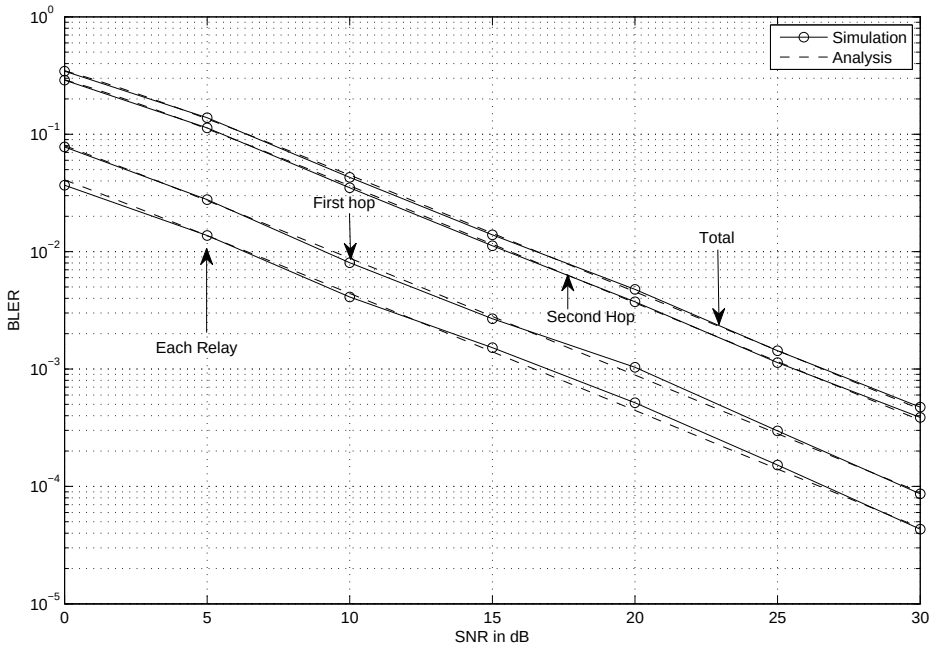

Figure 3.12: Simulation and analysis results of DSF V-BLAST for 16-QAM.

3.4.2 DSF Using the STBC Scheme

Table 3.2: DSF vMIMO with STBCfor $1 \times 2 \times 2$ relays

Number of time slots	Modulation type	Spectral efficiency
3	QPSK	0.66
3	16-QAM	1.33
3	64-QAM	2
3	256-QAM	2.66

Figure 3.13 compares the block error rate of a DSF-STBC vMIMO system with different modulation techniques 64-QAM and 256-QAM and relays are at distance 0.3 from the source. The Figure compares the analytical results obtained for the DSF-STBC vMIMO to those obtained from the simulation it is clear that the Monte Carlo simulation matches the analysis methods, which demonstrates the validity of the proposed analysis. Figures 3.14 and 3.15 similarly compare the block error rate of a DSF-STBC vMIMO system with different modulation techniques and relays at distances 0.5 and 0.7 from the source. Figure 3.16 compares the block error rate of a DSF-STBC vMIMO system with different relay locations from the source with 64-QAM. The closer to the source, the better the performance.

At certain SNR, we evaluate the performance of the system with different relay locations as in Figure 3.17. Figure 3.18 compares the channel average capacity of a DSF-STBC vMIMO system with different relay locations from the source. The closer to the source, the better the performance.

At certain SNR, we evaluate the performance of channel capacity with different relay locations and the best place for relays to support higher channel capacity is when the relays are in the range 0.2 and 0.5.

Figure 3.20 shows a comparison between DSF-STBC and DSF-V-BLAST in terms of

the BLER error rate. To get fair comparison between both systems, we use 64-QAM for the DSF-STBC and 16-QAM for the DSF-V-BLAST. The total bit rate for both systems are 2 bit/s/Hz using a total number of transmit antennas, N_T = 1, 2 relays set up at 0.3 from the source and the receiver is equipped with 2 antennas. The results show that there is a gain of 2 dB over DSF-V-BLAST.

Figure 3.21 shows a comparison between DSF-STBC and DSF-V-BLAST in terms of the BLER error rate. To get fair comparison between both systems, we use 64-QAM for the DSF-STBC and 16-QAM for the DSF-V-BLAST. The total bit rate for both systems are 2 bit/s/Hz using a total number of transmit antennas, N_T = 1, 2 relays set up at 0.5 from the source and the receiver is equipped with 2 antennas. The results show that there is a gain 5 dB over DSF-STBC.

Figure 3.22 shows a comparison between DSF-STBC and DSF-V-BLAST in terms of varying the relay locations. When the relays are closer to the source, the DSF-STBC performs better than DSF-V-BLAST. However, when the relays are placed farther than 0.4, the DSF-V-BLAST performs with a noticeable gain over DSF-STBC. From this result we propose to design a hybrid system where the relays use adaptive techniques to determinate the best scheme to use based on distances from the source as shown in Figure **??**

Figure 3.24 compares the channel average capacity of a DSF-STBC system and a DSF-V-BLAST system with relay locations at d=0.3 from the source. As we can notice when the relays are located close enough to the source the average channel capacity for DSF-V-BLAST becomes higher than DSF-STBC.

Figure 3.25 compares the channel average capacity of a DSF-STBC system and a DSF-

V-BLAST system with relay locations at d=0.7 from the source. As we can notice, when the relays are located farther from the source the average channel capacity for both DSF-V-BLAST and DSF-STBC will get same results.

As stated in the capacity analysis section, our system consists of SISO and MIMO channels, so at certain distances the SISO channel will dominate the overall channel capacity. Figure 3.26 shows that at distances greater than d=0.5 the DSF-V-BLAST channel capacity will perform the same as the DSF-STBC since both systems are dominated by the weakest channel, which is the SISO.

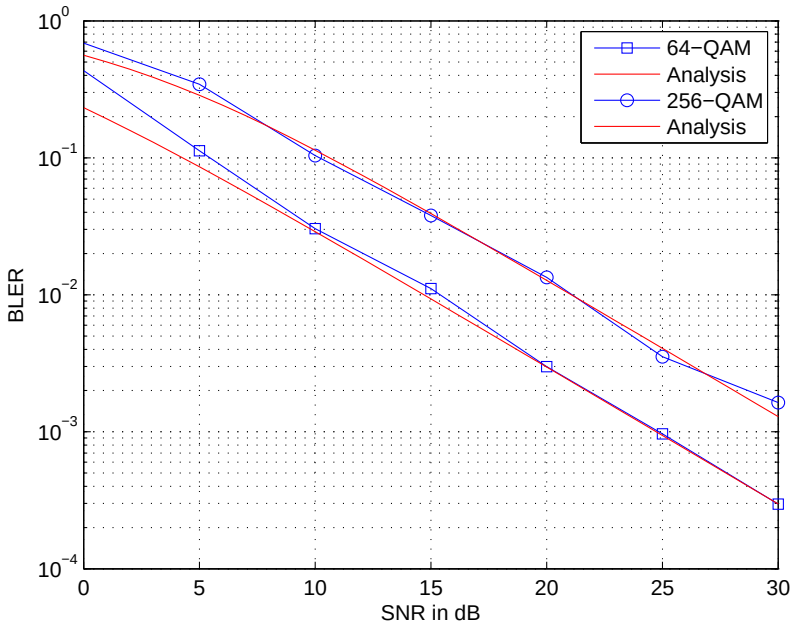

Figure 3.13: Simulation and analysis results of DSF with STBC for 64-QAM and 256-QAM relays 0.3 from the source.

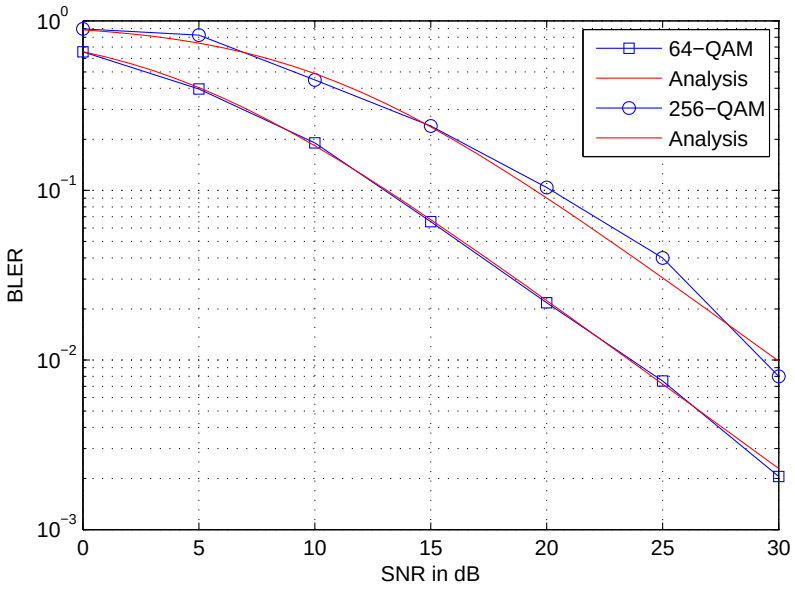

Figure 3.14: Simulation and analysis results of DSF with STBC for 64-QAM and 256-QAM relays 0.5 from the source.

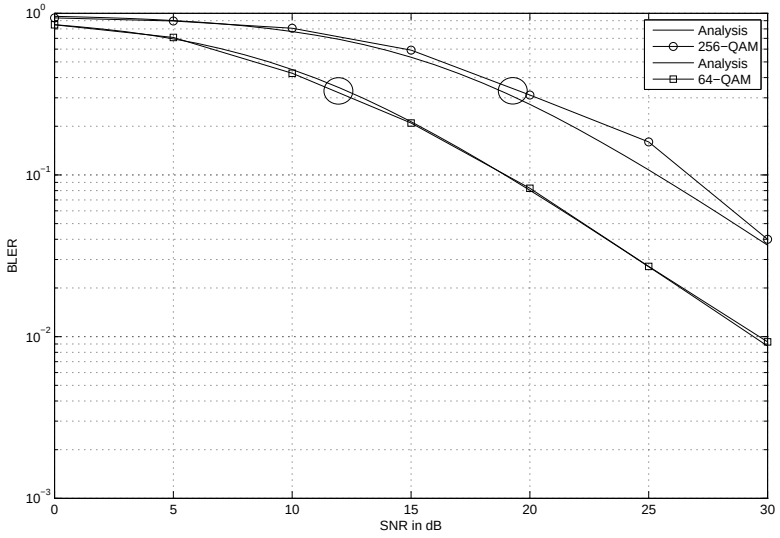

Figure 3.15: Simulation and analysis results of DSF with STBC for 64-QAM and 256-QAM relays 0.7 from the source.

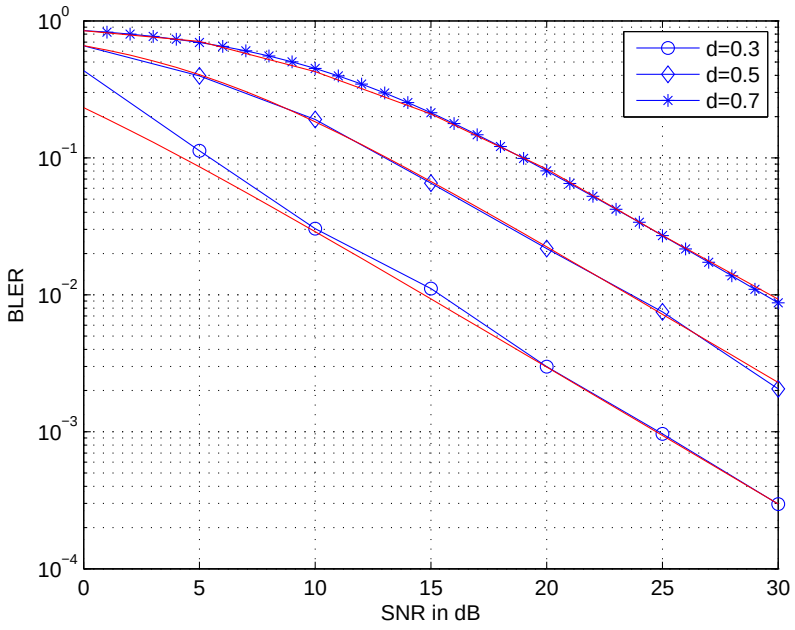

Figure 3.16: 64-QAM with different relay location of DSF-STBC vMIMO for $1 \times 2 \times 2$ relays.

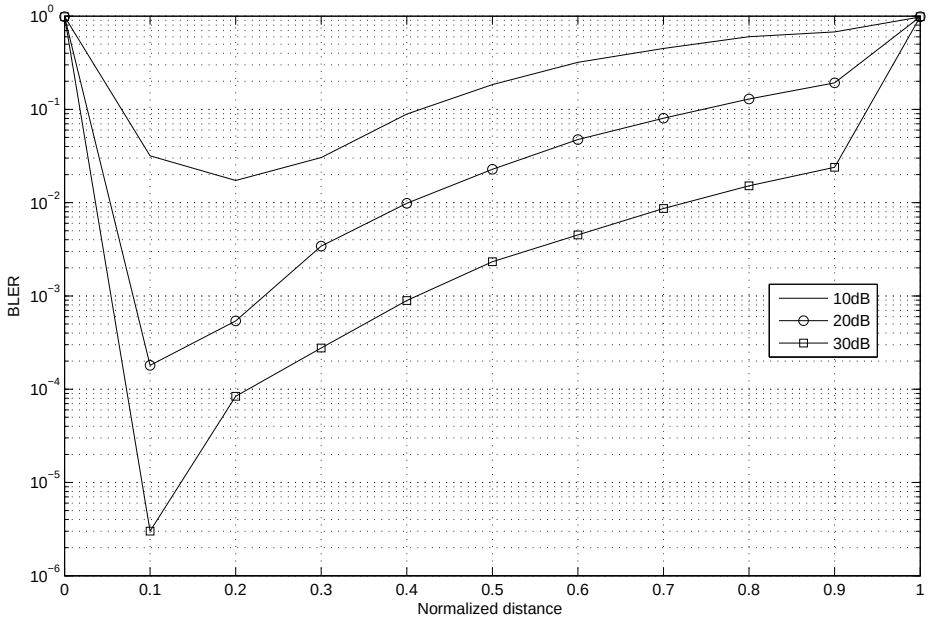

Figure 3.17: BLER performance various source-relay distances for DSF using STBC.

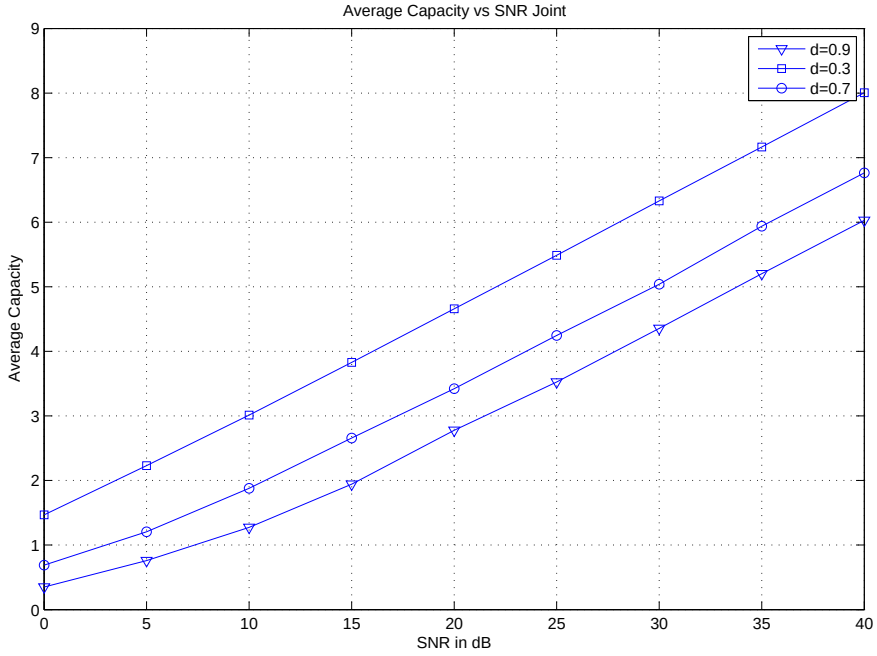

Figure 3.18: Average capacity with various source-relay distances for DSF using STBC.

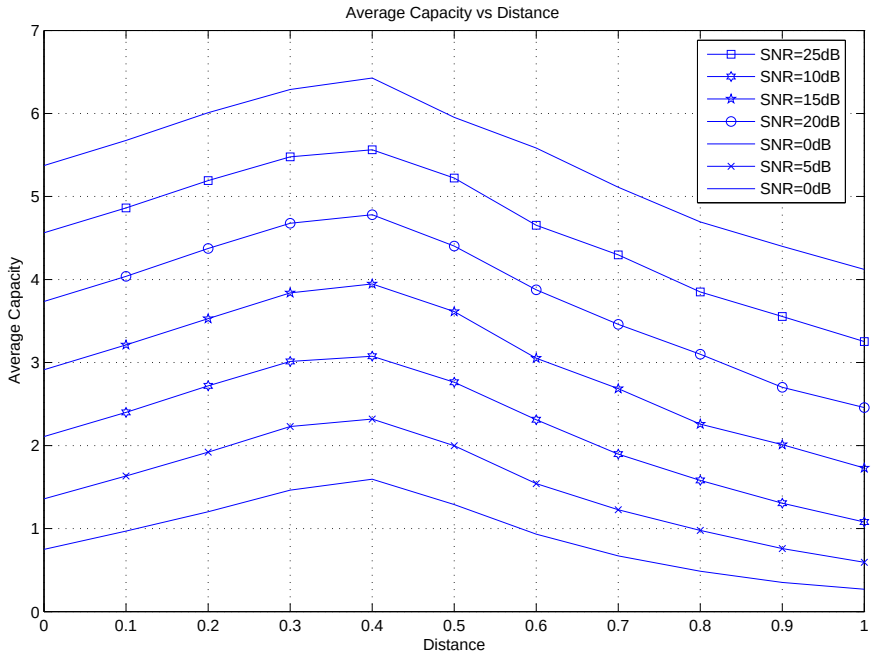

Figure 3.19: Average capacity with various source-relay distances for DSF using STBC at certain SNR value.

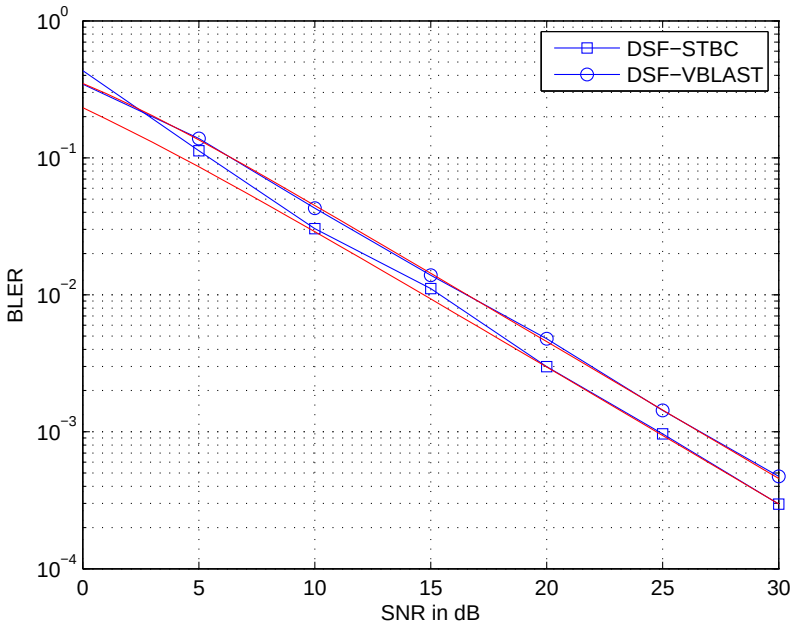

Figure 3.20: Comparing BLER performance for DSF using STBC and V-BLAST at d=0.3 from source-relay .

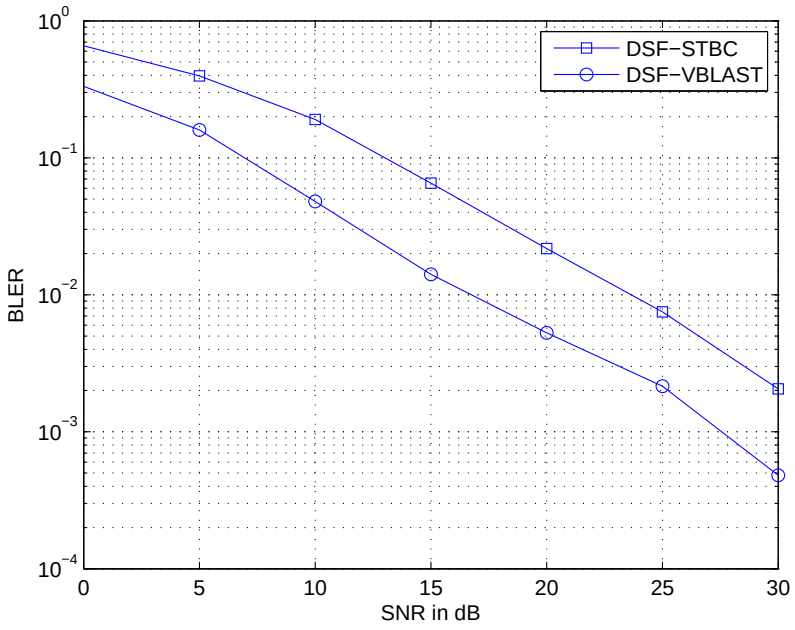

Figure 3.21: Comparing BLER performance for DSF using STBC and V-BLAST at d=0.5 from source-relay .

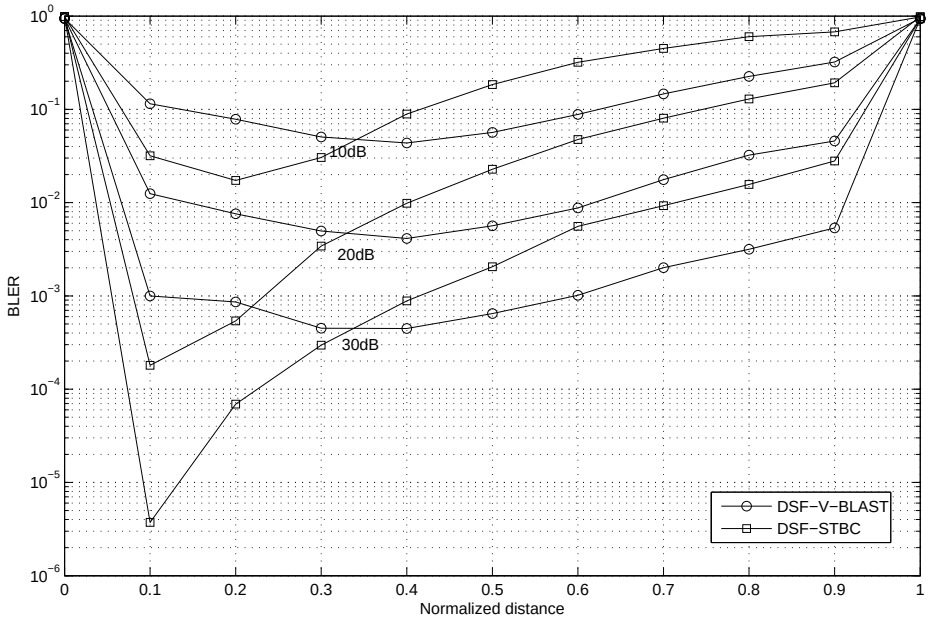

Figure 3.22: BLER performance for various source-relay distances of the DSF using STBC and V-BLAST.

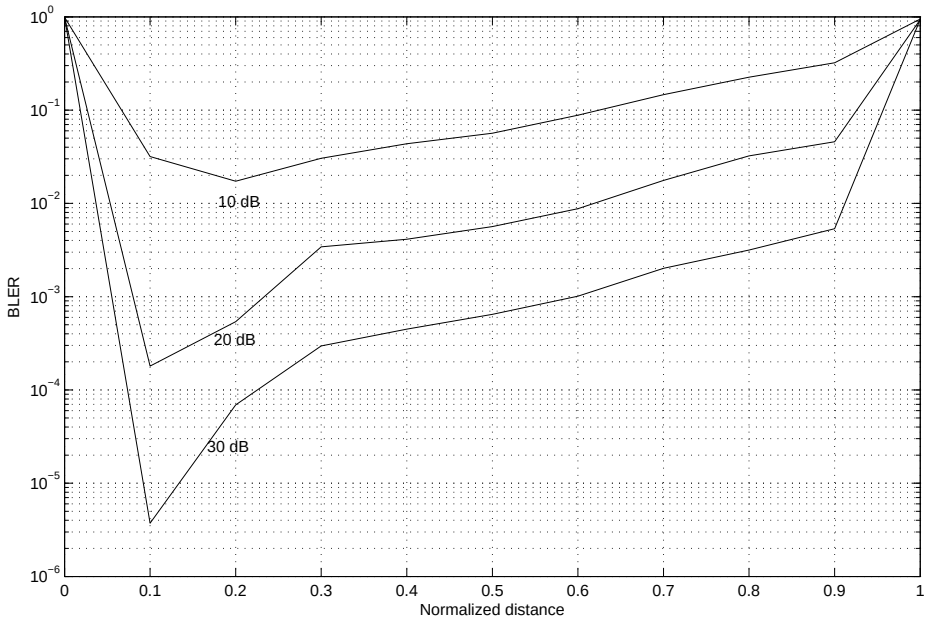

Figure 3.23: BLER performance for various source-relay distances of the hybrid vMIMO system for $1 \times 2 \times 2$ relays at 2 bit/s/Hz .

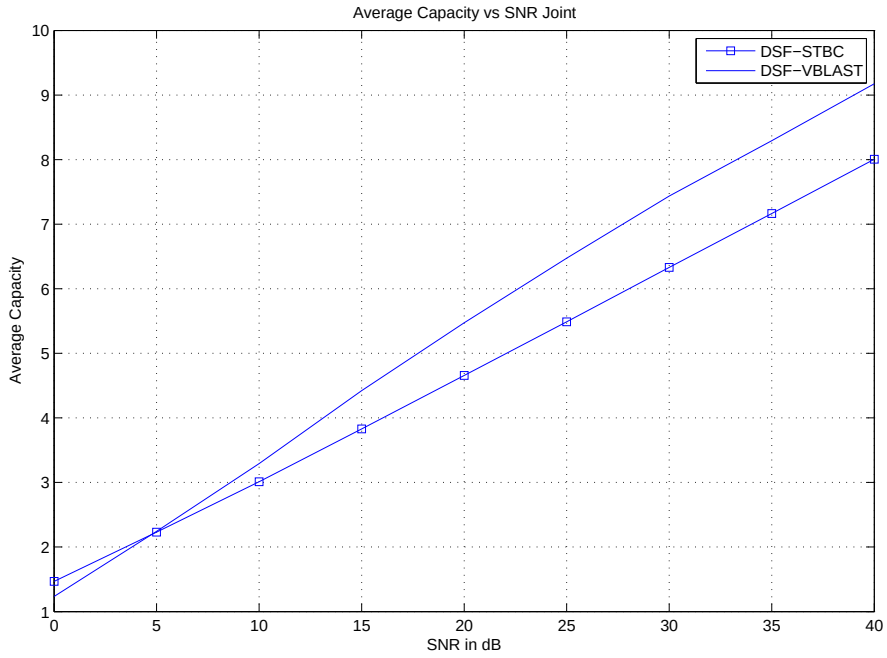

Figure 3.24: Average capacity with d=0.3 from source-relay for DSF using STBC and V-BLAST.

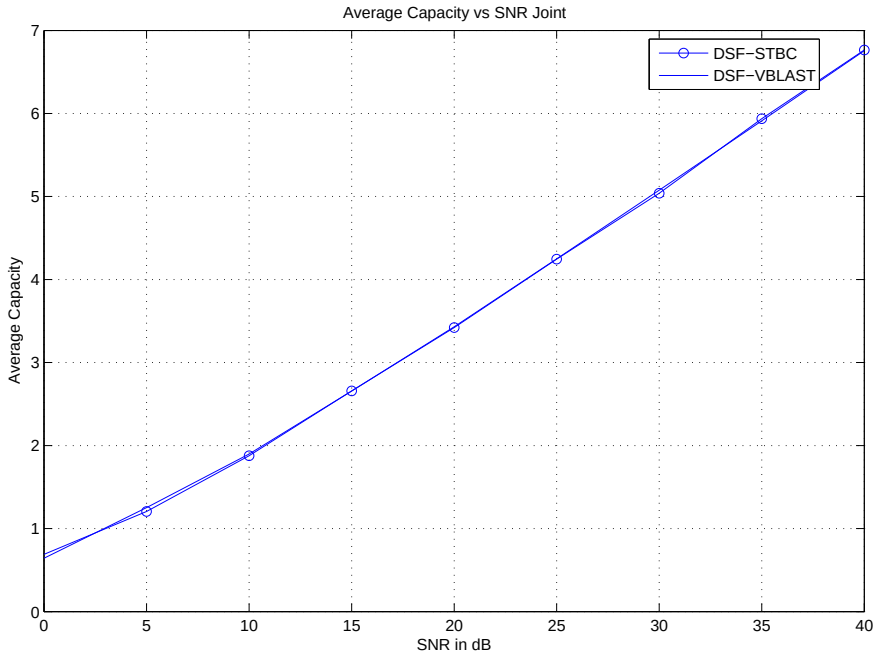

Figure 3.25: Average capacity with d=0.7 from source-relay for DSF using STBC and V-BLAST.

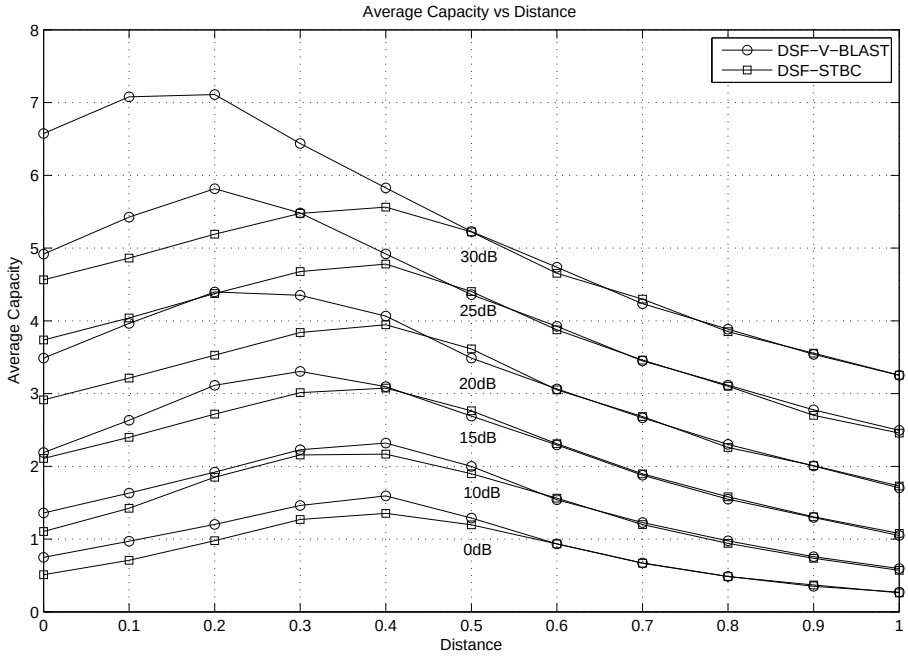

Figure 3.26: Average capacity with various source-relay distances for DSF-STBC and DSF-V-BLAST at certain SNR value.

3.4.3 Comparison Between the AF and the DSF V-BLAST Schemes

In this section, a fair comparison between AF vMIMO and DSF vMIMO is conducted. This fairness is achieved by structure and spectral efficiency fairness, that means that the total number of antennas at the transmitter and the relays is the same. In addition, the number of symbols sent every time-slot is the same for both systems.

Figure 3.27 shows a comparison between AF vMIMO and DSF vMIMO in terms of the BLER error rate. The two systems use a total number of transmit antennas, $N_T = 1$, and 2 relays and the receiver is equipped with 2 antennas. DSF vMIMO shows a 5 dB gain over AF vMIMO. The main reason for this gain is that the DSF lowers the modulation at the second hop and does not amplifying the noise.

Figure 3.28 shows a comparison between AF and DSF performances at fixed SNR's for relay locations.

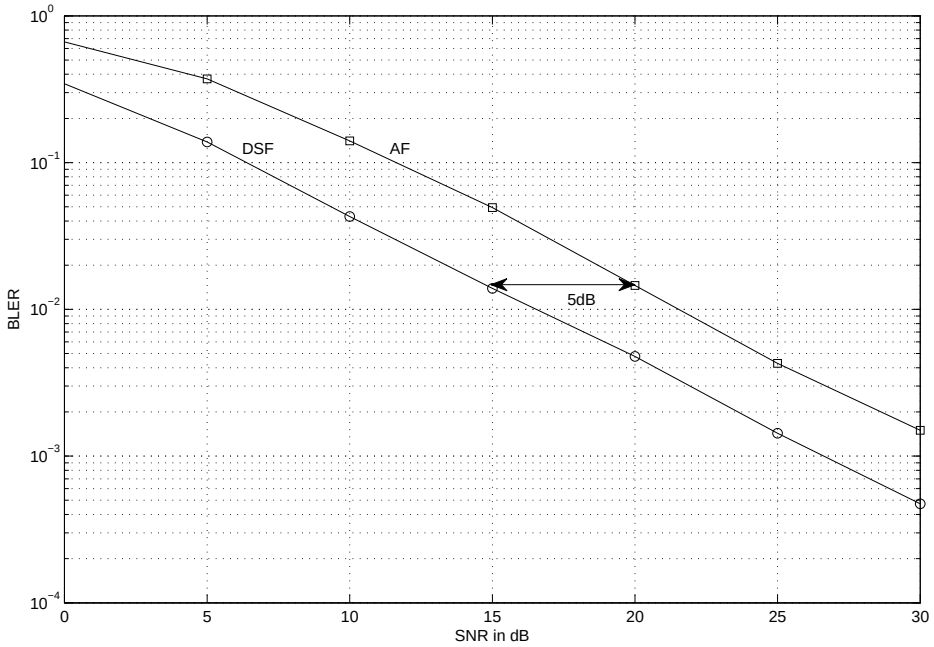

Figure 3.27: Comparing between AF and DSF .

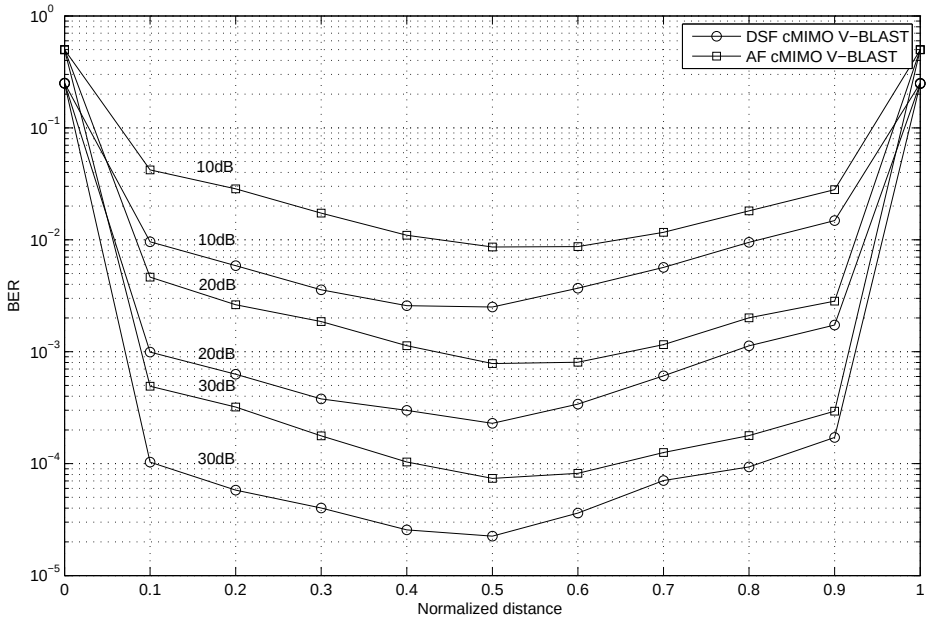

Figure 3.28: Comparing between AF and DSF source-relay distances.

3.5 Chapter Conclusions

In this chapter, we investigate the performance of uplink cooperative Spatial Multiplexing and STBC using the DSF scheme over MIMO relays. The analytical results match the simulation results. We evaluate the system performance in terms of several physical parameters such as distance, modulation type, and number of relays. DSF-V-BLAST vMIMO shows 5 dB gain over AF-V-BLAST vMIMO. The main reason for this gain is that DSF lowers the modulation at the second hop and controls the noise.

CHAPTER 4

MIMO RELAYING BASED ON SPATIAL MODULATION

As shown in the last two chapters, using a single antenna at the source eliminates the diversity order from the overall system performance. Another main effect is the capacity limitation caused by the single antenna at the Ms. As we conclude from Chapter 3, the SISO capacity will dominate over MIMO because after certain distance the weakest link will be SISO. In order to overcome the diversity order and capacity limitations, the source can be equipped with multi-antennas. This will allow us to introduce a relayed spatial modulation technique to guarantee the tradeoff between spatial multiplexing and diversity order.

The remainder of the chapter is organized as follows: The system model is described in the next section. In Sections 4.2 and 4.3 the BLER and average capacity of the relayed spatial modulation system are analyzed. Simulation results are presented in Section 4.4 and Section 4.5 presents the chapter's conclusions.

4.1 System Model

The general system model used in this chapter is shown in Figure 4.1. The relay is equipped with multi antenna. Several MIMO transmission techniques are used in this chapter: STBC, V-BLAST and SMod. The forwarding scheme is decode and forward. Relayed spatial modulation system model is described in Figure 4.2 where each antenna is used to transmit part of the information intended to be sent from the source. Then the relay detects the whole information block and forwards it the same way it was sent from the source.

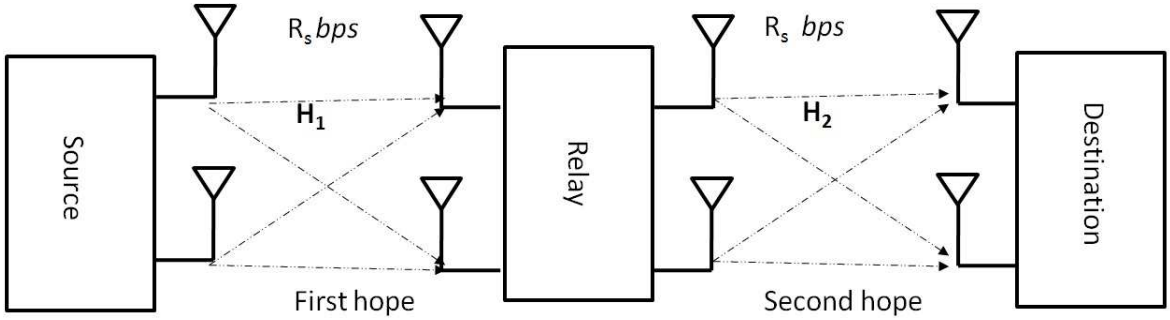

Figure 4.1: MIMO relayed system model.

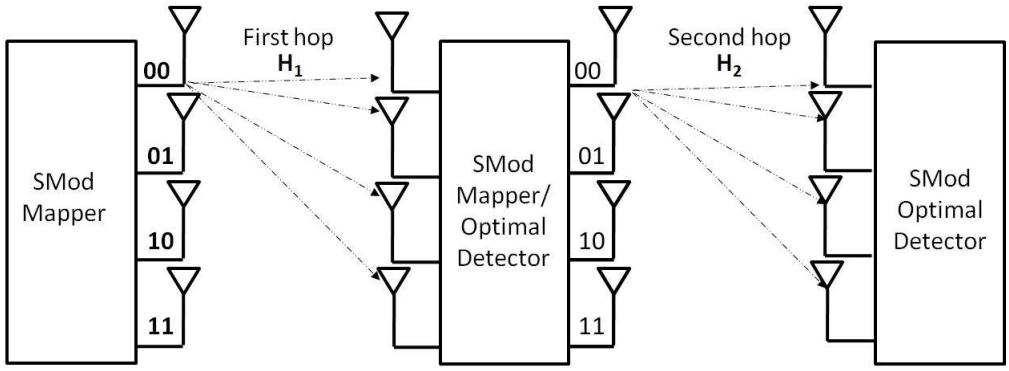

Figure 4.2: SMod relayed system model.

4.2 Performance Analysis

In this section, we derive the exact block-error probability analysis of MIMO relaying. Several MIMO transmission techniques are used in this chapter (STBC, V-BLAST and SMod) which employ M-QAM and M-PSK modulation schemes. In the analysis we consider the effect of errors propagating from the previous erroneous layers. We analyze the system assuming that the power is equally split among antennas at the transmitters.

4.2.1 MIMO V-BLAST Relaying

By applying Equation 3.7 to calculate the BLER of the MIMO V-BLAST relaying scheme, the BLER at each hop becomes:

$$P_{B,H_1} = 1 - \prod_{i=1}^{N_T}(1 - P_{e,i}), \tag{4.1}$$

where $P_{e,i}$ is the conditional symbol error probability of layer i (without error propagation) over Rayleigh fading channels.

4.2.2 MIMO STBC Relaying

For the MIMO STBC relaying scheme, performance analysis follows the same derivation done for V-BLAST considering the right diversity order and number of layers.

4.2.3 MIMO SMod Relaying

For SMod, the block consists of one symbol. Here, we use the modified derivation of [35] to analyze SER in order to get BLER at the first and second hop then substitute them in Equation 3.7. The SMod detector at each hop is responsible for two quantities: the active transmit antenna index and the transmitted symbol. The overall probability of symbol error is bounded by:

$$P_{B,H_i} \geq P_a + P_d - P_a P_d, \tag{4.2}$$

where P_a (as shown in equation 4.4) denote the symbol error probability of the transmit antenna index estimation given that the symbol is perfectly detected. and P_d (as shown in equation 4.3) is the symbol error probability of symbol given that the transmit antenna index is perfectly detected.

In SMod, only one antenna is active during transmission. Therefor, at any instant the $N_T \times M_R$ SMod model may be viewed as a $1 \times M_R$ SIMO configuration. In [36] Alamouti shows that Maximum likelihood detection (ML) is equivalent to an M_R branch MRRC of received signal followed by a regular symbol-by-symbol detection. The average symbol error rate of square M-QAM with MRRC reception over Rayleigh fading channels given by [[37], Eq.(15)] is:

$$P_d(\gamma_s) = \frac{a}{c}\{\frac{1}{2}(\frac{2}{b\gamma_s+2})^{M_R} - \frac{a}{2}(\frac{1}{b\gamma_s+1})^{M_R} + (1-a)\sum_{i=1}^{c-1}(\frac{S_i}{b\gamma_s+S_i})^{M_R} + \sum_{i=1}^{2c-1}(\frac{S_i}{b\gamma_s+S_i})^{M_R}\} \tag{4.3}$$

where $a = (1 - \frac{1}{\sqrt{M}})$, $b = \frac{3}{M-1}$, $m = \log_2(M)$, $S_i = 2\sin^2\theta_i$, $\theta_i = \frac{i\pi}{4n}$, M_R is the number of receive antennas,γ_s is the SNR per receive antenna and c is the number of

summations.

The symbol error probability of the transmit antenna index estimation is derived using the same approach of [38]. Given that the transmitted symbol is perfectly detected, the average SER of transmit antenna index estimation is union bounded by [[39], pp.261-262]

$$P_a \leq E_j[\sum_{\hat{j}} N(j,\hat{j}) P(x_{jq} \rightarrow x_{\hat{j}q})] \tag{4.4}$$

$$P_a = \sum_{j}^{N_T} \sum_{\hat{j}}^{N_T} \frac{N_T(M-1)P(x_{jq} \rightarrow x_{\hat{j}q})}{M}, \tag{4.5}$$

where $P(x_{jq} \rightarrow x_{\hat{j}q})$ denotes the pairwise error probability (PEP) of choosing signal vector $x_{\hat{j}q}$ given that x_{jq} was transmitted and $N(j,\hat{j})$ is the number of bits in error between transmit antenna index j and estimated transmit antenna index $\hat{j}$.

PEP can be computed as follows [[38], Eq. (6)]

$$P(x_{jq} \rightarrow x_{\hat{j}q}) = \int_{v=0}^{\infty} Q(\sqrt{v}) p_k(v)\, \mathrm{d}v, \tag{4.6}$$

where k has a known distribution then the closed form solution PEP and

$$P(x_{jq} \rightarrow x_{\hat{j}q}) = \mu_{\alpha}^{M_R} \sum_{w=0}^{M_R-1} \binom{M_R-1+w}{w} [1-\mu_{\alpha}]^w \tag{4.7}$$

and

$$P_a = \frac{N_T(M-1)\mu_{\alpha}^{M_R} \sum_{w=0}^{M_R-1} \binom{M_R-1+w}{w} [1-\mu_{\alpha}]^w}{M}. \tag{4.8}$$

where $\mu_\alpha = \frac{1}{2}(\sqrt{\frac{\gamma_s}{1+\gamma_s}})$

4.3 Capacity Analysis

4.3.1 MIMO V-BLAST Relaying

Similarly to the analysis presented in Section 3.3, the instantaneous capacity of relayed V-BLAST with K layers, with zero forcing interference nulling (ZF) and serial cancelation is determine by the weakest link, as in Equation 4.9:

$$C_{Relayed-V-BLAST} = \frac{min\{C^{ZF}_{V-BLAST_{H_1}}, C^{ZF}_{V-BLAST_{H_2}}\}}{N_H}. \tag{4.9}$$

4.3.2 MIMO STBC Relaying

For relayed STBC, the capacity is computed as:

$$C_{Relayed-STBC} = \frac{min\{C_{STBC_{H_1}}, C_{STBC_{H_2}}\}}{N_H}. \tag{4.10}$$

4.3.3 MIMO SMod Relaying

Capacity of spatial modulation is computed based on two quantities: the space shift keying C_{SSK} [[38], Eq(11)], and the single-input multiple-output (SIMO) scheme:

$$C_{SSK} = m - E_\theta[\log_2 \frac{\sum_{\acute{x}\epsilon\chi} p_Y(y \mid \acute{x}, H)}{p_Y(y \mid x, H)}], \tag{4.11}$$

where $m = \log_2(N_T)$, $\theta(x, y, H)$, and $p_Y(y \mid x, H)$ is given by:

$$p_Y(y \mid x, H) = \frac{\exp(-\|y - \sqrt{\gamma_s} H x_j\|^2_F)}{\pi^M_R}, \tag{4.12}$$

$$C_{SIMO} = E_h\{\log_2(1+\gamma_s)\ \sum_{i=1}^{M_R} |h_i|^2\}, \tag{4.13}$$

from the equations above, we obtain C_{SMod}:

$$C_{SMod} = C_{SIMO} + C_{SSK}, \tag{4.14}$$

Then, the overall relayed spatial modulation is determined by the weakest link:

$$C_{Relayed-SMod} = \frac{min\{C_{SMod_{H_1}}, C_{SMod_{H_2}}\}}{N_H}. \tag{4.15}$$

4.4 Numerical Results

In this section, the numerical results of different relayed MIMO schemes are shown. All sources, relays and destinations are equipped with multi-antenna. Different modulation schemes can be applied to obtain different spectral efficiencies as shown in Tables 4.1, 4.2 and 4.3.

Table 4.1: MIMO V-BLAST Relaying

Number of time slots	Modulation type	Spectral efficiency	Antenna configuration
2	QPSK	2	$2 \times 2 \times 2$
2	16-QAM	4	$2 \times 2 \times 2$
2	BPSK	2	$4 \times 4 \times 4$

Table 4.2: MIMO STBC Relaying

Number of time slots	Modulation type	Spectral efficiency	Antenna configuration
2	16-QAM	2	$2 \times 2 \times 2$
2	256-QAM	4	$2 \times 2 \times 2$
2	256-QAM	2	$4 \times 4 \times 4$

Table 4.3: MIMO SMod Relaying

Number of time slots	Modulation type	Spectral efficiency	Antenna configuration
2	8PSK	2	$2 \times 2 \times 2$
2	128-QAM	4	$2 \times 2 \times 2$
2	QPSK	2	$4 \times 4 \times 4$

Figure 4.3 compares the block error rate of a DSF-STBC and V-BLAST for a vMIMO system with rate 2 bits/s/Hz and relays at distance 0.3 from the source. With a MIMO relayed system, when the MIMO relay or vMIMO relays are close to the source (like this example) we get almost the same performance as for V-BLAST. However, MIMO relay STBC shows a very noticeable gain over DSF-STBC since there is diversity order at both hops.

Losing the diversity and spatial multiplexing gains is clearer when vMIMO relays are located far from the source and SISO channels dominate the overall performance. Figures 4.4 and 4.5 show the block error rate of a DSF of a vMIMO system and a MIMO relaying with rate 2 bits/s/Hz and relays at distances 0.5 and 0.7 from the source.

At fixed SNR's, we evaluate the performance of the system with different relay locations. From Figure 4.6, at low SNR and relays being very close to the source, vMIMO DSF-V-BLAST provides the best performance over a MIMO relay system. However, when the relays are placed beyond 0.3 from the source, MIMO STBC relay overcomes other relaying systems.

Figure 4.7 shows the performance of systems with different relay locations at high SNR value. Relays are very close to the source vMIMO DSF-V-BLAST provide better performance over MIMO V-BLAST relay and DSF-STBC systems. MIMO STBC relay overcomes on all other relaying systems.

The capacity of DSF-V-BLAST will be better than MIMO STBC relay. MIMO V-BLAST relay overcomes all other systems (since the two hops are MIMO multiplexing gain will be higher than vMIMO). As shown in Figure 4.8, relays are located at 0.3 of the distance from the source.

But when relays are placed further than of 0.3 of the distance, vMIMO relay systems are limited with the SISO capacity and MIMO relay will get better average capacity. In Figure 4.9, relays are located at 0.9 distances from the source.

At fixed SNR's, we evaluate the performance of the average capacity for vMIMO and MIMO relaying systems with different relay locations. When relays are very close to the

source, vMIMO DSF-V-BLAST provides the same capacity performance of MIMO V-BLAST relay because MIMO hops will dominate. Figure 4.10 shows average capacity at 20 dB SNR.

Figure 4.11 compares the block error rate of a DSF-STBC and a V-BLAST for vMIMO systems with a rate 4 bits/s/Hz and relays at distance 0.3 from the source with MIMO relayed systems. When the MIMO relays or vMIMO relays are close to the source like this example, we get almost the same performance for V-BLAST. However, MIMO relay STBC shows a noticeable gain over all relaying systems at higher SNR for the diversity order at both hops.

Losing the diversity and the spatial multiplexing gains becomes clearer when vMIMO relays are located far from the source so that SISO channels dominate the overall performance. Figures 4.12 and 4.13, the block error rate of a DSF of a vMIMO system and a MIMO relaying with rate 4 bits/s/Hz and relays at distance 0.5 and 0.7 from the source are presentesd.

At fixed SNR's and at rate 4 bit/s/Hz, we evaluate the performance of the system with different relay locations. From Figure 4.14, SNR and relays close to the source in vMIMO DSF-V-BLAST provide similar performance to MIMO V-BLAST relay systems. When relays are placed beyond 0.3 from the source MIMO V-BLAST relay overcomes on other relaying systems. However, MIMO relayed STBC gives very close performance of vMIMO DSF-V-BLAST.

Figure 4.15 shows the performance of the system at rate 4 bit/s/Hz with different relay locations at high SNR's. From the figure, relays close to the source vMIMO DSF-V-BLAST

will provide the same performance of MIMO V-BLAST relay systems. MIMO STBC relay overcomes on all relaying systems especially when the relay is placed over 0.3 from the source.

Bringing in relayed MIMO, allows us to study SMOd relays and their impact when benchmarked with other MIMO relay schemes. Figure 4.16 compares the block error rate of SMod relay and other MIMO relay systems with a rate 2 bits/s/Hz. Relays at distance 0.3 from the source with MIMO relayed systems. At low SNR's SMod relay perform better than V-BLAST and STBC. On the other hand, at higher SNR's STBC overcomes since it has a diversity order of 4. Figures 4.16, 4.17 and 4.18 compare the analytical results obtained for the relayed SMod to those obtained from the simulations. The Monte Carlo simulation is bounded to the analysis methods, which demonstrates the validity of the analysis proposed.

At fixed SNR's, the performances for SMod and MIMO relaying systems with different relay locations are evaluated. At a 10 dB SNR, SMod relay overcomes both STBC and V-BLAST. Figures 4.19 and 4.20 show the comparison between SMod, STBC and V-BLAST at 10 dB and different antenna setups.

At fixed SNR's, the performances of average capacity for SMod and MIMO relaying systems with different relay locations are evaluated. As expected, SMod has more average capacity comparing to STBC but it does not overcome V-BLAST average capacity. Figure 4.21 shows average capacity at 20 dB SNR. Figures 4.22, 4.23 and 4.24 show the block error rate of a SMod relay system and other MIMO relaying at rate 4 bits/s/Hz and relays at distances 0.3, 0.5 and 0.7 from the source. By comparing the analytical results obtained for

the relayed SMod to those obtained from the simulation, it becomes clear that the Monte Carlo simulation is bounded to the analysis methods, which demonstrates the validity of the proposed analysis.

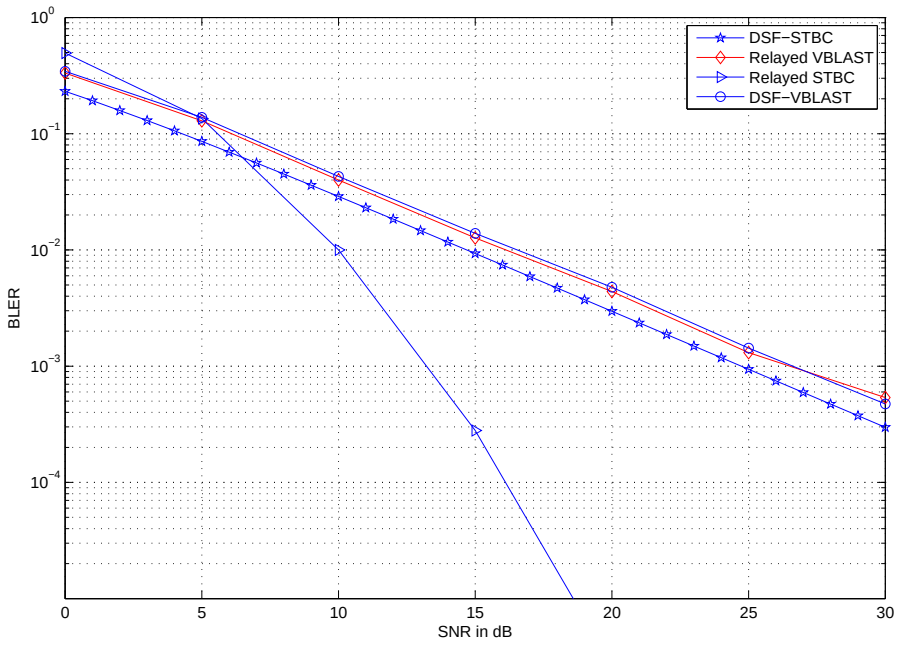

Figure 4.3: MIMO relaying versus DSF relays at 0.3 from the source with rate 2bit/s/Hz.

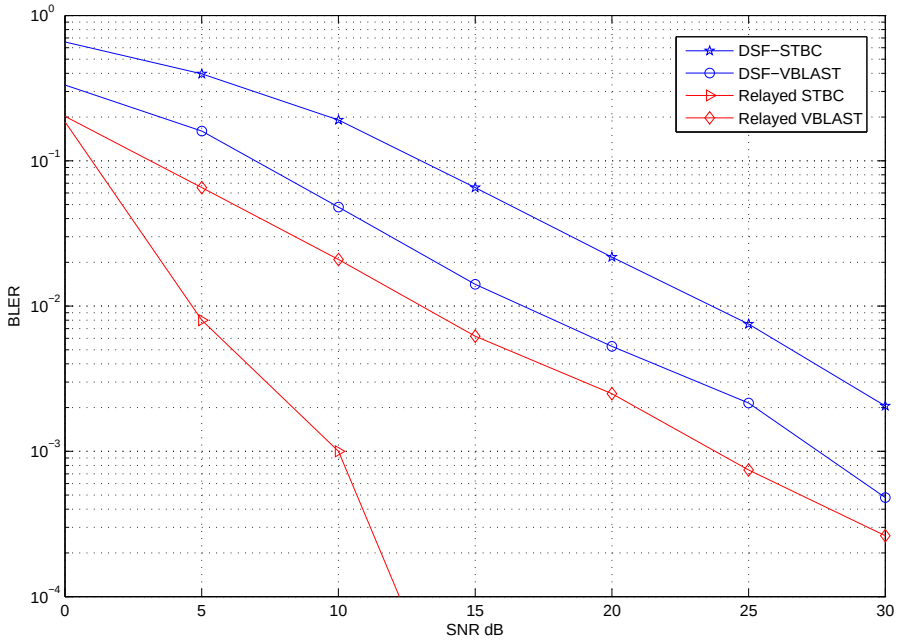

Figure 4.4: MIMO relaying versus DSF relays at 0.5 from the source with rate 2bit/s/Hz.

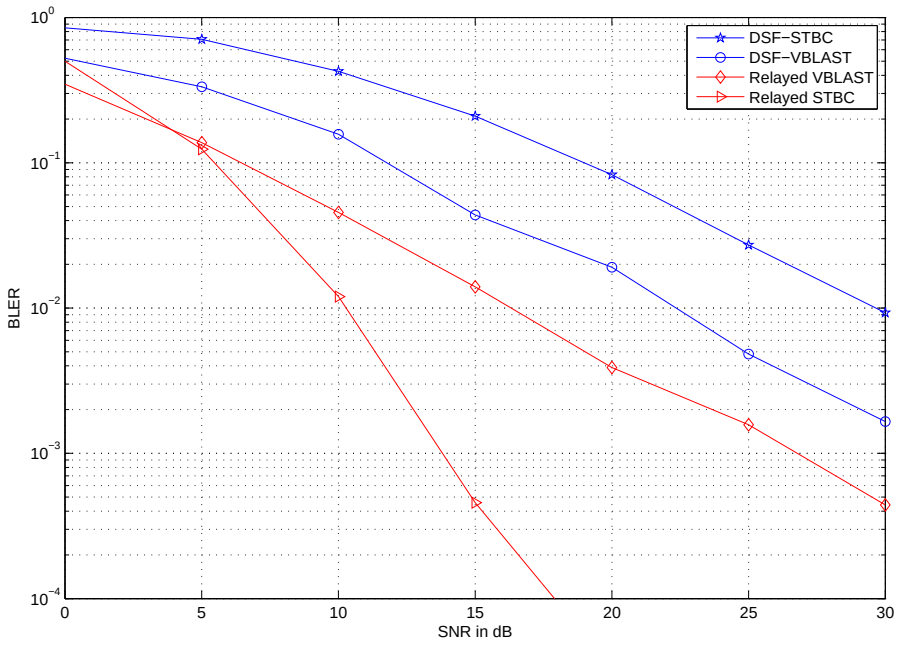

Figure 4.5: MIMO relaying versus DSF relays at 0.7 from the source with rate 2bit/s/Hz.

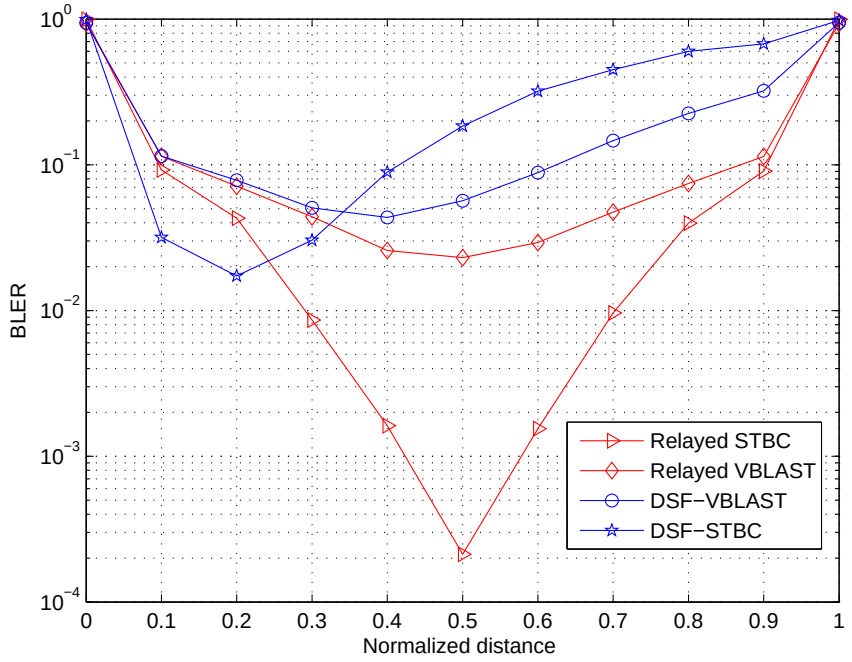

Figure 4.6: BLER performance various source-relay distances for MIMO relaying versus DSF with rate 2bit/s/Hz SNR=10 dB.

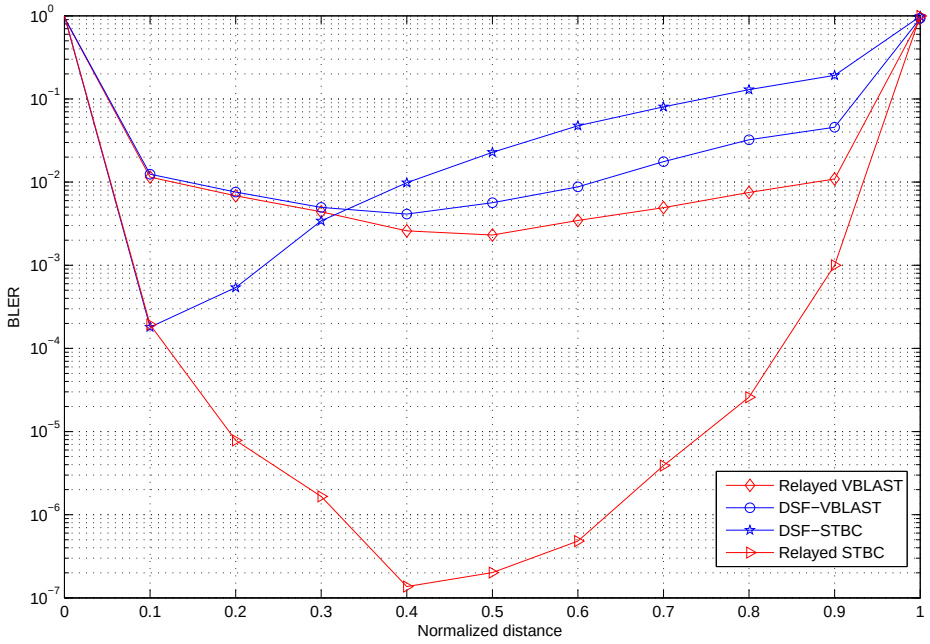

Figure 4.7: BLER performance various source-relay distances for MIMO relaying versus DSF with rate 2bit/s/Hz SNR=20 dB.

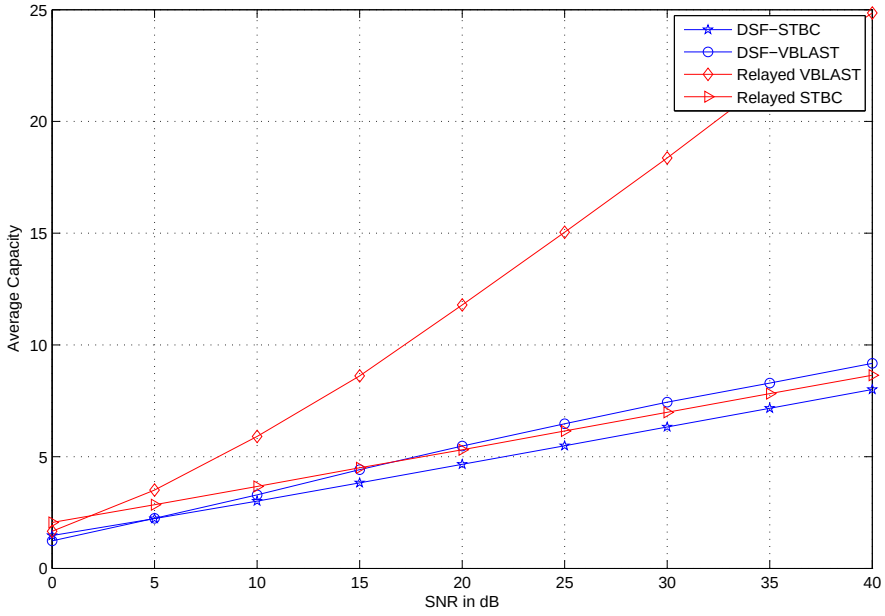

Figure 4.8: Average capacity at distance d=0.3 from source-relay for MIMO relaying versus DSF relaying.

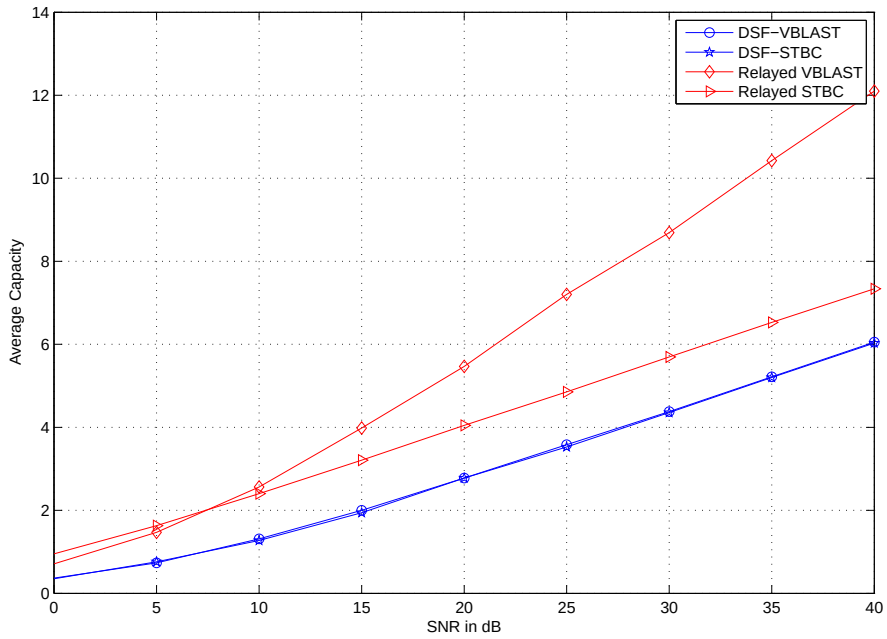

Figure 4.9: Average capacity at distance d=0.9 from source-relay for MIMO relaying versus DSF relaying.

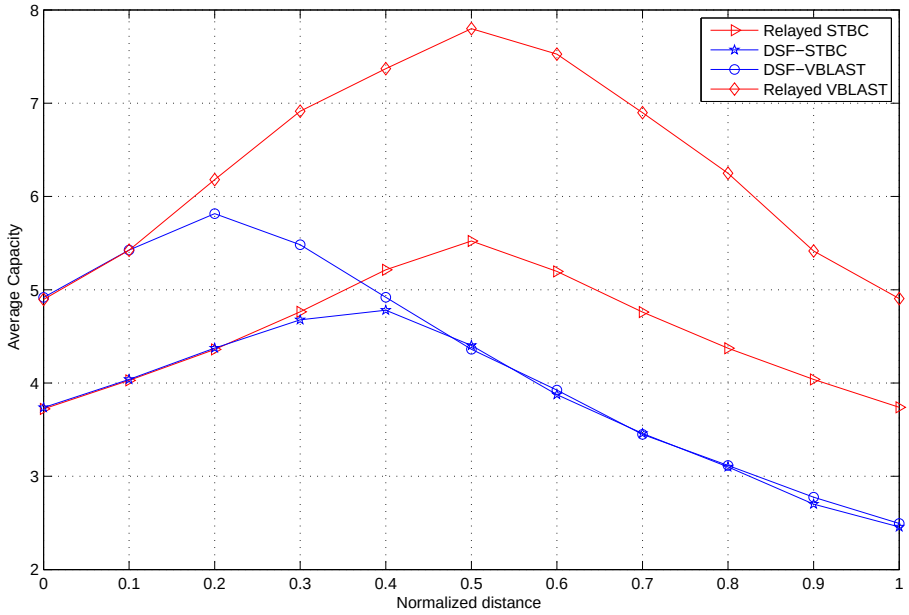

Figure 4.10: Average capacity various source-relay distances for MIMO relaying versus DSF with SNR=20 dB.

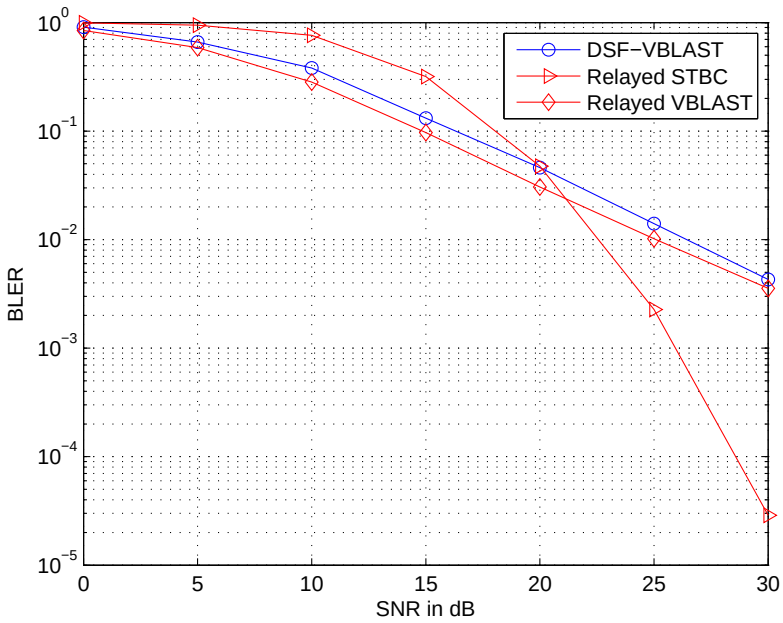

Figure 4.11: MIMO relaying versus DSF relays at 0.3 from the source with rate 4bit/s/Hz.

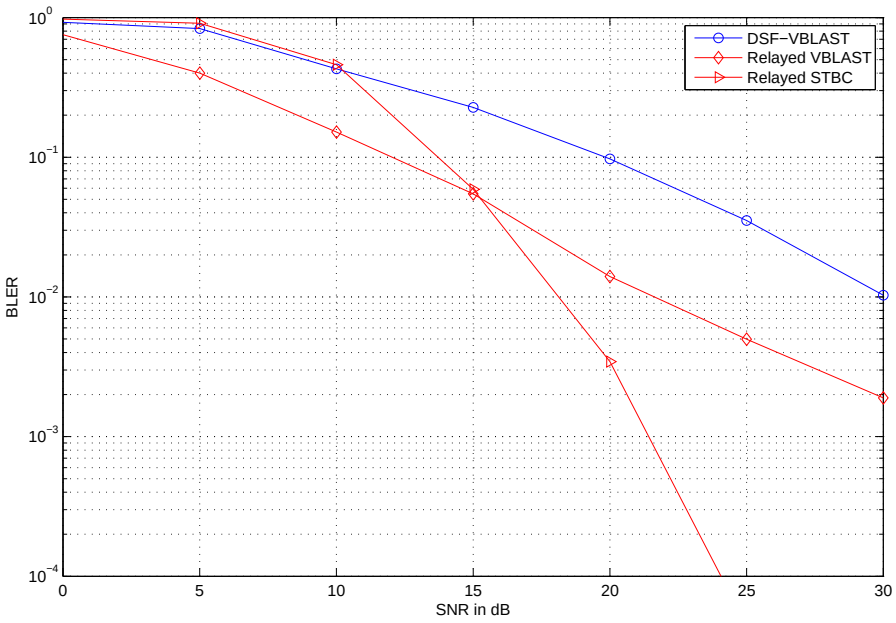

Figure 4.12: MIMO relaying versus DSF relays at 0.5 from the source with rate 4bit/s/Hz.

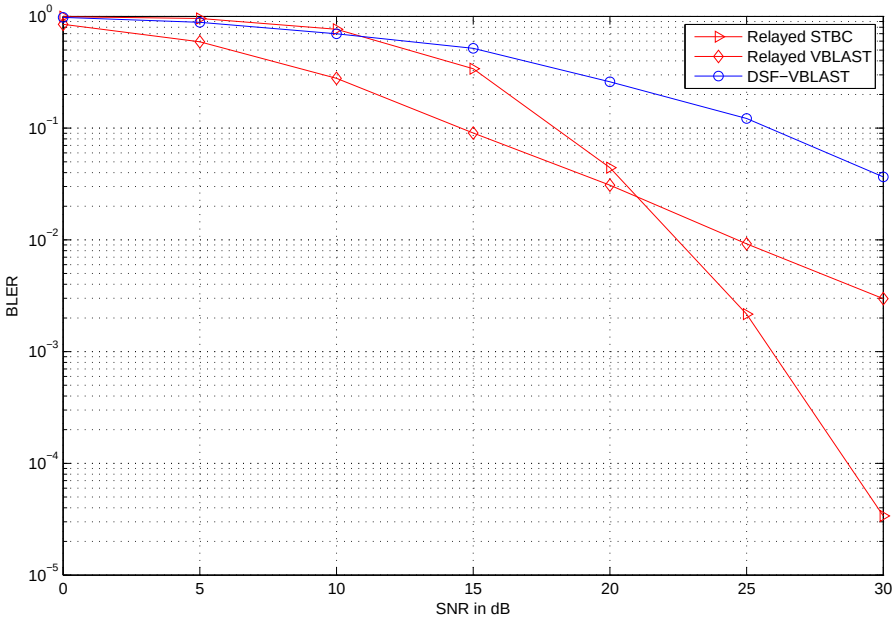

Figure 4.13: MIMO relaying versus DSF relays at 0.7 from the source with rate 4bit/s/Hz.

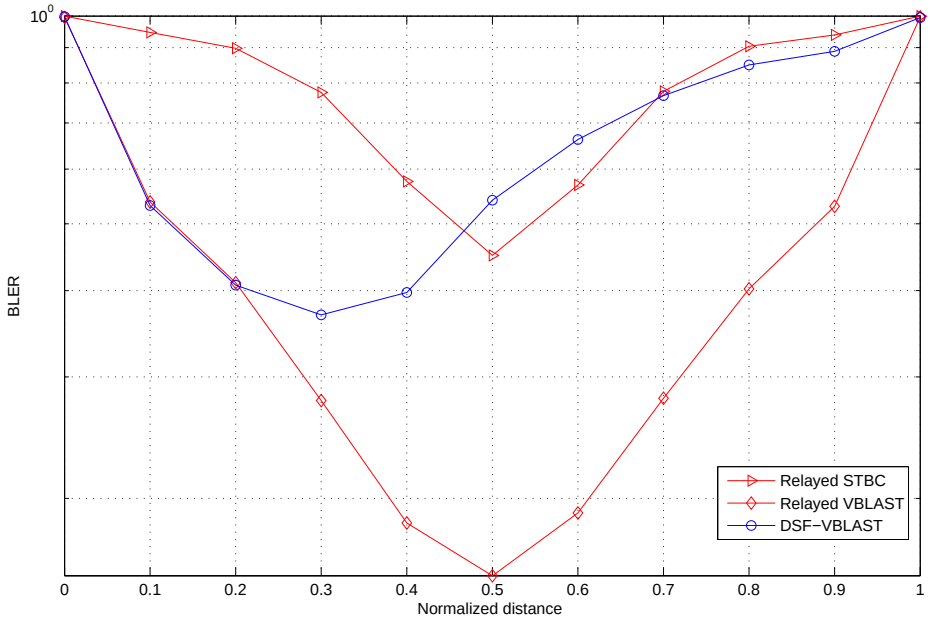

Figure 4.14: BLER performance various source-relay distances for MIMO relaying versus DSF with rate 4bit/s/Hz SNR=10 dB.

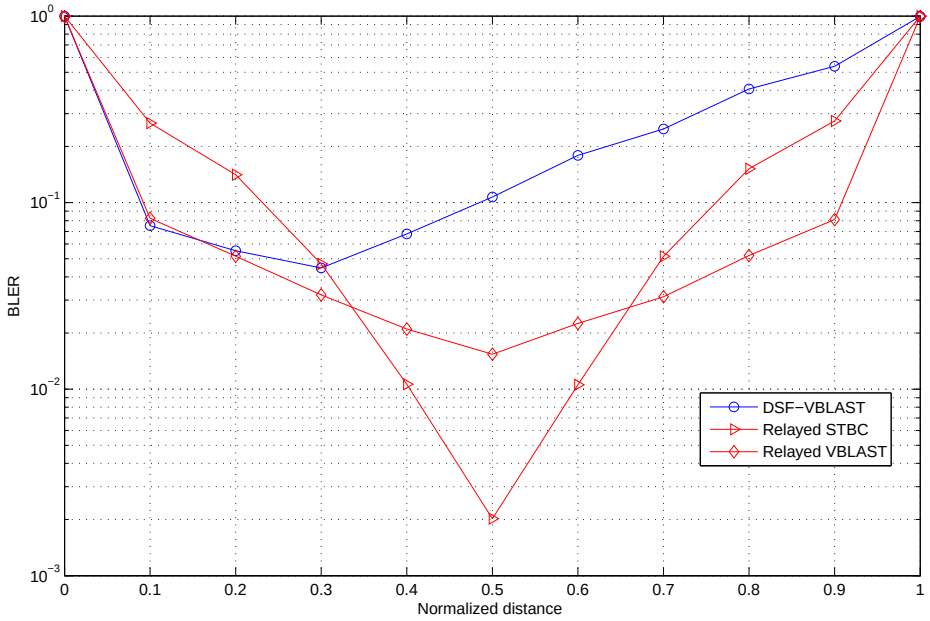

Figure 4.15: BLER performance various source-relay distances for MIMO relaying versus DSF with rate 4bit/s/Hz SNR=20 dB.

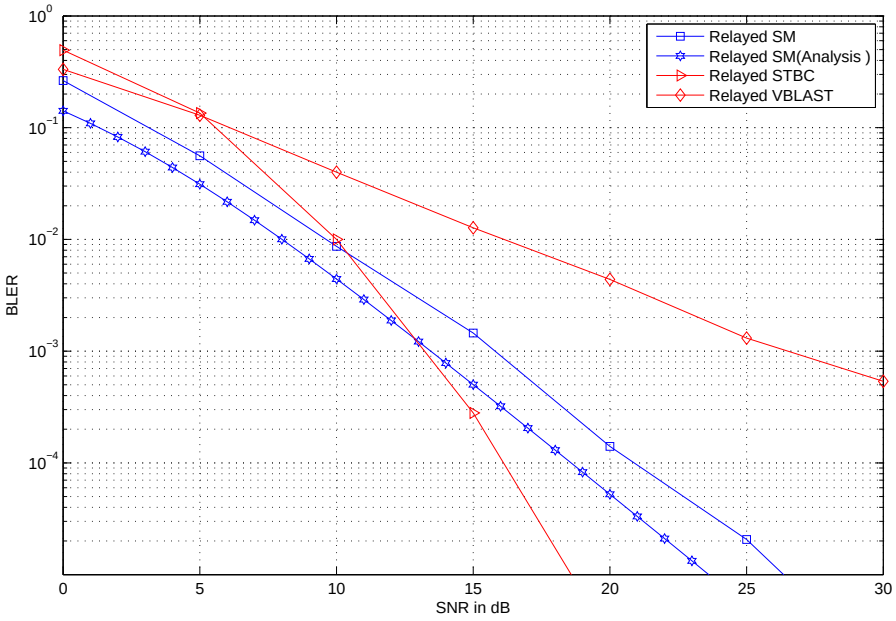

Figure 4.16: MIMO relaying versus Relayed Spatial Modulation at 0.3 from the source with rate 2bit/s/Hz.

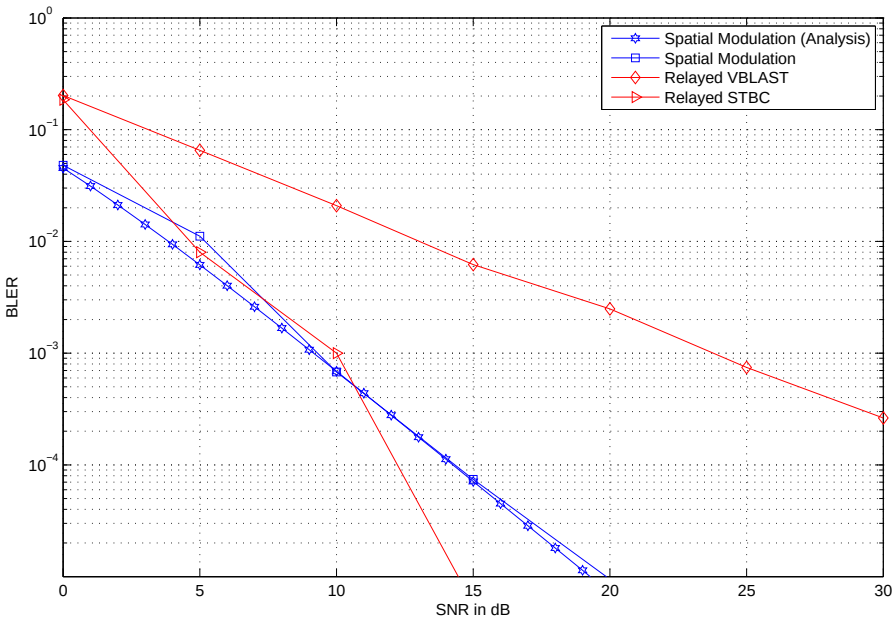

Figure 4.17: MIMO relaying versus Relayed Spatial Modulation at 0.5 from the source with rate 2bit/s/Hz.

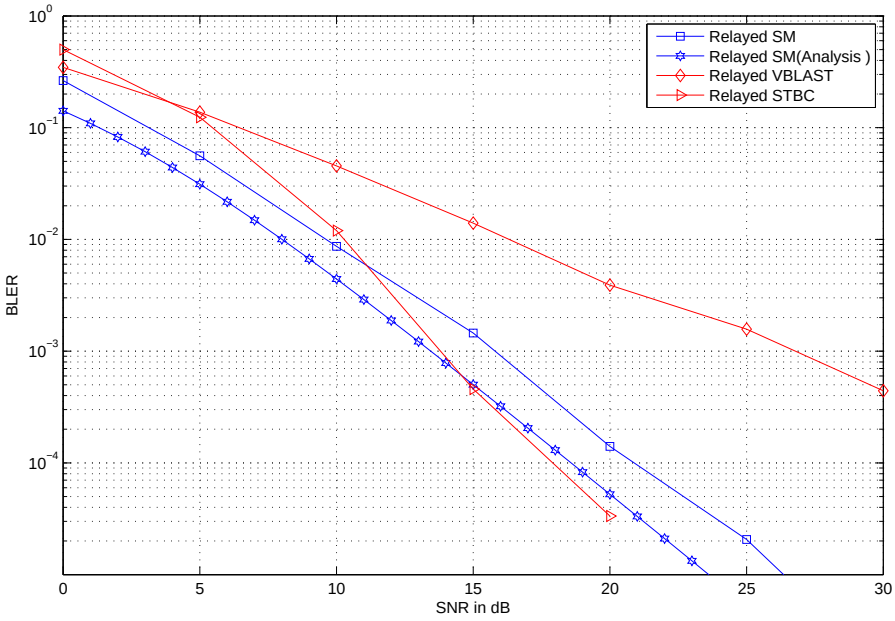

Figure 4.18: MIMO relaying versus Relayed Spatial Modulation at 0.7 from the source with rate 2bit/s/Hz.

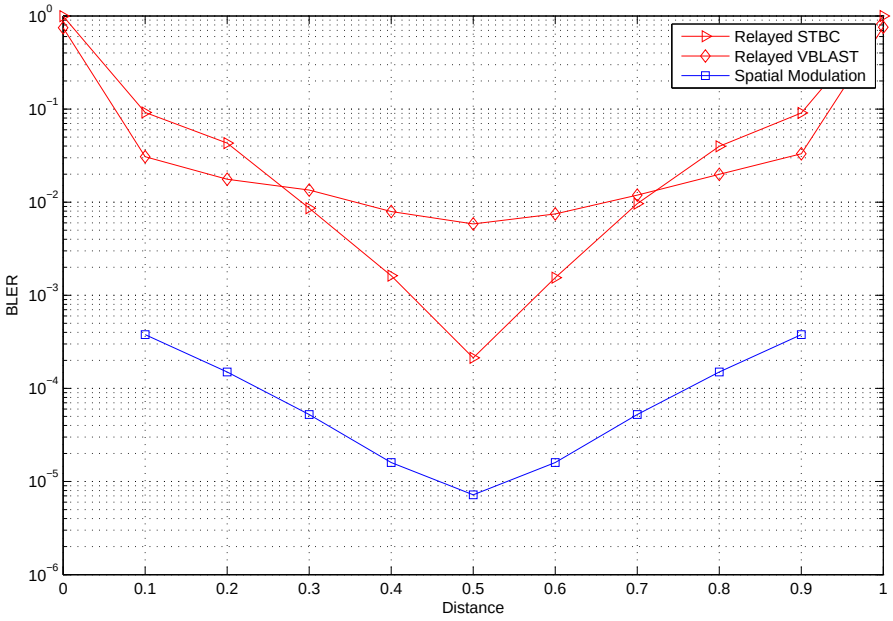

Figure 4.19: BLER performance various source-relay distances for MIMO relaying versus SMod with rate 2bit/s/Hz SNR=10 dB

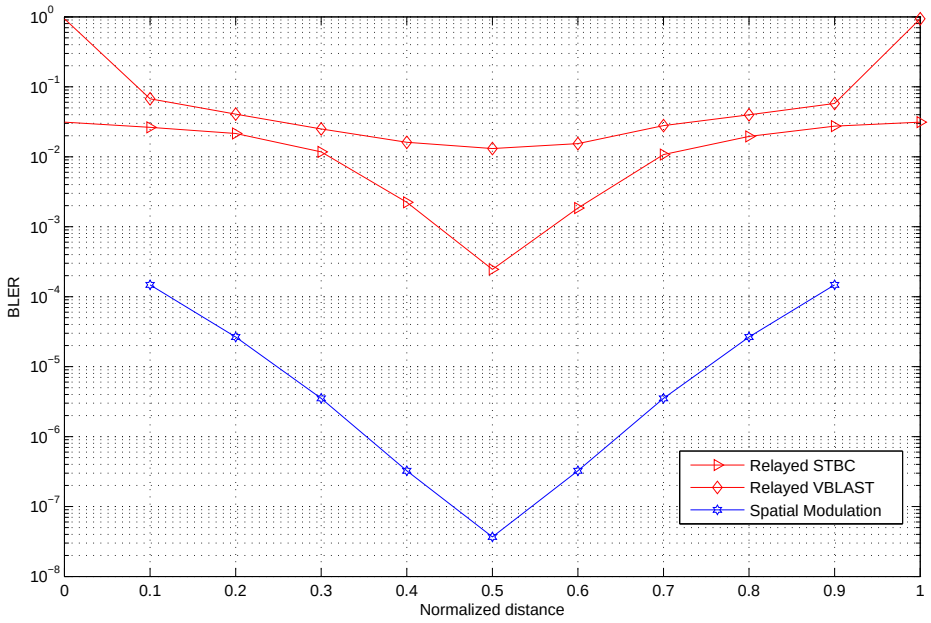

Figure 4.20: BLER performance various source-relay distances for MIMO relaying versus SMod with rate 2bit/s/Hz SNR=10 dB with 4×4 configuration.

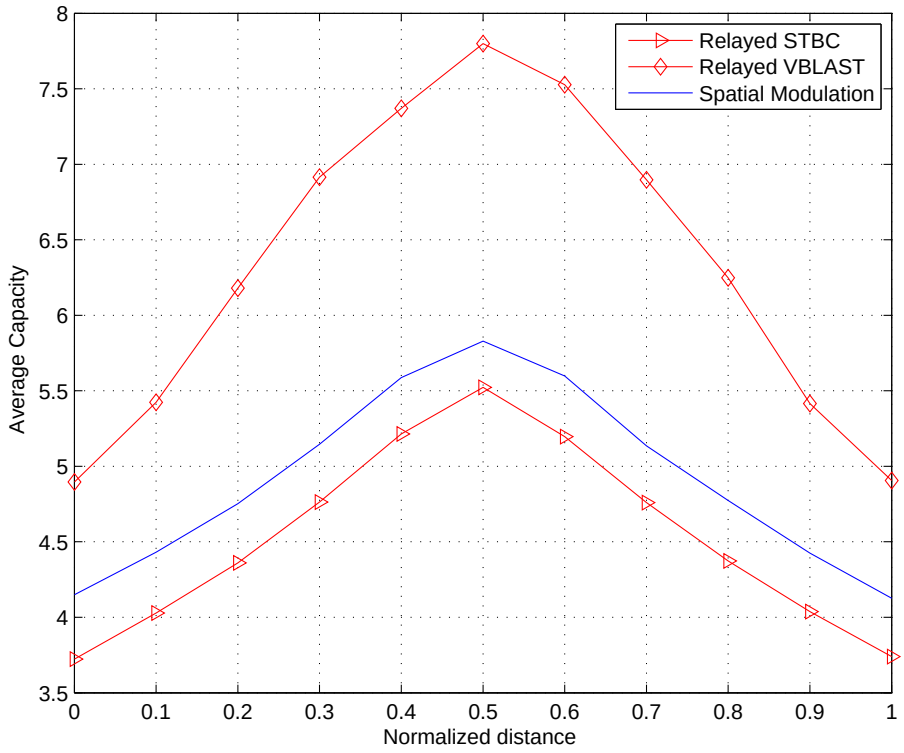

Figure 4.21: Average capacity various source-relay distances for MIMO relaying versus SMod with SNR=20 dB.

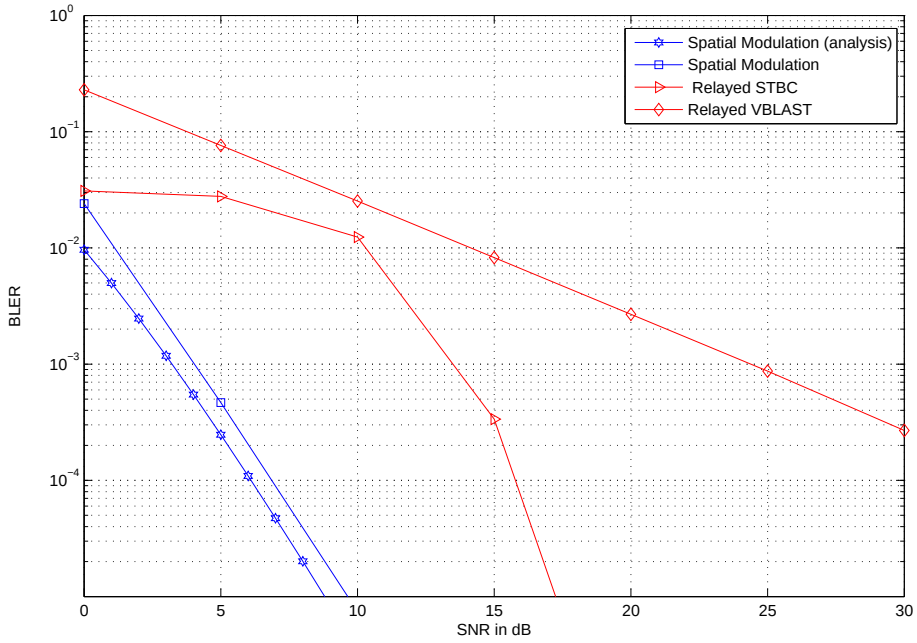

Figure 4.22: MIMO relaying versus Relayed Spatial Modulation at 0.3 from the source with rate 2bit/s/Hz.

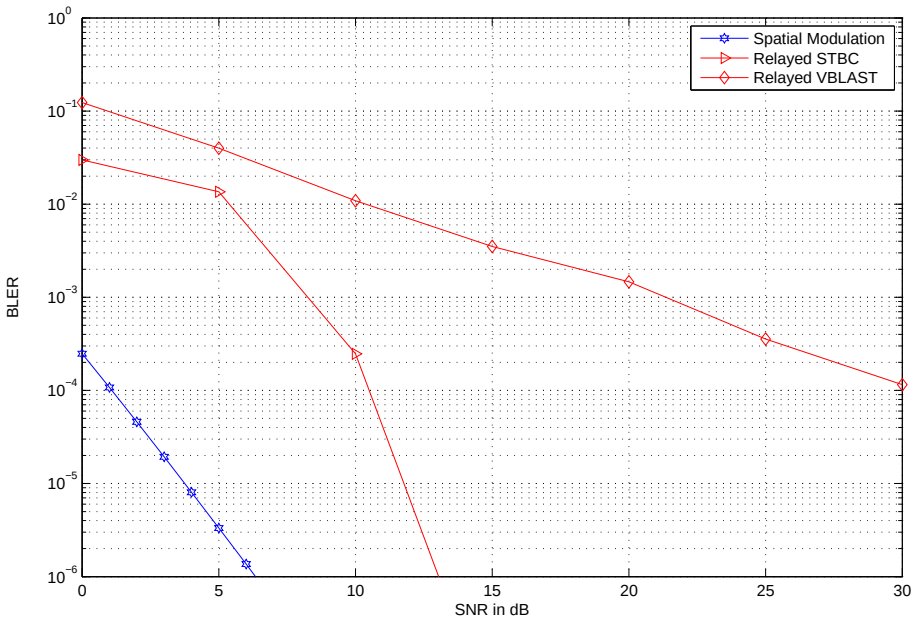

Figure 4.23: MIMO relaying versus Relayed Spatial Modulation at 0.5 from the source with rate 2bit/s/Hz.

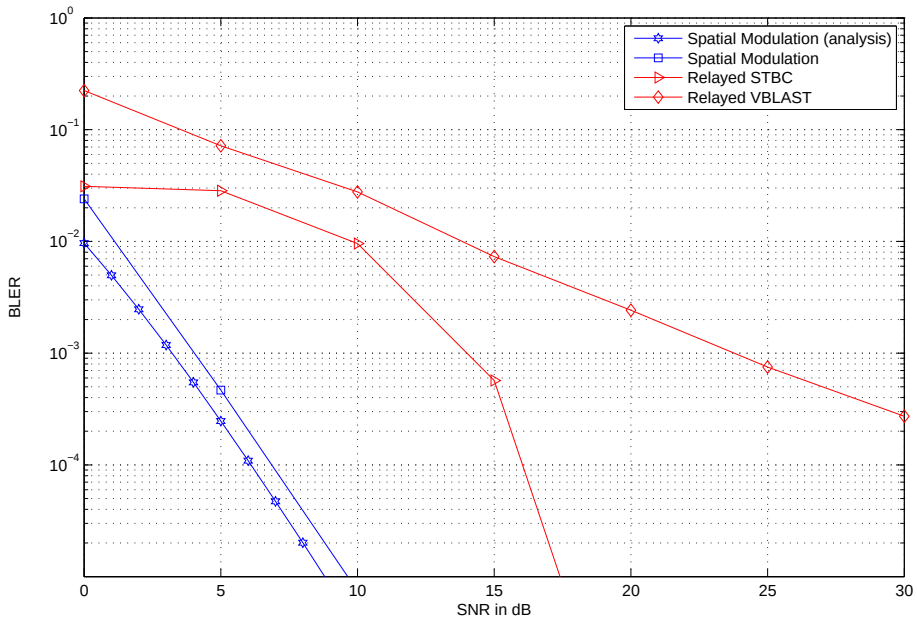

Figure 4.24: MIMO relaying versus Relayed Spatial Modulation at 0.7 from the source with rate 2bit/s/Hz.

4.5 Chapter Conclusions

In this chapter, we compare MIMO relaying over vMIMO. The SISO channels become the bottleneck of the vMIMO systems. Setting up MIMO relaying allows us to present relayed spatial modulation techniques to guarantee the tradeoff between spatial multiplexing and diversity order. The system performance in terms of distance, modulation type, and the number of relays is evaluated. The analytical results of relayed SMod in this thesis form a close upper bound for the simulation results demonstrated in the chapter

CHAPTER 5

CONCLUSIONS AND FUTURE RESEARCH

In this thesis, we investigated distributed and virtual MIMO relaying schemes. Both error and capacity analysis have been conducted and the analytical results have been verified by simulations.

In Chapter 2, we investigated the performance of uplink cooperative Spatial Multiplexing and non-orthogonal STBC MIMO using Amplify-and Forward (AF) relays. The analytical results matched the simulation results. The system performance in terms of distance, modulation type, and number of hops is evaluated. The gain is limited as we increase hops or relays because the noise and interference are also amplified along with the signal, so the performance will not enhance in proportion with the increase of hops.

In Chapter 3, we investigated the performance of uplink cooperative Spatial Multiplexing and STBC using the DSF scheme over MIMO relays. The analytical results matched the simulation results. The system performance in terms of distance, modulation type, and

number of relays is evaluated. The DSF-V-BLAST vMIMO shows 5 dB gain over the AF-V-BLAST vMIMO. The main reason for this gain is that the DSF lowers the modulation at the second hop and does not amplifying the noise.

In Chapter 4, we compared MIMO relaying over vMIMO since the SISO channels will be the bottleneck of the vMIMO systems. Setting up MIMO relaying allowed us to present relayed spatial modulation to guarantee the tradeoff between spatial multiplexing and diversity order. We evaluate the system performance in terms of distance, modulation type, and number of relays is evaluated. The analytical results of relayed SMod in this thesis form a very close upper bound for the simulation results demonstrated in this chapter.

The main contribution of this thesis is to provide analytical tools to evaluate the performance of distributed and virtual MIMO relaying schemes, including V-BLAST, STBC and spatial modulation.

As a future work, time and frequency siynchronization for vMIMO relay systems needs to be investigated. Adaptive vMIMO is another interesting research question as power allocation for vMIMO. Anotehr direction of investigation may include relay selection for scheduling techniques.

REFERENCES

[1] Samir Al-Ghadhban, *Multi-layered Space Frequency Time Codes*, Ph.D. thesis, Virginia Polytechnic Institute and State University, Blacksburg, Virginia, Nov 2005.

[2] Krishna Balachandran, Doru Calin, Nandu Gopalakrishnan, Joseph H. Kang, Achilles Kogiantis, Shupeng Li, Lawrence Ozarow, Sudhir Ramakrishna, Ashok N. Rudrapatna, and Russell Sun, "Design and performance analysis of collaborative spatial multiplexing for ieee 802.16e-based systems," *Bell Lab. Tech. J.*, vol. 13, no. 4, pp. 97–117, 2009.

[3] Moray Rumney, *LTE and the Evolution to 4G Wireless : Design and Measurement Challenges*, Wiley, USA, 2009.

[4] Ahmed K.Sadek K.J. rayliu and A.Kwasinski, *Cooperative Communications and Networking*, Cambridge University Press, Cambridge, 2009.

[5] S. Alamouti, "A simple transmit diversity technique for wireless communications," *Selected Areas in Communications,IEEE Journal*, vol. 16, pp. 14511458, Oct 1998.

[6] H. Jafarkhani V. Tarokh and A. R. Calderbank, "Space-time block codes from orthogonal designs," *IEEE Trans. Inform. Theory*, vol. 45, pp. 14561467, Oct 1999.

[7] S. Ganesan, R. Mesleh, H. Haas, Chang Wook Ahn, and S. Yun, "On the performance of spatial modulation ofdm," *Signals, Systems and Computers, 2006. ACSSC '06. Fortieth Asilomar Conference on*, pp. 1825 –1829, oct. 2006.

[8] R.Y. Mesleh, H. Haas, S. Sinanovic, Chang Wook Ahn, and Sangboh Yun, "Spatial modulation," *Vehicular Technology, IEEE Transactions on*, vol. 57, no. 4, pp. 2228 –2241, jul. 2008.

[9] J. Jeganathan, A. Ghrayeb, and L. Szczecinski, "Spatial modulation: optimal detection and performance analysis," *Communications Letters, IEEE*, vol. 12, no. 8, pp. 545 – 547, aug. 2008.

[10] R. Mesleh, R. Mehmood, H. Elgala, and H. Haas, "Indoor mimo optical wireless communication using spatial modulation," *Communications (ICC), 2010 IEEE International Conference on*, pp. 1 –5, may. 2010.

[11] Jose F. Monserrat Afif Osseiran and Werner Mohr, *MOBILE AND WIRELESS COMMUNICATIONS FOR IMT-ADVANCED AND BEYOND*, Wiley-IEEE Press, Jan. 2011.

[12] E. van der Meulen, "Three-terminal Communication Channels," .

[13] and G.W.Wornell J.N.Laneman, D.N.C.Tse, "Cooperative Diversity in Wireless Networks: Efficient Protocols and Outage Behavior," pp. 3062–3080, December 2004.

[14] "Ieee standard for local and metropolitan area networks part 16: Air interface for broadband wireless access systems amendment 1: Multiple relay specification," *IEEE Std 802.16j-2009 (Amendment to IEEE Std 802.16-2009)*, pp. c1 –290, jun. 2009.

[15] A. Wyner, "The rate-distortion function for source coding with side information at the decoder -ii: General sources," vol. 38, pp. 60– 80, 1978.

[16] S. Simoens, O. Muoz-Medina, J. Vidal, and A. Del Coso, "Compress-and-forward cooperative mimo relaying with full channel state information," *Signal Processing, IEEE Transactions on*, vol. 58, no. 2, pp. 781 –791, feb. 2010.

[17] M. Dohler, A. Gkelias, and H. Aghvami, "A resource allocation strategy for distributed mimo multi-hop communication systems," *Communications Letters, IEEE*, vol. 8, no. 2, pp. 99 – 101, feb. 2004.

[18] R. Pabst, B.H. Walke, D.C. Schultz, P. Herhold, H. Yanikomeroglu, S. Mukherjee, H. Viswanathan, M. Lott, W. Zirwas, M. Dohler, H. Aghvami, D.D. Falconer, and G.P. Fettweis, "Relay-based deployment concepts for wireless and mobile broadband radio," *Communications Magazine, IEEE*, vol. 42, no. 9, pp. 80 – 89, sep. 2004.

[19] B. Wang, J. Zhang, and A. Host-Madsen, "On the capacity of mimo relay channels," *Information Theory, IEEE Transactions on*, vol. 51, no. 1, pp. 29 –43, jan. 2005.

[20] Younsun Kim and Hui Liu, "Infrastructure relay transmission with cooperative mimo," *Vehicular Technology, IEEE Transactions on*, vol. 57, no. 4, pp. 2180 –2188, jul. 2008.

[21] A. Abdaoui, S.S. Ikki, M.H. Ahmed, and E. Chatelet, "On the performance analysis of a mimo-relaying scheme with space time block codes," *Vehicular Technology, IEEE Transactions on*, vol. 59, no. 7, pp. 3604 –3609, sep. 2010.

[22] H. Van Khuong and T. Le-Ngoc, "Performance analysis of a decode-and-forward cooperative relaying scheme for mimo systems," *Communications (QBSC), 2010 25th Biennial Symposium on*, pp. 400 –403, may. 2010.

[23] Changick Song, Kyoung-Jae Lee, and Inkyu Lee, "Performance analysis of amplify-and-forward spatial multiplexing mimo relaying systems," *Communications (ICC), 2010 IEEE International Conference on*, pp. 1 –5, may. 2010.

[24] Xiaolong Zhu, Yong Song, Hongwei Yang, and Liyu Cai, "2-d switching diversity aided collaborative spatial multiplexing for uplink wireless access," *Wireless Communications and Networking Conference, 2009. WCNC 2009. IEEE*, pp. 1 –4, apr. 2009.

[25] A. Darmawan, S.W. Kim, and H. Morikawa, "Amplify-and-forward scheme in cooperative spatial multiplexing," *Mobile and Wireless Communications Summit, 2007. 16th IST*, pp. 1 –5, jul. 2007.

[26] S.W. Kim and Ravi Cherukuri, "Cooperative spatial multiplexing for high-rate wireless communications," *Signal Processing Advances in Wireless Communications, 2005 IEEE 6th Workshop on*, pp. 181 – 185, jun. 2005.

[27] Sang Wu Kim, "Cooperative spatial multiplexing in mobile ad hoc networks," *Mobile Adhoc and Sensor Systems Conference, 2005. IEEE International Conference on*, pp. 8 pp. –387, nov. 2005.

[28] M.O. Hasna and M.-S. Alouini, "A performance study of dual-hop transmissions with fixed gain relays," *Wireless Communications, IEEE Transactions on*, vol. 3, no. 6, pp. 1963 – 1968, 2004.

[29] A. M Chan and Inkyu Lee, "A new reduced-complexity sphere decoder for multiple antenna systems," *IEEE International Conference on Communications*, vol. 1, pp. 460–464, may. 2002.

[30] F. Al-Shalan, *Performance of Quadrature Amplitude Modulation in Nakagami Fading Channels with Diversity*, Ph.D. thesis, King Fahd University of Petroleum and Minerals, Dhahran, Saudi Arabia, March 2000.

[31] C. Papadias and G. J. Foschini., "On the capacity of certain space-time coding schemes," *EURASIP Journal on Applied Signal Processing 2002*, vol. 5, pp. 447 –458, may. 2002.

[32] Gang Shen, Jimin Liu, Dongyao Wang, Jikang Wang, and Shan Jin, "Multi-hop relay for next-generation wireless access networks," *Bell Lab. Tech. J.*, vol. 13, no. 4, pp. 175–193, 2009.

[33] Marvin K. Simon and Mohamed-Slim Alouini, *Digital Communication over Fading Channels (Wiley Series in Telecommunications and Signal Processing)*, Wiley-IEEE Press, Dec. 2004.

[34] S. Sandhu and A. Paulraj, "Space-time block codes: A capacity perspective," *IEEE Comm. Letters*, vol. 4, no. 12, pp. 384:386, December. 2000.

[35] N.R. Naidoo, H.J. Xu, and T. Al-Mumit Quazi, "Spatial modulation: optimal detector asymptotic performance and multiple-stage detection," *Communications, IET*, vol. 5, no. 10, pp. 1368 –1376, 1 2011.

[36] S.M. Alamouti, "A simple transmit diversity technique for wireless communications," *Selected Areas in Communications, IEEE Journal on*, vol. 16, no. 8, pp. 1451 –1458, oct 1998.

[37] H. Xu, "symbol error probability for generalized selection combining reception of m-qam," *SAIEE Afr. Res.J.*, vol. 100, no. 3, pp. 68–71, 2009.

[38] J. Jeganathan, A. Ghrayeb, L. Szczecinski, and A. Ceron, "Space shift keying modulation for mimo channels," *Wireless Communications, IEEE Transactions on*, 2009.

[39] J.G. Proakis, *Digital communications*, McGraw-Hill, New York, 2001.

Vitae

- Suhaib Mohammed Al-Basit
- Nationality: Jordanian
- Current Address: P.O. Box 8050, K.F.U.P.M., Dhahran 31261, Saudi Arabia
- Permanent Address: Jubail Street, Alfakhria, Dhahran, Saudi Arabia
- Telephone: (+966) 502 451 933
- Email: *suhaib.albaseet@gmail.com*
- Born in Riyadh, Saudi Arabia on December 19, 1983
- Received Bachelor of Engineering (B.E.) in Electrical Engineering from King Fahd University of Petroleum & Minerals, Dhahran, Saudi Arabia in 2006.